

Dissertation

zur Erlangung des Doktorgrades der Fakultät für Chemie und
Pharmazie der Ludwig-Maximilian-Universität München



Cell culture models and novel gene therapeutic strategies for
colorectal cancer

vorgelegt von

Lars Gädtke

aus Leonberg

2006

Erklärung

Diese Dissertation wurde im Sinne von § 13 Abs. 3 bzw. 4 der Promotionsordnung vom 29. Januar 1998 von Prof. Dr. Ernst Wagner betreut.

Ehrenwörtliche Versicherung

Diese Dissertation wurde selbständig, ohne unerlaubte Hilfe erarbeitet.

München,

(Lars Gädtke)

Dissertation eingereicht am 12.01.2006

1. Gutacher: Prof. Dr. Ernst Wagner

2. Gutacher: PD. Dr. Carsten Culmsee

Mündliche Prüfung am 15.02.2006

Table of Contents

1. INTRODUCTION.....	8
1.1. Colorectal cancer	8
1.1.1. Pathogenesis of colorectal cancer	8
1.1.2. Human low passage colon cancer cell lines.....	10
1.1.3. Multicellular tumor spheroids.....	11
1.2. Chemotherapy of colorectal cancer	13
1.2.1. Chemoresistance against chemotherapeutic drugs	13
1.2.2. Mechanisms of action of 5-fluorouracil.....	14
1.3. Gene therapy of colorectal cancer.....	16
1.3.1. Gene delivery strategies	16
1.3.2. Tumor specific cell targeting strategies	17
1.3.3. Therapeutic genes	18
1.4. Specific aims of the PhD thesis	20
1.4.1. Initiation and characterization of relevant model systems for colorectal cancers	20
1.4.2. Elucidation of mechanisms involved in resistance of colorectal cancers against chemotherapy	20
1.4.3. Development of alternative therapy strategies for colorectal cancers	21
2. MATERIAL AND METHODS	22
2.1. Chemicals and reagents	22
2.2. Molecular biological methods	23
2.2.1. Restriction digestion of plasmid DNA	23
2.2.2. Dephosphorylation of plasmid DNA fragments.....	23
2.2.3. Converting of 5'-overhangs of DNA fragments to blunt ends	23
2.2.4. Isolation of DNA fragments from agarose gels.....	23
2.2.5. Ligation	23
2.2.6. Transformation of E.coli	24
2.2.7. Preparation of plasmid DNA.....	24
2.2.8. Cloning strategies	24

2.3. Cell biological methods	25
2.3.1. Cell culture	25
2.3.2. Multicellular spheroid culture.....	26
2.3.3. Formation of transfection complexes	26
2.3.4. Measurement of particle size and zeta-potential	27
2.3.5. Gene transfer to monolayer cultures	27
2.3.6. Gene transfer to multicellular spheroids.....	28
2.3.7. Luciferase assay	28
2.3.8. Human IL-2 ELISA	29
2.3.9. Treatment of cells with 5-fluorouracil.....	29
2.3.10. Proliferation and viability assays	29
2.3.10.1. Hoechst 33258-based proliferation assay.....	29
2.3.10.2. MTT assay	30
2.3.11. Flow cytometric analysis	30
2.3.11.1. Flow cytometric analysis of EGFP expression	30
2.3.11.2. Flow cytometric analysis of apoptosis.....	30
2.3.12. Transmission light and epifluorescence microscopy	31
2.3.13. Confocal laser scanning microscopy of multicellular spheroids.....	32
2.3.14. Cryosections of multicellular spheroids	32
2.4. 2D Electrophoresis and MALDI-TOF mass spectrometry	33
2.4.1. Sample preparation.....	33
2.4.2. Measurement of protein concentration.....	33
2.4.3. First dimension: Isoelectric focusing	33
2.4.4. Second dimension: SDS-page	34
2.4.5. Silver staining.....	35
2.4.6. 2D image analysis.....	35
2.4.7. In-gel digestion.....	36
2.4.8. Desalting and spotting of peptides onto the MALDI-TOF MS target.....	36
2.4.9. MALDI-TOF mass spectrometry and peptide mass fingerprinting.....	37

3. RESULTS	38
3.1. Multicellular spheroids of low passage colon cancer cell lines - A promising model system for colorectal cancer	38
3.1.1. Establishment of multicellular spheroids of low passage colon cancer cell lines	38
3.1.2. Differences in the expression profiles of multicellular spheroids compared to corresponding monolayer cultures	39
3.2. Chemotherapy of colorectal cancer – Detection of proteins associated with chemoresistance against 5-FU	50
3.2.1. Determination of 5-FU concentrations required for reduction of proliferation of selected low passage colon cancer cells	50
3.2.2. Long-term 5-FU treatment of selected low passage colon cancer cells	53
3.2.3. Effect of 5-FU on proliferation of the long-term 5-FU-pretreated sublines .	54
3.2.4. Effect of 5-FU on the induction of apoptosis in the long-term 5-FU pretreated subline COGA-12/G6	55
3.2.5. Effect of 5-FU on proliferation and apoptosis in long-term propagated COGA-12 cells	56
3.2.6. Differences in the expression profiles of chemoresistant cells compared to corresponding chemosensitive cells.....	58
3.3. Gene therapy of colorectal cancer	67
3.3.1. Optimization of nonviral gene transfer to colorectal cancer cells.....	67
3.3.1.1. Generation and biophysical properties of nonviral gene transfer formulations	67
3.3.1.2. Determination of the efficiencies of the most adequate formulations in gene transfer.....	69
3.3.1.3. Transfection of multicellular spheroids with lipopolyplexes	71
3.3.2. Transcriptional targeting of colorectal cancer cells.....	75
3.3.2.1. Gene expression levels after transcriptional targeting in various low passage colon cancer cell lines	75
3.3.2.2. Transfection of selected low passage colon cancer cell lines with transcriptionally targeted lipopolyplexes	77

3.3.2.3.	Influence of plasmid DNA concentration on gene expression levels with or without transcriptional targeting	78
3.3.2.4.	Percentage of transfected cells with or without transcriptionally targeted gene transfer	79
3.3.2.5.	Transfection of multicellular spheroids with transcriptionally targeted lipopolyplexes	82
3.3.3.	Therapeutic strategies for treatment of colorectal cancer	83
3.3.3.1.	Colorectal cancer specific expression of immune stimulatory IL-2.....	83
3.3.3.2.	Colorectal cancer specific coexpression of cytotoxic protease 2A and immune stimulatory IL-2.....	85
3.3.3.2.1.	Effect of protease 2A on the overall gene expression of transfected cells.....	86
3.3.3.2.2.	Effect of protease 2A on the metabolic activity of transfected cells ..	88
3.3.3.2.3.	Effect of protease 2A on the apoptosis rate of transfected cells	90
3.3.3.2.4.	IRES-mediated IL-2 expression	90
4.	DISCUSSION.....	92
4.1.	Protein expression pattern in multicellular spheroids compared to monolayer cultures of low passage colon cancer cells.....	92
4.2.	Regulation of cytoskeleton- and mitochondria-associated proteins related to chemoresistance against 5-FU.....	99
4.3.	Lipopolyplexes mediate efficient gene transfer to low passage colon cancer cells	108
4.4.	The artificial CTP4 promoter enables high colorectal cancer specific gene expression.....	112
4.5.	Transcriptionally targeted lipopolyplexes enable sufficient expression of the immune stimulatory gene IL-2	114
4.6.	Therapeutic potential of combined immune stimulatory and cytotoxic gene expression in colorectal cancer cells	116

5. SUMMARY.....	121
6. APPENDIX.....	123
6.1. Abbreviations	123
6.2. Publications	127
6.2.1. Original Papers	127
6.2.2. Poster presentation	127
7. REFERENCES.....	128
8. ACKNOWLEDGEMENTS.....	144
9. CURRICULUM VITAE	144

1. Introduction

1.1. Colorectal cancer

1.1.1. Pathogenesis of colorectal cancer

Colorectal cancer is one of the most frequent cancers in the western hemisphere besides lung and breast cancer (Ries et al., 2002). Colorectal carcinomas arise both sporadically at a median age of 67 years and hereditarily at a median age of 42 years (Kinzler and Vogelstein, 1996); about 5 - 15 % of all colorectal cancers are inherited. The most frequent inherited forms are familial adenomatous polyposis (FAP, characterized by germline mutations in the adenomatous polyposis coli (APC) gene) and hereditary nonpolyposis colorectal cancer (HNPCC, characterized by germline mutations in mismatch repair (MMR) genes) (Kinzler and Vogelstein, 1996; Weitz et al., 2005).

FAP and the majority of sporadic colorectal cancers develop via the adenoma-carcinoma sequence proposed by Fearon and Vogelstein (Fearon and Vogelstein, 1990): The pathologic transformation of normal colonic epithelium to benign tumors (called adenoma or adenomatous polyps) and finally invasive tumors (called cancers or carcinomas) requires several years and multiple genetic alterations. Mostly one oncogene (K-ras) and three tumor suppressor genes (APC, SMAD4 and p53) are sequentially genetically altered. Whereas the oncogene K-ras only requires a genetic event in one allele, the tumor suppressor genes require genetic events in both alleles (Kinzler and Vogelstein, 1996) according to Knudson's two-hit hypothesis (Knudson, 1971; Knudson, 1993). The event that triggers the adenoma-carcinoma sequence and thereby leads to the development of malignant cancers is the activation of the Wnt signaling pathway in consequence of mutations in the adenomatous polyposis coli (APC) tumor suppressor gene (reviewed in Smalley and Dale, 2001; Fodde, 2002). According to a current model, wild-type APC binds nuclear β -catenin and exports it to the cytoplasm (Henderson, 2000; Rosin-Arbesfeld et al., 2000), where it is phosphorylated by a complex of various proteins including APC. Phosphorylated β -

catenin becomes ubiquitinated and therefore targeted for degradation by the proteasome (Bienz and Clevers, 2000; Polakis, 1997). Mutations in APC prevent degradation of β -catenin and lead to its accumulation in the nucleus (Kinzler and Vogelstein, 1996). Nuclear β -catenin functions in association with the HMG box protein T cell factor 4 (TCF4) as a transcriptional coactivator and thereby enables the expression of genes controlled by promoters with TCF4 binding sites (Huber et al., 1996; Porfiri et al., 1997), for example, c-MYC (He et al., 1998) and Cyclin D2 (Shtutman et al., 1999; Tetsu and McCormick, 1999). These in turn activate cell proliferation. Furthermore, it has been reported that mutations in APC contribute to chromosomal instability in cancer cells (Fodde et al., 2001; Kaplan et al., 2001).

The subsequent genetic alteration occurring in the adenoma-carcinoma sequence affects the oncogene K-ras. The K-ras gene encodes a membrane-localized G-protein involved in signal transduction critical for normal proliferation. Mutations lead to constitutively activated Ras protein, which is stimulating cell proliferation (Leslie et al., 2002). Proceeding in the adenoma-carcinoma sequence, alterations in the tumor suppressor genes SMAD4 (also known as DPC4) and p53 take place. The SMAD4 protein is a mediator in the inhibitory transforming growth factor β (TGF- β) signaling pathway that suppresses cell growth (Miyaki and Kuroki, 2003). Through inactivation of SMAD4 cells become resistant against TGF- β -mediated growth suppression (Liu, 2001). The tumor suppressor gene p53 was termed as “guardian of the genome” (Lane, 1992), as p53 mediates growth arrest or apoptosis as response to various cellular stresses, like DNA-damage or oncogenic activation (Selivanova, 2004). Inactivation of p53 allows therefore the survival of aberrant cells. p53 is esteemed, for example, to be responsible for the transition from adenoma to carcinoma (Leslie et al., 2002).

In contrast to FAP, HNPCC and about 15 % percent of sporadic colorectal cancers develop as a consequence of mutations in one or more of the three mismatch repair genes hMSH2, hMLH1 and hPMS2, which usually maintaining genetic stability. This in turn leads to an accumulation of mutations amongst others in oncogenes and tumor suppressor genes accelerating tumor progression (Kinzler and Vogelstein, 1996). A marker for mismatch repair deficiency is the incidence of microsatellite

instabilities (MSI), as (frequently occurring) mistakes in the replication of these sequences are not sufficiently corrected (Lynch and de la Chapelle, 2003).

A major obstacle for further profound investigations of colorectal cancers and especially for the developing of successful therapy strategies is the lack of suitable model systems. Primary culture of colorectal carcinoma is difficult, very laborious, and difficult to standardize. In addition, the success rate in establishing cell lines is far below 10 %. Hence, there is an urgent demand for cell culture models that closely reflect the characteristics of *in vitro* tumor cells, which would, in general, facilitate the investigation of cancers and especially development of successful novel therapy strategies.

1.1.2. Human low passage colon cancer cell lines

The demand for colon cancer cell lines that closely reflect the *in vivo* tumor cells triggered efforts in the lab of E. Wagner which recently resulted in the generation of unique human low passage colon cancer cell lines originating directly from the clinic (Vecsey-Semjen et al., 2002). In contrast to other commercially available colon cancer cell lines these cell lines still closely resemble the phenotypes of their corresponding original tumor cells. Only 5 - 10 passages after harvesting the primary tumor cells from the patients were required for the generation of such low passage cell lines. Thereby accumulation of alterations due to long-term cultivation was avoided. On the other hand, this cell lines were stable enough to be continuously cultured, if required.

Eight novel cell lines were established and intensively characterized (Vecsey-Semjen et al., 2002). The established cell lines exhibit widely heterogeneous morphologies and can be divided into three categories of different phenotypic morphologies typical for the original tumor cells: epithelial-like, piled-up and rounded-up (**Fig. 1**). Cell lines that belong to the epithelial-like category (COGA-1, -5, -10) exhibit mainly an epithelial morphology. Piled-up cell lines (COGA-5L, -8, -12) grow preferentially in multilayers: COGA-5L cells, for example, formed ball-like clumps on top of an attached cell layer. Interestingly, COGA-5L cells originate from the same patient as COGA-5 cells, but COGA-5 cells were isolated from the primary tumor, whereas COGA-5L cells were derived from the respective lymph node metastasis. COGA-12

cells grew as multilayer aggregates surrounded by cells growing as single cell layers. Rounded-up cell lines (COGA-2, -3) were loosely attached to the surface of the cell culture dish without forming cell-cell contacts.

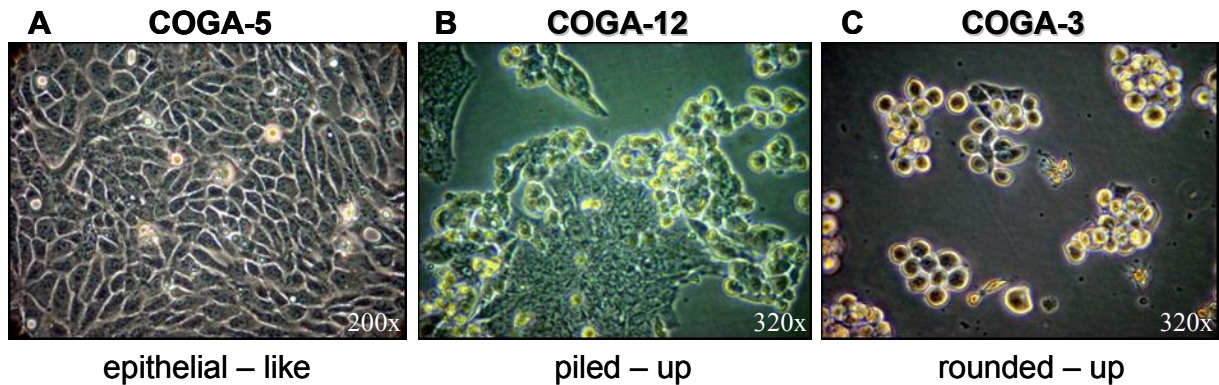


Fig. 1. Different morphologies of the low passage colon cancer cell lines. Epithelial-like (A), piled-up (B) and rounded-up (C) morphologies. Respective magnifications of transmission light microscopy are indicated.

Extensive investigations of the cell lines demonstrated an unexpected diversity of the individual tumor cells regarding, for example, mutations mediating oncogenic and tumor-suppressive effects. Since the established cell lines closely reflected all analyzed features of the corresponding original tumor cells, they are promising *in vitro* model systems for further investigations of colorectal cancers.

1.1.3. Multicellular tumor spheroids

The individual low passage colon cancer cells described above closely reflect the properties of individual *in vivo* tumor cells and are therefore very valuable for the general investigation of colon cancer and the development of novel therapeutic strategies. However, when these cells are grown as traditional monolayer cell cultures, the situation is still different from the three-dimensional growth situation of *in vivo* tumors. Therefore, additional requirements exist for an extended model system that recapitulates the three-dimensional *in vivo* situation of cancers better than monolayer cell cultures. Multicellular tumor spheroid cultures represent such a three-dimensional model system. They are intermediates between monolayer cultures and *in vivo* tumors as they resemble the latter more closely with regard to cell shape and cell environment. A major feature of multicellular spheroids is that they consist of a proliferating cell population at the periphery followed by an intermediate zone with

quiescent, yet viable cells passing into a necrotic or apoptotic core in the center of the spheroid (Mueller-Klieser, 2000), thereby providing a model system closely to *in vivo* tumors. Recent investigations demonstrated that insufficient nutrient and oxygen supply and resultant hypoxia are not or only partly responsible for cell death in multicellular spheroids. Processes leading to cell death in multicellular spheroids besides hypoxia-induced signaling are yet not well understood (Mueller-Klieser, 1997). The higher relevance of multicellular spheroids compared to traditional monolayer cultures was demonstrated for example by Kobayashi and co-workers (Kobayashi et al., 1993). They isolated cells from murine EMT6 tumors exhibiting chemoresistance after treatment of the mice with chemotherapeutic drugs. Monolayer cultures of these cells failed to exhibit chemoresistance, while multicellular spheroids fully recapitulated the chemoresistant phenotype of the respective *in vivo* tumors.

Multicellular spheroids can be generated by preventing the adhesion of cells to the surface of the cell culture dish forcing the cells to develop cell-cell contacts and finally form multicellular spheroids. Adhesion can be prevented by three different methods. The spinner flask method hinders the cells from adhesion to the flask by stirring and the gyratory rotation system by shaking. Inhibition of adhesion by covering of the culture plates with a non-adhesive surface (agar, agarose) is accomplished in the so called liquid overlay technique (Santini and Rainaldi, 1999). This technique results in the formation of multicellular spheroids all with the same defined size and number of cells. Whether a certain cell line will form multicellular spheroids (characterized by the formation of cell-cell interactions) or only multicellular aggregates, is not predictable.

For the reasons listed above it was concluded at the start of this thesis that the low passage colon cancer cells (closely reflecting the original *in vivo* tumor cells) grown as multicellular spheroids (reflecting the three-dimensional growth of *in vivo* tumors) might be very promising model systems for investigation of colon cancers and developing of novel therapy strategies.

1.2. Chemotherapy of colorectal cancer

1.2.1. Chemoresistance against chemotherapeutic drugs

The standard treatment of colorectal cancer is surgery complemented by chemotherapeutic drugs (Macdonald and Astrow, 2001). However, despite advances in therapeutic strategies, the five-year survival period in colorectal cancer patients still remains unsatisfying. One reason is that cancers or their metastases often develop resistance against chemotherapeutic drugs. Chemoresistance can be primary (intrinsic) or secondary (acquired). Primary resistant cancers are not sensitive to a chemotherapeutic drug from the beginning of the treatment, while secondary resistance appears as a consequence of treatment with a chemotherapeutic drug that induced a response at the beginning of the treatment (Hutter and Sinha, 2001). While it is possible to investigate secondary resistance *in vitro* by generation of chemoresistant sublines through long-term treatment with the respective chemotherapeutic drug, primary chemoresistance cannot easily be mimicked with traditional monolayer cultures *in vitro*. The reason for primary chemoresistance is the so called multicellular community effect. This means that primary resistance, in contrast to secondary resistance, is dictated by the collective properties of tumor cell populations rather than by features of the individual tumor cells. Primary resistance is hence mediated by interactions of the tumor cells with each other and with their surrounding microenvironment and is therefore also called multicellular resistance (MCR). Multicellular resistance can be caused as a consequence of cell-cell contacts (contact inhibition resistance) or of the heterogeneous three-dimensional structure of tumors (Desoize and Jardillier, 2000). One possibility to evaluate primary resistance *in vitro* are multicellular spheroids (as described above).

In contrast to primary resistance, secondary resistance is called unicellular resistance. Secondary chemoresistance can be subdivided into typical multidrug resistance (MDR) and atypical resistance. Typical MDR is accomplished by effective efflux of the chemotherapeutic drug by overexpression of P-glycoprotein (Pgp). Pgp (coded by the *mdr-1* gene) is a 170 kDa transmembrane protein belonging to the unspecific ABC transporter family (Kerb et al., 2001; van Tellingen, 2001). Secondary

chemoresistant cells that do not overexpress Pgp are allocated to atypical resistance. Atypical resistance can be mediated by alternative ABC transporters, intracellular detoxification of chemotherapeutic drugs (by glutathione-S-transferases), increased DNA repair, modifications of drug targets or modulation of apoptotic pathways (Hutter and Sinha, 2001).

The various forms of resistance described above must not be seen as independent events; moreover they must be taken together to understand the versatile phenomenon of chemoresistant cancers.

1.2.2. Mechanisms of action of 5-fluorouracil

The standard chemotherapeutic drug used for the treatment of colorectal cancer is 5-fluorouracil (5-FU) (Schmoll et al., 1999). 5-FU is an analogue of uracil with a fluorine atom at the C-5 position in place of hydrogen (**Fig. 2**).

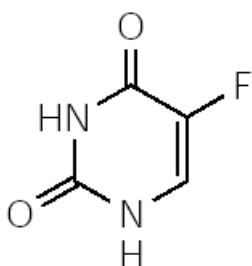


Fig. 2. 5-fluorouracil

It was demonstrated that rat hepatomas utilized the pyrimidine uracil more rapidly than normal tissue (Rutman et al., 1954). 5-FU is taken up into the cells in the same manner as uracil (Wohlhueter et al., 1980) and is intracellularly converted to three main active metabolites: fluorodeoxyuridine monophosphate (FdUMP), fluorodeoxyuridine triphosphate (FdUTP) and fluorouridine triphosphate (FUTP). The cytotoxicity of 5-FU can be ascribed to two distinct mechanisms: The inhibition of the nucleotide synthetic enzyme thymidylate synthase (TS) and the misincorporation of fluoronucleotides into RNA and DNA (reviewed in Longley et al., 2003).

Thymidylate synthase catalyses the reductive methylation of deoxyuridine monophosphate (dUMP) to deoxythymidine monophosphate (dTMP) necessary for the generation of deoxythymidine triphosphate (dTTP). dTTP is essential for DNA replication. The 5-FU metabolite FdUMP forms a stable complex with TS and thereby

inhibits dTMP synthesis, which finally leads to a lack of dTTP. The downstream events are not fully understood. Most likely, the imbalance in the deoxynucleotide pool leads to disruption of DNA synthesis and repair, and consequently to lethal DNA damage.

In addition, the accumulation of dUMP and FdUMP (as a result of TS inhibition) will lead to an accumulation of dUTP and FdUTP, which are both misincorporated into DNA. These misincorporations eventually lead to DNA strand breaks and cell death. Moreover, the 5-FU metabolite FUTP is misincorporated into RNA, leading to disruption of normal RNA processing. This in turn affects cellular metabolism and viability (reviewed in Longley et al., 2003).

Apoptosis is induced via the death receptor pathway in 5-FU treated cells (Kaufmann and Earnshaw, 2000; Eichhorst et al., 2001; Schwartzberg et al., 2002). This pathway is activated by increased levels of Fas and Fas ligand, which are mainly up-regulated by p53 in response to DNA damage (Petak et al., 2000; Petak and Houghton, 2001). In addition, initiation of apoptosis via the mitochondrial pathway may also play a role in 5-FU-induced apoptosis (Backus et al., 2003). It was demonstrated that 5-FU-induced activation of p53 led to upregulation of Bax, a major regulator of the mitochondrial apoptosis pathway (Koshiji et al., 1997; Osaki et al., 1997).

The novel low passage colon cancer cell lines could represent a powerful model system for the investigation of chemoresistance of colorectal cancers. In particular, 5-FU resistant sublines could provide important insights in the mechanisms involved in the development of such resistance against the chemotherapeutic drug.

1.3. Gene therapy of colorectal cancer

Besides solving the problems of chemotherapeutic strategies, alternatives of conventional treatment have to be developed. In particular, gene therapy could provide a powerful alternative to conventional treatment and lead to novel approaches in cancer therapy. Gene therapy, as first proposed 1972 by Friedman and Roblin (Friedmann and Roblin, 1972), aims at the delivery of nucleic acids (DNA or RNA) into target cells in order to cure patients suffering from different diseases. The transferred nucleic acids can be used to turn on or restore a gene function. For example, a therapeutic gene can be expressed ('gain of function'). A relatively new field in gene therapy applies nucleic acids to suppress specific gene functions ('loss of function') by turning off genes with antisense oligonucleotides or double-stranded small interfering RNA (siRNA). Although gene therapy has not yet been established as standard treatment, it was already applied in various clinical studies, e.g. in the field of cancer therapy (most clinical trials), monogenic diseases (Hemophilia A and B, cystic fibrosis, severe combined immunodeficiency syndrome), infectious diseases, vascular diseases, or DNA vaccination (The Journal of Gene Medicine web site, www.wiley.co.uk/genmed/clinical). Gene therapy may hold the potential to revolutionize modern molecular medicine, provided that appropriate nucleic acid delivery systems ('vector systems') are available.

1.3.1. Gene delivery strategies

Current gene therapy vectors can be divided into two major groups, namely viral vectors derived from natural viruses and nonviral, synthetically manufactured vectors. Viruses in general and therefore also viral vectors are highly efficient regarding cellular uptake and intracellular delivery of therapeutic genes to the nucleus. Therefore, few viral particles are sufficient for the transduction of cells. On the other hand, they often cause inflammatory and immune host response and some viral vectors even bear the risk of insertional oncogenesis. Nonviral vectors exhibit only low immunogenicity, since synthetic vectors present far less or no immunogenic proteins or peptides in comparison to viral vectors. An obvious weakness of nonviral vectors, however, is their low efficiency in intracellular nucleic acid delivery which currently is partly compensated by administration of large amounts of the vectors.

Therefore, extensive efforts are necessary to improve the efficiency of nonviral vectors. Nonviral vectors are usually based on chemically defined cationic lipids or cationic polymers and can be generated protein-free or using non-immunogenic human proteins and peptides only. Cationic lipids condensed with DNA are called lipoplexes; cationic polymers that are condensed with DNA are called polyplexes. Lipoplexes and polyplexes became widely used technique for gene delivery both *in vitro* and *in vivo* (Felgner et al., 1987; Godbey et al., 1999; Kircheis et al., 2001; Liu et al., 2003). Despite significant improvements in lipoplex or polyplex formulations, still many obstacles must be overcome (Bally et al., 1999; Godbey et al., 1999; Templeton, 2002). For efficient transfection, the delivery vector must ensure a sufficient uptake into the cell, endosomal release and uptake into the nucleus. For gene delivery *in vivo*, small particles are necessary without specific interactions with biological fluids and non-target cells. The combination of cationic lipids and cationic polymers to form lipopolyplexes can be a very promising approach to enhance gene transfer efficiency of nonviral vectors. It was reported that the synergistic effects of both contribute to their enhanced efficiency (Lampela et al., 2002; Lampela et al., 2003; Lampela et al., 2004; Lee et al., 2003). Furthermore, the delivery vector should guarantee a highly specific cell targeting and expression for *in vivo* applications.

1.3.2. Tumor specific cell targeting strategies

Tumor specific gene transfer can be achieved by modifying gene transfer vectors in a way that they only target tumor cells but not other cells. This is, for example, possible by integration of ligands into the vectors, which are preferentially taken up by tumor cells. Such ligands are, for example, transferrin or EGF. Another strategy is transcriptional targeting by tumor specific gene expression mediated through tumor specific promoters (Miller and Whelan, 1997). Several approaches have been made to develop such promoters. Albeit most of them enabled tumor specific expression, they only led to inadequate expression levels (Nettelbeck et al., 1998). Lipinski and co-workers (Lipinski et al., 2004) recently developed a promising new promoter, CTP4, which is specific for tumors with constitutively activated Wnt signaling pathway. The activation of this pathway leads to nuclear accumulation of β -catenin. In association with the HMG box protein T cell factor 4 (TCF4), nuclear β -catenin

enables the expression of genes controlled by promoters with TCF4 binding sites (Huber et al., 1996; Porfiri et al., 1997). The artificial CTP4 promoter contains ten such TCF4 binding sites (**Fig. 3**), which make the CTP4 promoter very specific for tumor cells with deregulated levels of β -catenin such as most colorectal carcinomas. In addition, it was demonstrated that the CTP4 promoter enabled expression levels comparable to expression levels obtained by the strong but non-tissue-specific human cytomegalovirus immediate early enhancer/promoter (CMV) in the colorectal cancer cell line SW480 (Lipinski et al., 2004). Therefore, it would be very interesting to investigate the efficiency of the CTP4 promoter also in the various low passage colon cancer cell lines exhibiting widely heterogeneous properties.

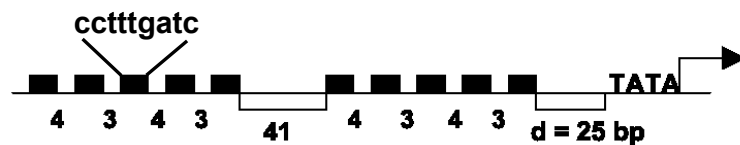


Fig. 3. Composition of the CTP4 promoter. Numbers indicate the base pairs between the TCF4 binding sites (filled boxes) and the distance from the end of the most proximal site to the start of the TATA box (adapted from Lipinski et al., 2004).

1.3.3. Therapeutic genes

Tumor specific vector systems enable the delivery of therapeutic genes into cancer cells. A promising approach is the delivery of genes that encode immune stimulatory factors. These in turn activate the immune system against the tumor cells. Therefore, also tumor cells that have not been transfected and do not express the therapeutic gene can be eliminated. Interleukin-2 (IL-2) was already reported as an effective immune stimulatory factor in immunotherapy studies (Rosenberg et al., 1985; Huland and Huland, 1989). This cytokine provides the stimulatory signal necessary for the activation of the tumor defense effectors, T and NK lymphocytes (Bubenik, 2004) or macrophages (Zatloukal et al., 1995). However, the systemic application of high IL-2 protein amounts often exhibits side effects, like capillary leakage syndrome or hepato- and nephrotoxicity (Bubenik, 2004). Therefore, the selective application of IL-2 to the tumors via gene therapy is a promising alternative to avoid these side effects. Another cancer gene therapy approach is the expression of cytotoxic genes in tumor cells that, for example, lead to death of the transfected individual tumor cells. However, if the particular cytotoxic gene does not exhibit a so called bystander effect, only the transfected cells will be eliminated. Bystander effect means that the

therapeutic gene product also acts on cells surrounding the transfected cell. Therapeutic gene transfer without such bystander effects is insufficient, since the extent of gene transfer is often low. This problem can be circumvented by simultaneously expression of an immune stimulatory gene in addition to the cytotoxic gene. The efficiency of such a combination gene therapy with suicide and cytokine genes could already be demonstrated by combining IL-2 with herpes simplex virus thymidine kinase. This enzyme phosphorylates the prodrug ganciclovir (9-[(2-hydroxy-1-(hydroxymethyl)ethoxy)methyl]guanine) (Moolten, 1986) and such activated ganciclovir is highly toxic to dividing cells (Kwong et al., 1997; Pizzato et al., 1998). Recently another bicistronic construct was generated, named 2A-IRES-IL2 (Kisser, 2003). 2A-IRES-IL2 combines sequences encoding the rhinovirus protease 2A and IL-2. Rhinoviruses use protease 2A for shutdown of host cell biosynthesis after infection. The major substrate of the protease 2A is the translation initiation factor eIF4G (Lloyd et al., 1988; Seipelt et al., 1999). By cleaving of eIF4G cellular, cap-dependent translation becomes impossible. At the same time the biosynthesis of viral proteins is guaranteed by IRES (internal ribosomal entry site) mediated, cap-independent translation. Thus, heterologous expression of the protease 2A via the 2A-IRES-IL2 construct will prevent cap-dependent translation of cellular mRNAs and therefore reduce viability and proliferation of the transfected cells. Simultaneously, an IRES sequence located upstream of the IL-2 encoding sequence enables cap-independent translation of the IL-2 mRNA. Therefore, efficient expression of the immune stimulatory gene is guaranteed although expression of other cellular genes is reduced by the protease 2A. It has already been demonstrated that transfection of the 2A-IRES-IL2 construct leads to sufficient expression of IL-2 in addition to protease 2A expression. For easy monitoring of protease 2A expression the gene has been fused with the gene encoding enhanced green fluorescent protein (EGFP) in the 2A-IRES-IL2 construct. It was also demonstrated that the expressed protease 2A is active, as cleaved eIF4G could be detected by western blotting (Kisser, 2003). However, the evaluation of reduced viability or proliferation levels in the 2A-IRES-IL2 transfected cells failed so far. Therefore, it would be interesting to test this novel therapeutic gene construct in the low passage human colon cancer cell lines.

1.4. Specific aims of the PhD thesis

For development of drugs against colorectal cancer i) the provision of suitable cell model systems, ii) the elucidation of mechanisms limiting the efficiencies of existing therapeutic strategies with the objective to find adequate solutions to overcome these limitations, and iii) the development of novel therapeutic strategies are important issues. These issues have been the basis for the aims of the thesis.

1.4.1. Initiation and characterization of relevant model systems for colorectal cancers

As a first aim, suitable cellular model systems had to be established and characterized for the evaluation of colorectal cancer specific therapeutic strategies. The recently generated low passage colon cancer cells, reflecting the characteristics of the corresponding original tumor cells (Vecsey-Semjen et al., 2002), were used as a starting point. Besides traditional monolayer cultures, multicellular spheroid cultures were established with these cells to obtain even more relevant model systems. It has been reported that multicellular spheroids exhibit different characteristics compared to the corresponding monolayer cultures, such as, for example, higher resistance against chemotherapeutic drugs. Therefore, in this thesis differences between monolayer cultures and multicellular spheroids were characterized on the level of total protein expression. To this end, a proteomics approach using 2D electrophoresis followed by protein detection via mass spectrometry was applied.

1.4.2. Elucidation of mechanisms involved in resistance of colorectal cancers against chemotherapy

The chemotherapeutic drug 5-FU is the standard in the treatment of colorectal cancers. A major problem, however, is that treated cells often develop resistance against 5-FU. Hence, the second aim of this thesis was the detection of proteins associated with chemoresistance against 5-FU. Knowledge of the proteins that are involved in mediating 5-FU chemoresistance can lead to the development of successful therapeutic strategies to overcome chemoresistance. At first, chemoresistant sublines of the low passage colon cancer cells had to be generated. Afterwards differences in the protein expression profiles between 5-FU sensitive and

resistant sublines should be investigated by 2D electrophoresis. Such differences in protein expression may contribute to chemoresistance against 5-FU. Moreover, the differences in the expression profiles found between multicellular spheroids and monolayer cultures could be associated with intrinsic chemoresistance.

1.4.3. Development of alternative therapy strategies for colorectal cancers

Since the available established colorectal cancer therapies are dealing with several limitations, alternative therapeutic strategies have to be developed. A promising alternative is represented by colorectal cancer specific gene therapy. The third aim of this thesis was therefore the development of a novel tumor specific gene therapy concept that combines novel strategies for (i) gene transfer, (ii) cancer cell targeting and (iii) therapeutic treatment of cancer cells. Therefore, different lipopolyplex formulations of reporter gene DNA constructs were generated and their efficiencies in gene transfer were investigated using the novel colon carcinoma models. Tumor specificity, that was necessary for an *in vivo* application of these novel gene transfer vectors, was obtained by using the artificial promoter CTP4. The efficiency and specificity of such tumor specific transcriptionally targeted gene transfer vectors containing the CTP4 promoter was compared to corresponding unspecific vectors containing the CMV promoter. Finally, the expression of the immune stimulatory gene IL-2 alone or in combination with the cytotoxic gene protease 2A and the influence of the latter on the proliferation or viability of the transfected cells was investigated. Transfer of the therapeutic genes was accomplished with the tumor specific gene transfer vectors (transcriptionally targeted lipopolyplexes) developed within the scope of this thesis. This novel gene therapy concept was evaluated on traditional monolayer cultures of the low passage colon cancer cell lines and also on multicellular spheroids of these cells.

2. Material and methods

2.1. Chemicals and reagents

Multivalent non-biodegradable cationic lipid DOSPER and monovalent cationic lipid DOTAP were obtained from Roche (Mannheim, Germany). Multivalent biodegradable cationic lipid DOCSPER was 1,3-dioleoyloxy-2-(N5-carbamoyl-spermine)-propane (Groth et al., 1998). Linear PEI (PEI22lin) with an average molecular weight of 22 kDa was achieved from Euromedex (Exgen 500, Euromedex, Souffelweyersheim, France). Branched PEIs (PEI2k and PEI25br) with an average molecular weight of 2 kDa and 25 kDa were obtained from Sigma-Aldrich (Vienna, Austria). PEIs were used at a 1 mg/ml stock solution, neutralized with HCl. PLL18 (18 lysine residues) was synthesized by Dr. Arnold (Gene Centrum, Munich, Germany) and was used at a concentrations of 5 mg/ml.

Plasmid pCMV-Luc (Photinus pyralis luciferase under control of the CMV promoter/enhancer) described in Plank et al. (1992) was produced endotoxin-free by Elim Biopharmaceuticals (San Francisco, CA, USA) or Aldevron (Fargo, ND, USA). Plasmid pEGFP-N1 (encoding enhanced green fluorescent protein (EGFP) under the control of the CMV promoter/enhancer) and pEGFP-Luc (encoding a fusion of EGFP and luciferase under the control of the CMV promoter/enhancer) were purchased from Clontech Laboratories, Inc. (Palo Alto, CA, USA). Further, pCTP4-Luc (encoding luciferase under the control of the CTP4 promoter) (Lipinski et al., 2004), p2A-IRES-IL2 (encoding rhinoviral protease 2A and simultaneously human interleukin-2 under the control of the CMV promoter/enhancer) (Kisser, 2003) and pGShIL-2tet (encoding the human interleukin-2 protein under the control of the CMV promoter/enhancer) (Buschle et al., 1995; Schreiber et al., 1999) were used and amplified endotoxin-free using an EndoFree Plasmid Maxi Kit (Qiagen, Hilden, Germany) according to manufacturer's instructions in our lab.

2.2. Molecular biological methods

2.2.1. Restriction digestion of plasmid DNA

Plasmid DNA was incubated 1 - 3 h with 3 - 5 units of the desired restriction enzymes (Promega, Mannheim, Germany) per μg DNA in the appropriate restriction enzyme buffer according to manufacturer's instructions. Success of digestion was tested by agarose gel electrophoresis.

2.2.2. Dephosphorylation of plasmid DNA fragments

Digested plasmid DNA fragments were dephosphorylated directly in the restriction enzyme buffer by adding 2 - 3 units shrimp alkaline phosphatase (Promega, Mannheim, Germany) per μg DNA and incubation for 45 minutes at 37°C. Dephosphorylation was stopped by incubation at 65°C for 15 minutes.

2.2.3. Converting of 5'-overhangs of DNA fragments to blunt ends

5'-overhangs of digested (and if desired dephosphorylated) plasmid DNA fragments were filled to blunt ends directly in the restriction enzyme buffer by adding 1 unit Klenow fragment (Promega, Mannheim, Germany) per μg DNA, 40 μM of each dNTP and 50 $\mu\text{g/ml}$ acetylated BSA. Reaction was carried out for 10 minutes at RT and the reaction was stopped by incubation at 75°C for 10 minutes.

2.2.4. Isolation of DNA fragments from agarose gels

DNA fragments were excised from agarose gels with a clean, sharp scalpel. The following extraction and cleaning was performed with the QIAquick Gel Extraction Kit (Qiagen, Hilden, Germany) according to the manufacturer's instructions.

2.2.5. Ligation

A molar ratio of 1:3 of vector DNA (100 ng) and fragment DNA was used for sticky end ligations, for blunt end ligations a molar ratio of 1:5 was used. Ligations were carried out using 1 – 3 units T4 DNA ligase (Roche, Mannheim) in ATP containing ligation buffer in a final volume of 15 μl – 30 μl . Sticky end ligations were incubated at

16°C overnight. Blunt end ligations were incubated at 16°C for 3 h and subsequently at RT overnight.

2.2.6. Transformation of E.coli

Competent E.coli cells (DH5 α or JM109) were thawed on ice. 50 – 200 ng DNA were mixed with 100 μ l bacteria suspension and incubated on ice for 30 minutes. The competent E.coli cells were then heat-pulsed at 42°C for 90 seconds and subsequently incubated on ice for 2 minutes. 0.9 ml of LB-medium were added prior incubation at 37°C for 1 h with shaking. 10 – 300 μ l were spread on antibiotic (ampicillin or kanamycin) agar plates and incubated at 37°C overnight.

2.2.7. Preparation of plasmid DNA

All plasmid DNA preparations were carried out with QIAprep Spin Miniprep Kit or EndoFree Plasmid Maxi Kit (Qiagen, Hilden, Germany) according to the manufacturer's instructions.

2.2.8. Cloning strategies

pEGFP-LG-CTP4 (encoding EGFP under the control of the CTP4 promoter) was constructed by substitution of the CMV promoter of pEGFP-N1 by the CTP4 promoter from pCTP4-Luc (Lipinski et al., 2004). First, a fragment containing the CMV promoter was removed from pEGFP-N1 by cleaving the plasmid with Ase I and Eco47 III. The cohesive ends originating from the digestion by Ase I were converted to blunt ends by Klenow polymerase prior to religation of the vector, leading to the plasmid pEGFP-N1-0. Finally a Sac I - Bgl II digested fragment of the pCTP4-Luc plasmid, containing the CTP4 promoter, was inserted into the Sac I – BamH I restrictions sites of the MCS of the pEGFP-N1-0 plasmid.

pCTP4-hIL-2 (encoding IL-2 under the control of the CTP4 promoter) was constructed by replacement of the luciferase gene of pCTP4-Luc against the hIL-2 gene from pGShIL-2tet (Buschle et al., 1995; Schreiber et al., 1999). The luciferase gene was removed by digestion with Bgl II and BamH I and the Bgl II - Not I digested hIL-2 gene from pGShIL-2tet was inserted into the dephosphorylated vector. Both the

vector and the insert were converted to blunt ends prior to insertion using Klenow polymerase.

pCTP4-2A-IRES-IL2 (encoding the 2A-IRES-IL2 sequence under control of the CTP4 promoter) was constructed by inserting a fragment containing the 2A-IRES-IL2 sequence and a fragment harboring the CTP4 promoter into the pEGFP-N1-0 vector (created during the construction of pEGFP-LG-CTP4). The EGFP gene was removed from pEGFP-N1-0 by digestion with Sac I and Not I. The fragment containing the CTP4 promoter was excised from pCTP4-Luc by digestion with Sac I and Pst I and the 2A-IRES-IL2 sequence was excised from p2A-IRES-IL2 (Kisser, 2003) by digestion with Pst I and Not I. The fragments containing the CTP4 promoter and the 2A-IRES-IL2 sequence were inserted into the restriction sites Sac I and Not I of the pEGFP-N1-0 vector in a single ligation reaction. As the thereby generated pCTP4-2A-IRES-IL2 plasmid was smaller than the p2A-IRES-IL2 plasmid (containing the CMV promoter), additionally, a plasmid was created that has nearly the same size as pCTP4-2A-IRES-IL2 and is harboring the 2A-IRES-IL2 sequence under control of the CMV promoter. Therefore, the EGFP gene was removed from the plasmid pEGFP-N1 (containing the CMV promoter) by digestion with Pst I and Not I and the Pst I - Not I digested fragment from p2A-IRES-IL2 harboring the 2A-IRES-IL2 sequence was inserted into it, resulting in the plasmid pCMV-2A-IRES-IL2, similar to the plasmid pCTP4-2A-IRES-IL2 besides its promoter region.

2.3. Cell biological methods

2.3.1. Cell culture

Cell culture media, antibiotics and fetal calf serum (FCS) were purchased from Invitrogen (Karlsruhe, Germany). All cultured cells were grown at 37° C in 5 % CO₂ humidified atmosphere. HeLa (ATCC CCL-2, cervix epithelial adenocarcinoma, non-colorectal cells) and SW480 (ATCC CCL-228, human colorectal adenocarcinoma cells) cells were grown in DMEM medium, supplemented with 10 % serum. Human low passage colon carcinoma cells COGA-1, COGA-2, COGA-3, COGA-5, COGA-5L, COGA-10 and COGA-12 (Vecsey-Semjen et al., 2002) were cultured in RPMI 1640 medium containing 10 % serum. These cells are originating directly from

colorectal cancers in the clinic. All cells were cultured in T25 or T75 flasks purchased from Corning Incorporated (Corning, NY, USA) or various well plates purchased from TPP (Trasadingen, Switzerland). Harvesting of the cells was performed as followed: The cells were shortly washed with 0.05 % trypsin/0.02 % EDTA in PBS solution (Invitrogen, Karlsruhe, Germany) and subsequently incubated with fresh trypsin/EDTA solution at 37°C. After the detachment of the cells trypsin was inhibited by addition of serum containing growth medium. EDTA was removed by centrifugation at 180 g to 500 g and subsequently uptake of the cell pellet in fresh growth medium.

2.3.2. Multicellular spheroid culture

Multicellular spheroids were generated as previously described (Lieubeau-Teillet et al., 1998), using the liquid overlay technique. This technique prevents the cells from growing on the surface of the culture plates and the cells are thereby forced to interact with each other and finally form multicellular spheroids. Briefly, 24-well culture plates (Nalge Nunc International, Naperville, IL, USA) were coated with 300 µl of 1 % SeaPlaque agarose (Biozym, Hess, Germany) in serum-free growth medium. Cells from a single-cell suspension were added at 10^5 per well in a total volume of 1 ml growth medium with 2 % or 10 % serum. Multicellular spheroids were allowed to form over 48 h or 96 h. Multicellular spheroids are resistant against mechanical disruption. If they do not exhibit resistance against mechanical disruption they are not considered as multicellular spheroids but rather as multicellular aggregates.

2.3.3. Formation of transfection complexes

Different cationic lipids (DOCSPER, DOSPER, DOTAP) and/or polycations (PLL18, PEI22lin, PEI25br, PEI2k) were mixed with DNA to form various lipoplex, polyplex or lipopolyplex formulations. The mixing was performed either in low ionic strength solution (water) or in physiological solution (HBS; 150 mM NaCl, 20 mM HEPES, pH 7.4) as described below.

Lipopolyplexes were prepared as follows: first plasmid DNA was diluted in water or HBS at DNA concentrations ranging from 2.5 to 20 µg/ml. For cotransfection assays equal amounts of two different plasmids were mixed together in the same tube.

Immediately, polycations were added at optimized molar ratios of PEI nitrogen/DNA phosphate (N/P) of 8/1 or a charge ratio of PLL18/DNA of 5/1 (Pelisek et al., 2005) and incubated at room temperature for 5 - 10 min. Cationic lipids were diluted in similar manner in a separate tube, added to the DNA/polycation pre-complexes at optimized w/w ratios of DOCSPER/DNA of 10/1, DOSPER/DNA of 8/1 and DOTAP/DNA of 4/1 (Pelisek et al., 2005) and incubated at room temperature for 30 – 40 min.

Lipoplexes were prepared as described before (Pelisek et al., 2002). In brief, the cationic lipids and the plasmid DNA were diluted at the same ratios as described above in separate tubes in water or HBS, mixed together and incubated for 30 – 40 min at room temperature. Polyplexes were prepared in the same way (Kursa et al., 2003) at molar ratios as described above.

Lipofectamine 2000 (Invitrogen, Karlsruhe, Germany) containing complexes were prepared according to the manufacturer's instructions. Briefly, plasmid DNA and Lipofectamine 2000 at a DNA (in μg)/Lipofectamine 2000 (in μl) ratio of 2:3 were diluted in separate tubes in Opti-MEM (Invitrogen, Karlsruhe, Germany) at a DNA concentration of 20 $\mu\text{g}/\text{ml}$, mixed together and incubated for 30 min at room temperature.

2.3.4. Measurement of particle size and zeta-potential

Particle size was measured by dynamic laser-light scattering using a Malvern Zetasizer 3000HS (Malvern Instruments, Worcestershire, UK). For particle sizing complexes were prepared as for gene transfer and diluted either in low ionic strength solution (water) or in physiological solution (HBS) to give a final DNA concentration of 5 $\mu\text{g}/\text{ml}$. For estimation of the zeta-potential, transfection complexes were diluted in 10 mM NaCl and the particle charge was determined. The data represent the mean of at least three measurements.

2.3.5. Gene transfer to monolayer cultures

For luciferase assays 0.5 - 2 x 10⁴ cells were seeded in 96-well plates; for IL-2 detection and EGFP analysis 0.5 - 2 x 10⁵ cells were seeded in 24-well or 12-well plates; for proliferation assays with protease 2A 0.5 - 1 x 10⁴ cells were seeded in 96-

well plates and for analysis of protease 2A-mediated apoptosis $1 - 2 \times 10^5$ cells were seeded in 24-well or 12-well plates 24 hours prior transfection. The growth medium was removed and replaced with 50 μ l (96-well), 200 μ l (24-well) or 400 μ l (12 well) of serum-free medium or medium containing 10 % FCS. Transfection complexes (96-well: 20 μ l, 0.1 μ g plasmid DNA; 24-well: 50 μ l, 0.25 μ g - 1 μ g DNA; 12-well: 100 μ l, 0.25 μ g - 1 μ g DNA) were then added drop-wise to each well. 4 hours following incubation at 37°C/5 % CO₂, transfection medium was replaced by 100 μ l (96-well), 600 μ l (24-well) or 1 ml (12-well) of fresh growth medium. Gene transfer was performed in two to five wells/group and experiments were at least repeated twice.

2.3.6. Gene transfer to multicellular spheroids

Multicellular spheroids were grown in 1 ml medium containing 10 % serum or in serum-reduced (2 %) medium to enhance transfection efficiency. Transfection was performed directly in the growth medium to avoid disturbance of the spheroids. Forty-eight or 96 h after multicellular spheroid formation 700 μ l of growth medium were removed of each well and lipopolyplex formulation, diluted in a small volume (50 μ l), was added to the multicellular spheroid cultures. Transfection medium was not exchanged after transfection.

2.3.7. Luciferase assay

Twenty-four hours following gene transfer, medium was removed and the cells were washed with phosphate-buffered saline. The cells were then lysed with 50 μ l of lysis buffer (25 mM Tris, pH 7.8, 2 mM EDTA, 2 mM DTT, 10 % glycerol, 1 % Triton X-100) and 30 min later the luciferase activity was measured using a Lumat LB9507 instrument (Berthold, Bad Wildbad, Germany) as described recently (Ogris et al., 2001). In brief, luciferase light units were recorded from an aliquot of the cell lysate with 10 s integration after automatic injection of freshly prepared luciferin substrate solution using the Luciferase Assay system (Promega, Mannheim, Germany). Luciferase activity was measured in triplicates and the relative light unit (RLU) were determined per 1×10^4 cells. 10^7 light units correspond to two ng of recombinant luciferase (Promega, Mannheim, Germany).

2.3.8. Human IL-2 ELISA

Twenty-four hours after transfection growth medium was replaced by fresh medium. Forty-eight hours after transfection the supernatants were collected and stored at -80°C until IL-2 ELISA was performed. Human IL-2 expression was determined using a human IL-2 ELISA kit (Bender MedSystems, Vienna, Austria) according to the manufacturer's instructions.

2.3.9. Treatment of cells with 5-fluorouracil

The treatment with different concentrations of 5-fluorouracil (Sigma-Aldrich, Taufkirchen, Germany) was performed with 1.5×10^4 cells per well in 96 well plates in the case of COGA-5L and COGA-12 cells and 0.4×10^4 cells per well in the case of COGA-5 cells. For the determination of the percentage of apoptotic cells 28×10^4 COGA-12 cells per well in 12 well plates were used. Growth medium was replaced with fresh medium every day, to ensure constant concentration of 5-FU. For long-term (> one week) 5-FU incubations medium was exchanged 3 times per week.

5-FU was dissolved in DMSO. To exclude effects resulting from DMSO also control cells used for comparison were incubated with the same amount of DMSO as the 5-FU-treated cells received.

2.3.10. Proliferation and viability assays

2.3.10.1. Hoechst 33258-based proliferation assay

Cells were cultured in black 96 well-plates with transparent bottom (Greiner-Bio One, Frickenhausen, Germany). At the desired endpoint growth medium was removed and the 96 well-plate was frozen at -80°C . After thawing, 100 μl distilled water were added per well and the plate was incubated at 37°C for 1 hour. The plate was frozen to -80°C and thawed again. This procedure causes rapid cell lysis, resulting in release of DNA to form a relatively homogenous solution. 100 μl of 2 x TNE Buffer (5 M NaCl, 20 mM Tris, 2 mM EDTA, pH 7.4) containing 2 $\mu\text{g/ml}$ Hoechst 33258 (Sigma-Aldrich, Taufkirchen, Germany) were added and fluorescence was measured in a SPECTRAFluor Plus plate reader (Tecan, Austria) using excitation and emission filters centered at 360 nm and 465 nm, respectively.

2.3.10.2. MTT assay

Cells were cultured in 200 µl growth medium in 96 well-plates. At the desired endpoint 20 µl of MTT solution (5mg/ml in PBS) were added and cells were incubated 1 h – 4 h at 37° C in 5 % CO₂ humidified atmosphere. After forming of blue crystals cell culture medium was removed and crystals were solubilized by adding 100 µl DMSO. Absorbance was measured at a primary wave length of 590 nm and a reference wave length of 630 nm in a SPECTRAFluor Plus plate reader (Tecan, Austria).

2.3.11. Flow cytometric analysis

2.3.11.1. Flow cytometric analysis of EGFP expression

Forty-eight hours after transfection cells were harvested after incubation with trypsin/EDTA solution and kept on ice until analysis. The DNA stain propidium iodide (PI) (Sigma-Aldrich, Taufkirchen, Germany) was added to the cell suspension at 1 µg/ml to discriminate between viable and dead cells. PI only penetrates the nucleus after cell membrane integrity is lost. The number of dead cells and EGFP-positive cells was quantified using a CyanTM MLE flow cytometer (DakoCytomation, Copenhagen, Denmark). PI and EGFP fluorescence were excited at 488 nm. Emission of PI fluorescence was detected using a 613±20 nm bandpass filter. Dead cells were excluded by gating PI-positive cells by forward scatter versus PI fluorescence. Emission of EGFP was detected using a 530±40 nm bandpass filter and a 613±20 nm bandpass filter to analyze EGFP positive cells by diagonal gating (Ogris et al., 1998). To exclude cell debris and doublets, cells were appropriately gated by forward versus side scatter and pulse width, and 2 x 10⁴ gated events per sample were collected. Furthermore, the geometric mean channel number as measure for the mean fluorescence intensity (MFI) of a EGFP-positive cell population was determined.

2.3.11.2. Flow cytometric analysis of apoptosis

Apoptotic cells were detected by labeling of apoptotic cells with annexin V and following flow cytometry. Annexin V binds to phosphatidylserine in presence of calcium. At the onset of apoptosis, phosphatidylserine which is normally found on the

internal part of the plasma membrane becomes translocated to the external portion of the membrane and thereby available to bind to annexin V (van Engeland et al., 1998).

Cells were harvested 48 or 72 hours after transfection or beginning of the treatment by using trypsin/EDTA, washed once in PBS and resuspended in annexin V binding buffer (Sigma-Aldrich, Taufkirchen, Germany or BioVision, Mountain View, CA, USA) at a concentration of approximately 1×10^6 cells/ml. The DNA stain propidium iodide (PI) and annexin V-FITC (Sigma-Aldrich, Taufkirchen, Germany) or annexin V-Cy5 (BioVision, Mountain View, CA, USA) were added at 1 μ g/ml each and incubated for 10 min at RT. Following apoptotic and necrotic cells were determined using a Cyan™ MLE flow cytometer (DaKoCytomation, Copenhagen, Denmark). Annexin V-FITC fluorescence was excited at 488 nm and emission was detected using a 530 \pm 40 nm bandpass filter. Annexin V-Cy5 fluorescence was excited at 633 nm and emission was detected using a 680 \pm 30 nm bandpass filter. PI fluorescence was excited at 356 nm or 488 nm and emission was detected using a 700 \pm 20 nm or 575 \pm 25 nm bandpass filter, respectively. To exclude cell debris and doublets, cells were appropriately gated by forward versus side scatter and pulse width, and 2×10^4 gated events per sample were collected. Cells which are early in the apoptotic process will be stained with annexin V alone. Living cells will not show staining by neither annexin V nor PI. Necrotic cells will be stained by both annexin V and PI, as PI only penetrates the nucleus after cell membrane integrity is lost.

2.3.12. Transmission light and epifluorescence microscopy

Transmission light microscopy of living cells growing as monolayers or multicellular spheroids was performed using an Axiovert 200 microscope (Carl Zeiss, Jena, Germany) equipped with a Sony DSC-S75 digital camera (Sony Corporation, Tokyo, Japan). Light was collected through 5 x 0.12 NA, 10 x 0.25 NA or 32 x 0.40 NA objectives (Carl Zeiss, Jena, Germany), and images were captured using phase contrast.

Living or 4 % PFA (para-formaldehyde) fixed cell imaging of EGFP expressing cells was performed 48 h after transfection using an Axiovert 200 fluorescence microscope (Carl Zeiss, Jena, Germany) equipped with a Zeiss Axiocam camera.

Light was collected through a 5 x 0.12 NA or a 10 x 0.25 NA objective (Carl Zeiss, Jena, Germany). EGFP fluorescence was excited using a 470±20 nm bandpass filter, and emission was collected using a 540±25 nm bandpass filter. Digital image recording and image analysis were performed with the Axiovision 3.1 software (Carl Zeiss, Jena, Germany).

2.3.13. Confocal laser scanning microscopy of multicellular spheroids

Multicellular spheroids were transferred to Lab-Tek 8 chambered coverglasses (Nalge Nunc International, Naperville, IL, USA) and fixed in 4 % PFA for 30 – 60 min. For counterstaining cells were incubated with DAPI (4',6-Diamidino-2-phenylindole) at a concentration of 1 µg/ml in PBS for 15 min. Imaging of EGFP expression of transfected multicellular spheroids was performed 48 h after transfection using a confocal laser scanning microscope (LSM 510 Meta, Carl Zeiss, Jena, Germany) equipped with an UV and an argon laser delivering light at 364 nm and 488 nm, respectively. Light was collected through a 10 x 0.3 NA objective (Carl Zeiss, Jena, Germany). DAPI fluorescence was excited with the 364 nm line; emission was collected using a 385 nm long-pass filter. Excitation of EGFP fluorescence was achieved by using the 488 nm line, with the resulting fluorescent wavelengths observed using a 505 nm long-pass filter. No signal overspill between the individual fluorescence channels was observed. An optical section thickness of 10 µm was chosen. Digital image recording and image analysis were performed with the LSM 5 software, version 3.0 (Carl Zeiss, Jena, Germany).

2.3.14. Cryosections of multicellular spheroids

Multicellular spheroids were transferred to a 48-well plate prior fixation in 4 % PFA for 2 h at 4°C. Subsequently the multicellular spheroids were incubated in 30 % sucrose (in water) over night at 4°C. The fixed multicellular spheroids were then embedded in tissue freezing medium (Leica Microsystems, Nussloch, Germany) and frozen at -20°C. Cryosections were made using a Leica CM3050S cryostat (Leica Microsystems, Nussloch, Germany) with a section thickness of 10 µm. Sections were transferred to SuperFrost microscope slides (Menzel, Braunschweig, Germany) prior to analysis by epifluorescence microscopy.

2.4. 2D Electrophoresis and MALDI-TOF mass spectrometry

2.4.1. Sample preparation

Cells grown as monolayers were harvested by treatment with trypsin/EDTA, washed with 40 ml PBS and 40 ml of 0.5 x PBS (to reduce salt concentration) in a Greiner tube, resuspended in 1 ml 0.5 x PBS and transferred to an Eppendorf tube. Washing solution was quantitatively removed by centrifugation prior adding of 460µl 2D-lysis-buffer (9 M Urea, 5 mM EDTA, 4 % CHAPS, 1 % DTE). Cells were lysed for 15 minutes. All centrifugation steps were carried out at 500 g for 10 min.

Multicellular spheroids were transferred directly into 40 ml PBS provided in a Greiner tube, washed twice with 0.5 x PBS and lysed for 15 minutes directly in the Greiner tube after quantitative removal of washing solution. All centrifugation steps were carried out at 500 g for 5 min with subsequently removal of the solution by aspiration.

Cell lysates were homogenized by centrifugation at 17.500 g in a QIAshredder Homogenizer (Qiagen, Hilden, Germany) for 2 minutes. After the following centrifugation at 17.600 x g for 30 minutes supernatants were transferred into fresh Eppendorf tubes. Samples were stored at -80°C.

2.4.2. Measurement of protein concentration

The concentration of protein samples was measured with the BIO-RAD protein assay (BIO-RAD, Munich, Germany) according to the manufacturer's instructions. Samples were diluted 1:2, as the assay only tolerates 6 M urea. BSA was used for the protein standard curve and was therefore diluted in urea 2D-lysis-buffer.

2.4.3. First dimension: Isoelectric focusing

In the first dimension proteins were separated according to their isoelectric point. Isoelectric focusing (IEF) was carried out by using an Ettan IPGphor Isoelectric Focusing System (Amersham Biosciences, Uppsala, Sweden) according to the manufacturer's instructions. Briefly, protein samples (containing 200 µg protein) were mixed with 3 µl IPG-Buffer of the appropriate pH and 2 µl of 3 mM bromophenol blue in resolving buffer (1.5 M Tris, 0.4 % SDS, pH 8.8) and were filled up to a final volume of 460 µl with 2D-lysis-buffer. The total solution was dispensed over the Ettan

IPGphor strip holder, a 24 cm pH 4 - 7 IPG DryStrip gel was applied and finally covered with 1 – 1.5 ml DryStrip Cover Fluid to prevent evaporation of the sample solution. Ettan IPGphor strip holders were placed on the top of the Ettan IPGphor platform and IEF was carried out according to the protocol shown in **Table 1**. Focusing took about 30 h at 20°C and 50 μ A/strip, until in total 90 kVh were reached. Focused IPG DryStrip gels were stored at -80°C. IPG DryStrip gels and all materials used for IEF were purchased from Amersham Biosciences (Uppsala, Sweden).

Step	Voltage (V)	Step Duration (h:min)
Rehydration	0	0:10
1 Step – n – hold	30	8:00
2 Step – n – hold	50	4:00
3 Step – n – hold	200	2:00
4 Step – n – hold	500	2:00
5 Step – n – hold	2000	2:00
6 Step – n – hold	4000	2:00
7 Gradient	8000	1:00
8 Step – n – hold	8000	8:00 – 12:00

Table 1. Running conditions for isoelectric focusing. “Step-n-Hold” sets the voltage at the selected value for the new step and then holds the voltage constant for the step duration. “Gradient” increases the voltage limit linearly with respect to time from the value set for the previous step to the value set for current step.

2.4.4. Second dimension: SDS-page

In the second dimension proteins were separated according to their molecular weight. Second dimension gel electrophoresis was carried out by using an Ettan DALTtwelve System (Amersham Biosciences, Uppsala, Sweden). First IPG DryStrip gels were equilibrated in equilibration buffer (6 M urea, 3.3 M glycerol, 70 mM SDS, 3.3 % resolving buffer) containing 65 mM DTE and subsequent in equilibration buffer containing 215 mM iodoacetamide for 15 minutes each. The equilibrated IPG DryStrip gels were transferred on the top of 11 % SDS-polyacrylamidgels and sealed by adding of 1 - 2 ml of 0.5 % agarose (in SDS-running buffer: 1.9 M glycine, 0.25 M Tris, 1 % SDS). Second dimension gel electrophoresis was carried out according to the protocol shown in **Table 2**.

Step	Constant power (W/gel)	Time (h:min)	Temperature (°C)
Entry phase	2.5	0:45	20
Second phase	18	4:00 – 6:00	20

Table 2. Running conditions for second dimension gel electrophoresis.

2.4.5. Silver staining

Silver staining is the most sensitive non-radioactive method (below 1ng) to visualize proteins in SDS gels. A modified silver staining protocol, that makes the method compatible with mass spectrometry analysis, is shown in **Table 3**.

Step	Solution	Time
1 Fixation	40 % Ethanol 10 % Acetic acid, glacial	45 min or o/n
2 Ethanol Washing	50 % Ethanol	3 x 20 min
3 Sensitizing	1.3 mM Sodium thiosulfate	2 min
4 Washing	Distilled water	2 x 2 min
5 Silver reaction	12 mM Silver nitrate 0.075 % Formaldehyde (37 %)	20 min – 30 min
6 Washing	Distilled water	2 min
7 Developing	0.57 M Sodium carbonate 0.05 % Formaldehyde (37 %) 0.03 mM Sodium thiosulfate	0.2 min – 5 min
8 Stop	40 mM EDTA	20 min
9 Preservation	20 % Ethanol 4 % Glycerol	20 min or o/n

Table 3. Mass spectrometry compatible silver staining protocol.

2.4.6. 2D image analysis

Transparency scanning of the silver-stained 2D gels was performed using the Amersham Biosciences ImageScanner (Amersham Biosciences, Uppsala, Sweden) and the Umax MagicScan 4.5 software (Umax, Duesseldorf, Germany). 2D image computer analysis was carried out using the Definiens Proteomweaver 2.2 software (Definiens, Munich, Germany) allowing automatic spot detection, spot matching and normalization. A protein was considered as differently expressed when the expression was at least two-fold up- or down-regulated and the alteration was at least detected in three separate gels of at least two independent 2D electrophoresis runs.

2.4.7. In-gel digestion

Protein spots of interest were cut out of the gel with a sharp scalpel, stored at -80°C or immediately cut into approximately 1 mm x 1 mm pieces and transferred to Eppendorf tubes. The gel pieces were washed with 100 μl water for 30 minutes with shaking at 650 rpm. Destaining was carried out with 15 mM potassium ferricyanide and 50 mM sodium thiosulfate until dark color disappeared (approx. 5 minutes). Destaining was stopped by 3 x washing with 100 μl water for 5 minutes until the yellow color was removed. The gel pieces were then successively washed with 100 μl acetonitrile, 50 mM ammonium bicarbonate and 50 % acetonitrile for 15 minutes each with shaking at 650 rpm. All steps were performed at room temperature. Digestion was carried out by incubation of the gel pieces in 50 mM ammonium bicarbonate containing 160 ng sequencing grade modified Porcine Trypsin (Promega, Mannheim, Germany) at 37°C overnight. Supernatants of overnight trypsin digestion and of two successive incubations with 100 μl extraction solution (75 % acetonitrile, 12.5 mM ammonium bicarbonate) at 25°C with full speed shaking for 30 minutes were transferred to the same fresh Eppendorf tube. The peptide containing supernatant was rapidly frozen in liquid nitrogen and lyophilized using a speed vac.

2.4.8. Desalting and spotting of peptides onto the MALDI-TOF MS target

Lyophilized peptides were solubilized in 0.1 % trifluoroacetic acid (TFA) and desalted by using C18 ZipTip pipette tips (Millipore, Bedford, USA). C18 ZipTip pipette tips were equilibrated by washing with 50 % acetonitrile and successive 0.1 % TFA each 10 times. Peptides were bound to the ZipTip by ten aspiration and dispensation cycles. The Zip Tip was subsequently washed three times with 0.1 % TFA. Desalted peptides were then directly eluted onto a clean MALDI-TOF MS (matrix assisted laser desorption ionization time of flight mass spectrometry) target with 2 μl of 50 % acetonitrile/0.1 % TFA saturated with alpha-cyano-4-hydroxy-cinnamic acid (Bruker Daltonics, Leipzig, Germany).

2.4.9. MALDI-TOF mass spectrometry and peptide mass fingerprinting

MALDI-TOF mass spectrometry was carried out using an autoflex II spectrometer (Bruker Daltonics, Leipzig, Germany) in the reflector mode. The mass spectrometer was calibrated using a peptide calibration standard (Bruker Daltonics, Leipzig, Germany). For an enhanced resolution and sensitivity the pulsed ion extraction was adjusted. Mass spectra were processed and analyzed using the flexAnalysis software (Bruker Daltonics, Leipzig, Germany). Briefly, mass spectra were smoothed using the Savitzky Golay algorithm, baseline was subtracted using the Convex Hull algorithm and peaks were detected using the SNAP algorithm. Internal recalibration of the mass spectra was performed using peaks derived from autoproteolysis of trypsin. Peptide mass fingerprinting was performed by using the BioTools software (Bruker Daltonics, Leipzig, Germany). Briefly, proteins were identified by database search on MASCOT server (<http://www.matrixscience.com>) using the MSDB database. Searches were performed with carboxymethyl as fixed modification and oxidation as variable modification. A peptide mass tolerance of 50 ppm and maximal one missing cleavage were allowed.

2D electrophoresis and MALDI-TOF mass spectrometry were established in the lab in the context of this PhD thesis.

3. Results

3.1. Multicellular spheroids of low passage colon cancer cell lines - A promising model system for colorectal cancer

The lack of suitable cancer model systems is a major obstacle for the investigation of cancer in general and for the development of effective therapy strategies in particular. A promising prospect is provided by recently developed low passage colon cancer cell lines, closely reflecting the phenotypes of the corresponding original tumors. These cell lines provided the starting point of this PhD thesis. It was reported previously that tumor cells grown as multicellular spheroids recapitulate the properties of *in vivo* tumors better than the same cells cultured as monolayers (Mayer et al., 2001). Therefore, multicellular tumor spheroid cultures of the low passage colon cancer cell lines were established which are expected to mirror the three-dimensional structure of the original tumors even more closely. Differences on the level of protein expression between monolayers and multicellular spheroids of the low passage colon cancer cells were analyzed in this thesis.

3.1.1. Establishment of multicellular spheroids of low passage colon cancer cell lines

Five low passage colon cancer cell lines of three different phenotypic morphologies (epithelial-like: COGA-5, piled-up: COGA-5L and COGA-12, rounded-up: COGA-2 and COGA-3) were tested for their ability to form multicellular spheroids. The multicellular spheroid formation was performed with the liquid overlay technique. The cell line COGA-5 formed fully compact spheroids, the cell lines COGA-5L and COGA-12 formed partly compact spheroids with local areas of compaction as shown in **Fig. 4**. The other cell lines tested did not form multicellular spheroids.

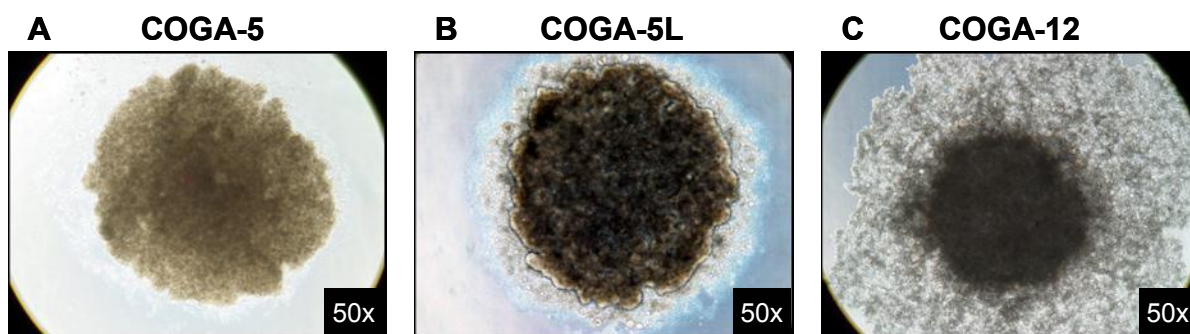


Fig. 4. Multicellular spheroids of COGA-5 (A), COGA-5L (B) and COGA-12 (C) cells using the liquid overlay technique. 1×10^5 cells were seeded in agarose-covered 24 well plates and cultivated in medium containing 10 % serum for 96 h (COGA-5 and COGA-5L) or 72 h (COGA-12). COGA-5 cells are forming fully compact spheroids, the cell lines COGA-5L and COGA-12 are forming partly compact spheroids with local areas of compaction. Respective magnifications of transmission light microscopy are indicated.

3.1.2. Differences in the expression profiles of multicellular spheroids compared to corresponding monolayer cultures

In order to analyze potential differences in protein expression protein extracts of monolayer cultures of the cell lines COGA-5, COGA-5L and COGA-12 were compared with protein extracts from respective multicellular spheroids by 2D electrophoresis. For this purpose, ten multicellular spheroids grown for 96 hours were pooled and 200 μ g total protein thereof were compared with 200 μ g total protein of the corresponding monolayer cultures. To have always comparable growing conditions monolayer cultures were grown to near confluence prior multicellular spheroid formation and sample preparation. As shown in **Fig. 5 - 7** 2D electrophoresis revealed differences in the expression of six proteins in multicellular spheroids of COGA-5 cells (five up- and one down-regulated), of four in COGA-5L multicellular spheroids (all up-regulated) and of four (all up-regulated) in COGA-12 multicellular spheroids compared to the respective monolayer cultures. The respective abbreviations used for numbering the spots are explained as follows: e.g. SPH12-U1 stands for multicellular **s**pheroid of COGA-**12** cells, **u**p-regulated spot number **1**. Two of the differentially regulated proteins in COGA-5L multicellular spheroids, i.e. SPH5L-U1 and SPH5L-U2, are probably identical to SPH5-U1 and SPH5-U2 that were up-regulated in COGA-5 multicellular spheroids. Moreover, SPH5L-U4a and SPH5L-U4b that were up-regulated in COGA-5L multicellular spheroids localize at the same position on the 2D gel as SPH12-U3a and SPH12-

U3b that were up-regulated in COGA-12 multicellular spheroids. The average intensities of all detected proteins altered between monolayers and corresponding multicellular spheroids are shown in **Table 4**.

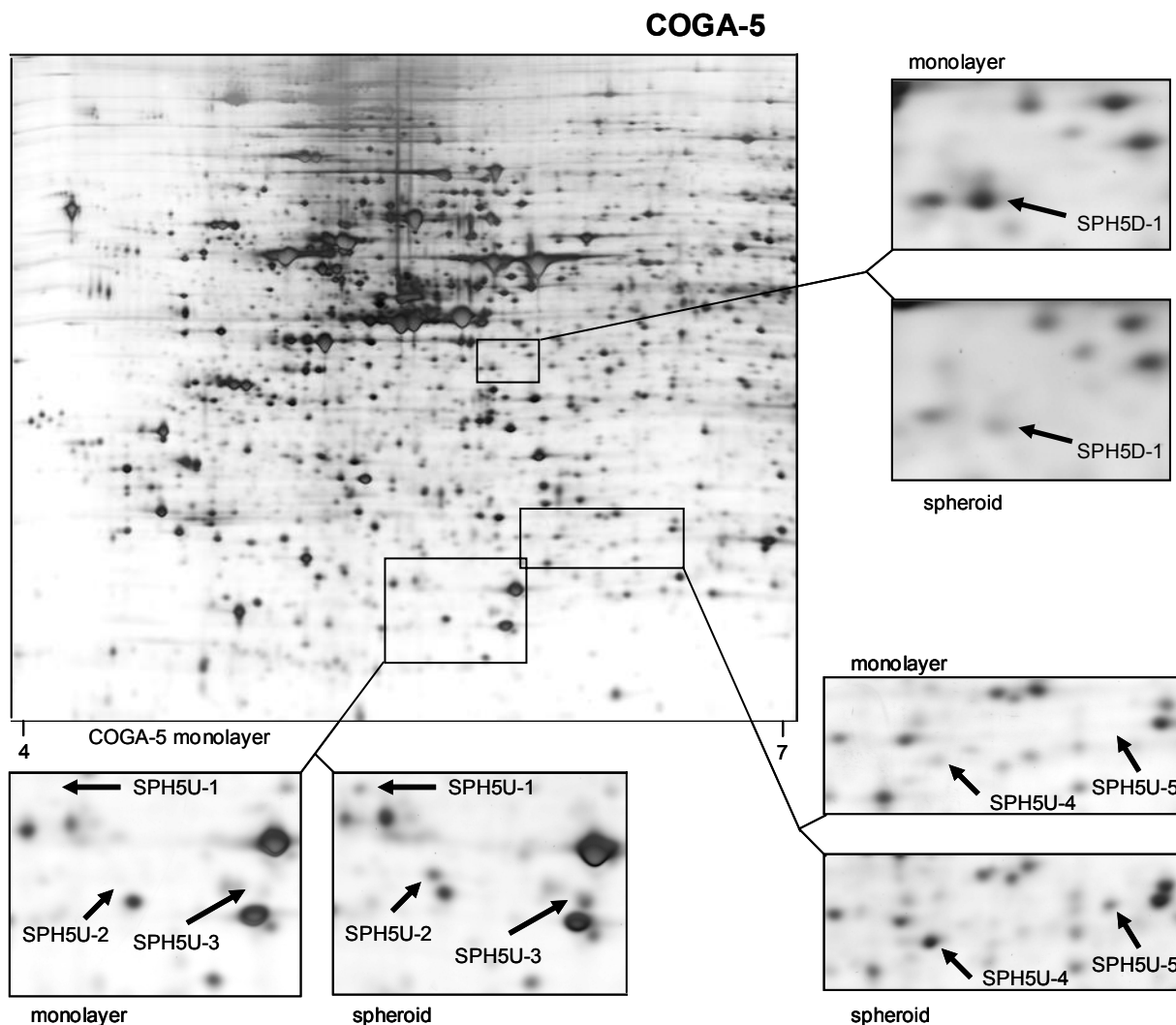


Fig. 5. Differences in the expression profiles of multicellular spheroids of COGA-5 cells and their corresponding monolayer cultures obtained by 2D electrophoresis. 2D electrophoresis was performed with IPG dry strips pH 4 - 7 in the first dimension and 11 % SDS-polyacrylamide gels in the second dimension. Representative silver-stained gels are shown. Differences in the expression profiles are marked with an arrow. The respective spot intensities are listed in Table 4 and corresponding proteins identified by MALDI-TOF mass spectrometry are listed in Table 5. Respective abbreviations for numbering of spots: e.g. SPH5-U1: multicellular **spheroid** of COGA-5 cells, **up**-regulated spot number 1.

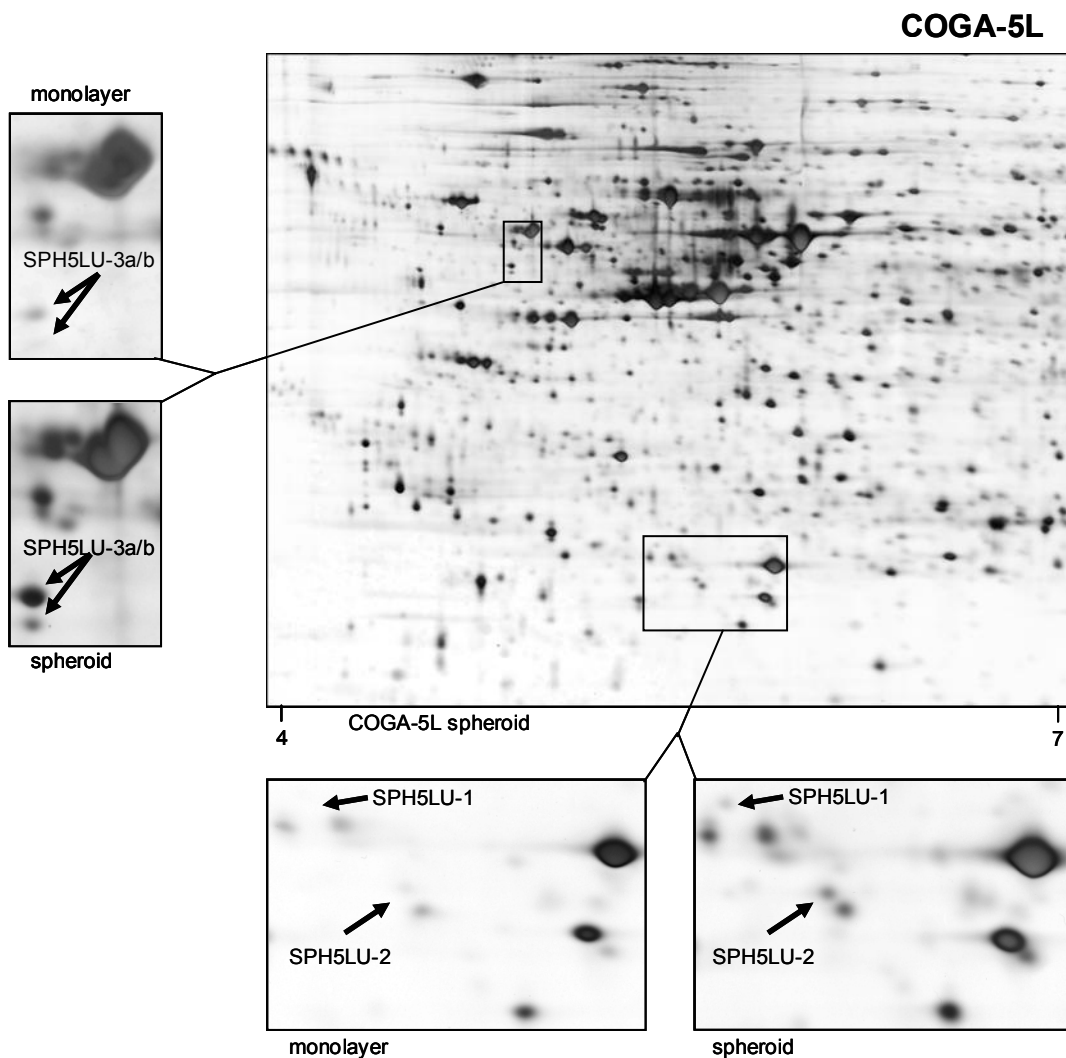


Fig. 6. Differences in the expression profiles of multicellular spheroids of COGA-5L cells and their corresponding monolayer cultures obtained by 2D electrophoresis. 2D electrophoresis was performed as described in Fig. 5. Representative silver-stained gels are shown. Differences in the expression profiles are marked with an arrow. The respective spot intensities are listed in Table 4. Respective abbreviations for numbering of spots: e.g. SPH5LU-1: multicellular **spheroid** of COGA-5L cells, **up-regulated** spot number 1.

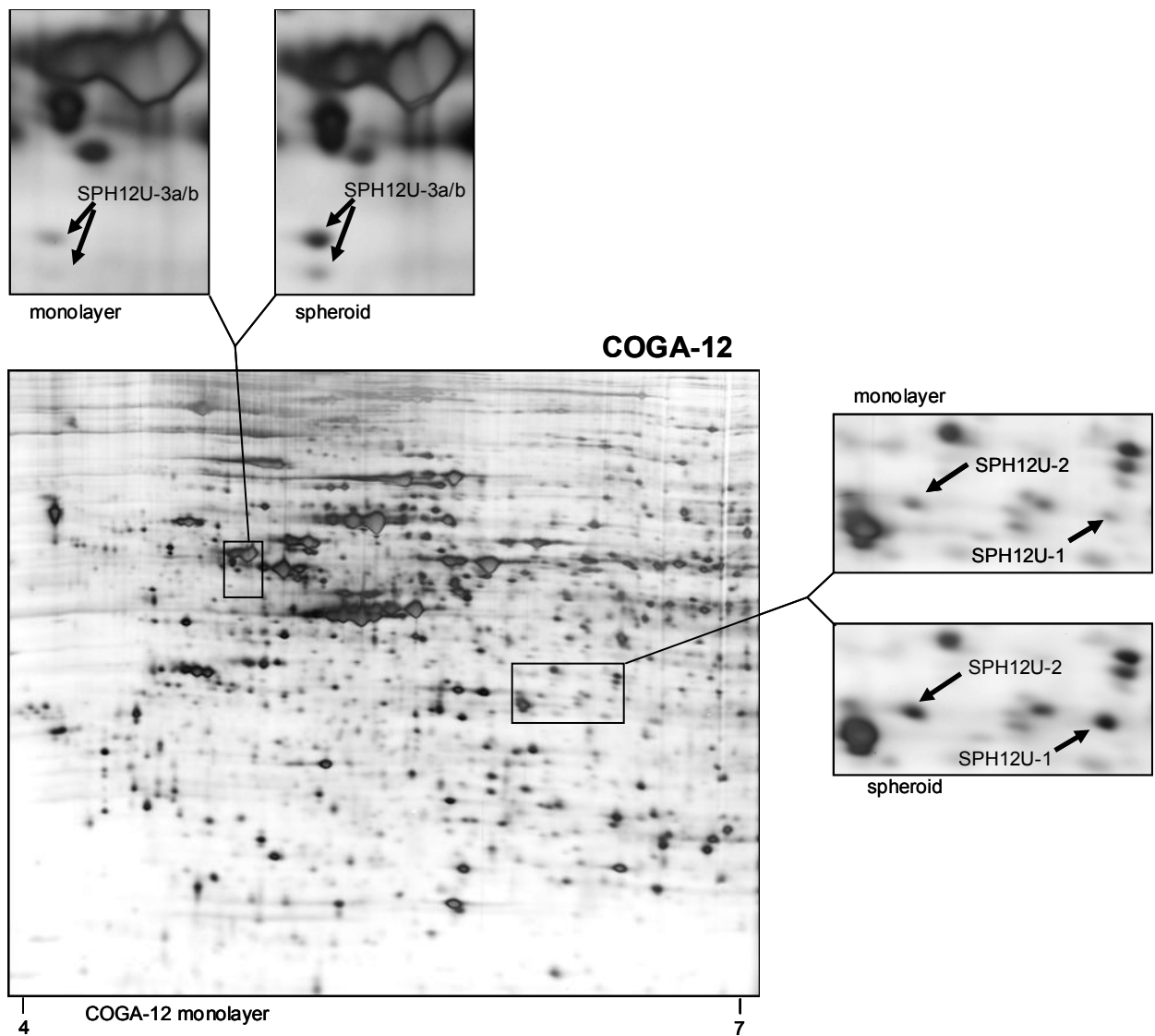


Fig. 7. Differences in the expression profiles of multicellular spheroids of COGA-12 cells and their corresponding monolayer cultures obtained by 2D electrophoresis. 2D electrophoresis was performed as described in Fig. 5. Representative silver-stained gels are shown. Differences in the expression profiles are marked with an arrow. The respective spot intensities are listed in Table 4 and corresponding proteins identified by MALDI-TOF mass spectrometry are listed in Table 5. Respective abbreviations for numbering of spots: e.g. SPH12-U1: multicellular **spheroid** of COGA-12 cells, **up**-regulated spot number 1.

Spot number	Average intensity in monolayer cultures	Average intensity in multicellular spheroids	Ratio multicellular spheroids / monolayers
SPH5U-1	0.098 ± 0.041	0.210 ± 0.075	2.15
SPH5U-2	---	0.264 ± 0.222	only expressed in multicellular spheroids
SPH5U-3	0.261 ± 0.223	0.635 ± 0.103	2.44
SPH5U-4	0.220 ± 0.064	0.762 ± 0.096	3.47
SPH5U-5	---	0.256 ± 0.021	only expressed in multicellular spheroids
SPH5D-1	0.551 ± 0.046	0.198 ± 0.051	0.36
SPH5LU-1	---	0.054 ± 0.003	only expressed in multicellular spheroids
SPH5LU-2*	0.122* ± 0.000	0.191* ± 0.025	1.56*
SPH5LU-3a	0.80 ± 0.259	0.247 ± 0.013	3.07
SPH5LU-3b	---	0.060 ± 0.013	only expressed in multicellular spheroids
SPH12U-1	0.179 ± 0.083	0.461 ± 0.060	2.57
SPH12U-2	0.301 ± 0.025	0.609 ± 0.086	2.02
SPH12U-3a	0.057 ± 0.003	0.136 ± 0.026	2.37
SPH12U-3b	---	0.048 ± 0.002	only expressed in multicellular spheroids

Table 4. Average intensities of the protein spots altered between 2D gels of monolayers and corresponding multicellular spheroids of cell lines COGA-5, COGA-5L and COGA-12. The respective normalized average intensities ± SE of at least three separate 2D gels analyzed with the Proteomweaver software are listed. (*) does not fulfill the requirement to be at least two-fold up- or down-regulated (as described in material and methods).

The proteins in the differently expressed spots were analyzed by MALDI-TOF mass spectrometry and subsequent peptide mass fingerprinting. Therefore, the protein spots of interest were cut out of the 2D gel, trypsin-digested and spotted on a MALDI-TOF target plate. However, MALDI-TOF mass spectrometry did not lead to identification of spots from a standard 2D gel with a total protein load of 200 µg (corresponding to approximately 0.075×10^6 cells). Therefore, preparative 2D gels (of monolayer cultures) were made with total protein of about 10×10^6 cells. In this case, staining time of the gels had to be reduced drastically. By using spots of these preparative 2D gels for mass spectrometry three of the differently expressed proteins in COGA-5 multicellular spheroids could be identified as 15-hydroxyprostaglandin

dehydrogenase, LMNA protein and acidic calponin (**Table 5**). It was also possible to identify two differently regulated proteins in COGA-12 multicellular spheroids as the same protein, namely acidic ribosomal protein P0 (**Table 5**). This protein appears at two neighboring positions on the 2D gel most likely as a result of different posttranslational modifications (PTMs). Corresponding mass spectra and protein identifications results are shown in **Fig. 8 - 12**. None of the changes in the expression profile of multicellular spheroids of COGA-5L cells could be ascribed to known proteins.

Spot number	Protein name identified by MALDI-TOF mass spectrometry	Cell line	Regulation in multicellular spheroids
SPH5U-1	not identified	COGA-5	up
SPH5U-2	not identified	COGA-5	up
SPH5U-3	not identified	COGA-5	up
SPH5U-4	15-Hydroxyprostaglandin Dehydrogenase	COGA-5	up
SPH5U-5	LMNA protein	COGA-5	up
SPH5D-1	Calponin, acidic isoform	COGA-5	down
SPH5LU-1	not identified	COGA-5L	up
SPH5LU-2	not identified	COGA-5L	up
SPH5LU-3a	not identified	COGA-5L	up
SPH5LU-3b	not identified	COGA-5L	up
SPH12U-1	Acidic Ribosomal Protein P0	COGA-12	up
SPH12U-2	Acidic Ribosomal Protein P0	COGA-12	up
SPH12U-3a	not identified	COGA-12	up
SPH12U-3b	not identified	COGA-12	up

Table 5. Proteins differentially expressed between multicellular spheroids of cell lines COGA-5, COGA-5L and COGA-12 and corresponding monolayers.

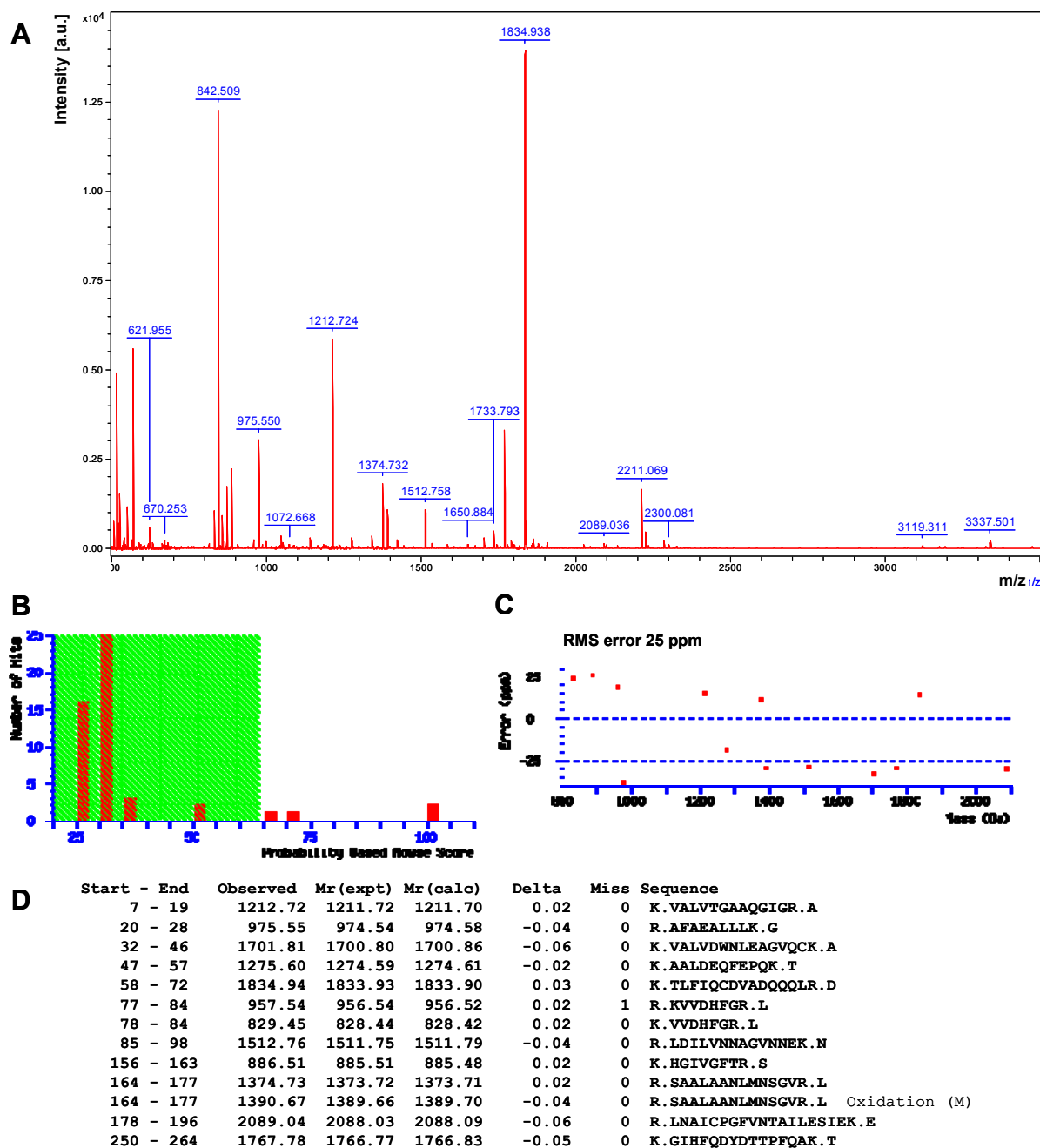


Fig. 8. Identification of spot SPH5U-1. (A) Mass spectrum of SPH5U-1 obtained after in-gel digestion and MALDI-TOF analysis. (B-D) Protein identification results obtained by database search on MASCOT server. Identifications were obtained after internal recalibration of the mass spectrum using peaks deriving from autoproteolysis of trypsin, with 50 ppm, as mass tolerance, and allowing only 1 missing cleavage. (B) Probability based mowse score. Ions score is $-10 \cdot \log(P)$, where P is the probability that the observed match is a random event. Protein scores greater than 64 are significant ($p < 0.05$). (C) Root mean square (RMS) error graph. (D) Peptides matched with the sequence of 15-hydroxyprostaglandin dehydrogenase and their molecular mass are reported.

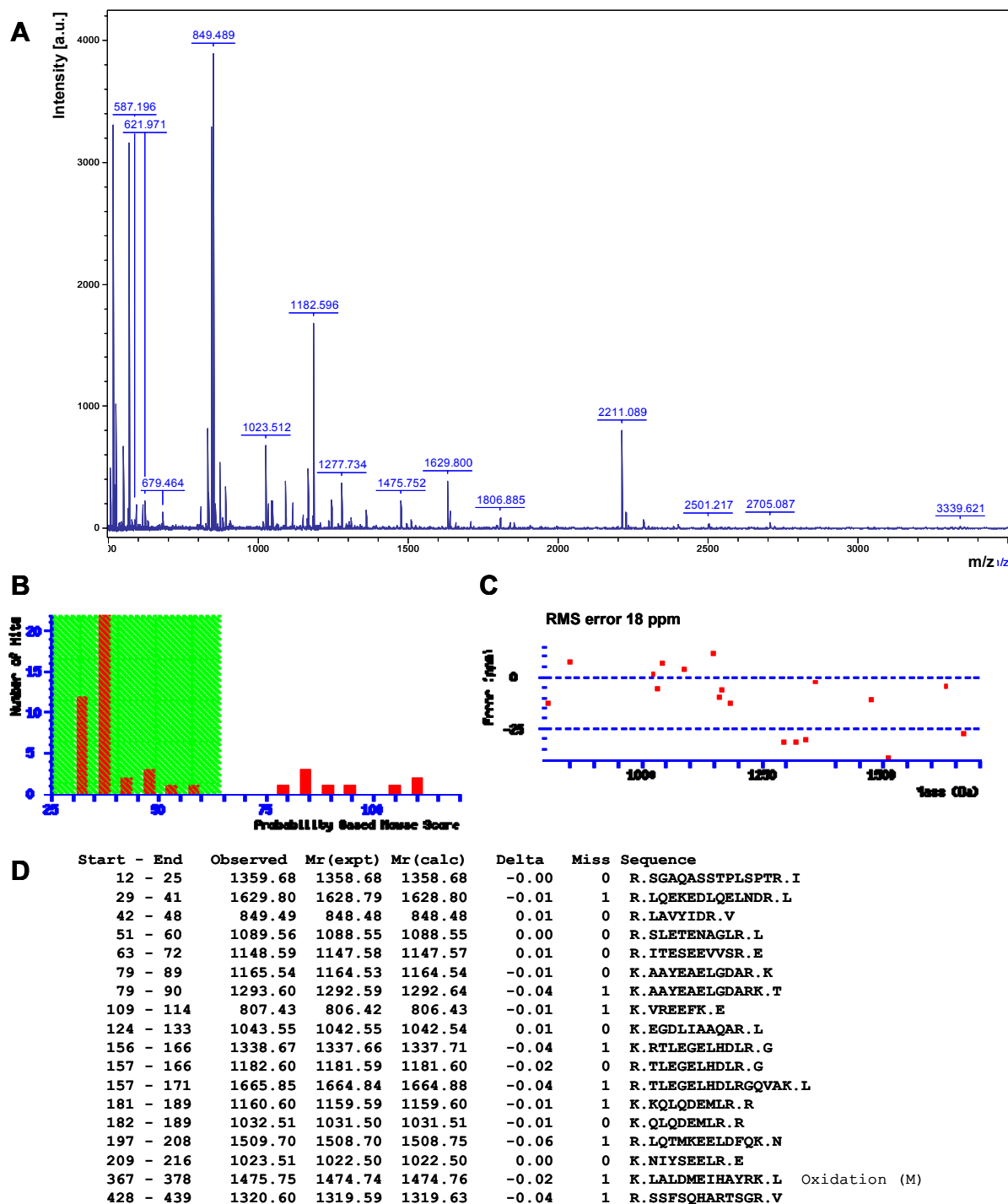


Fig. 9. Identification of spot SPH5U-2. (A) Mass spectrum of SPH5U-2 obtained after in-gel digestion and MALDI-TOF analysis. (B-D) Protein identification results obtained by database search on MASCOT server. Identifications were obtained after internal recalibration of the mass spectrum using peaks deriving from autoproteolysis of trypsin, with 50 ppm, as mass tolerance, and allowing only 1 missing cleavage. (B) Probability based mowse score. Ions score is $-10 \cdot \log(P)$, where P is the probability that the observed match is a random event. Protein scores greater than 64 are significant ($p < 0.05$). (C) Root mean square (RMS) error graph. (D) Peptides matched with the sequence of LMNA protein and their molecular mass are reported.

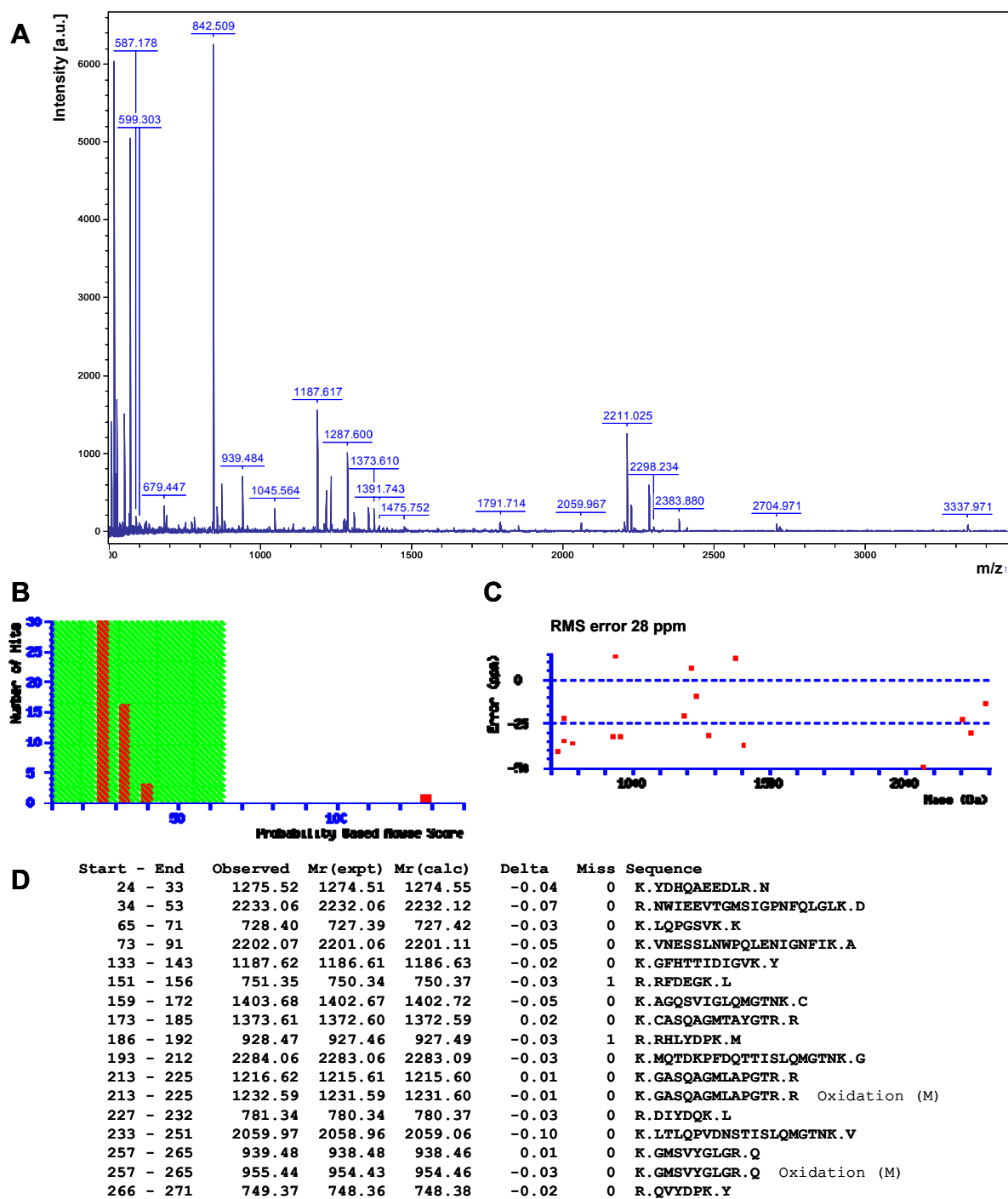


Fig. 10. Identification of spot SPH5D-1. (A) Mass spectrum of SPH5D-1 obtained after in-gel digestion and MALDI-TOF analysis. (B-D) Protein identification results obtained by database search on MASCOT server. Identifications were obtained after internal recalibration of the mass spectrum using peaks deriving from autoproteolysis of trypsin, with 50 ppm, as mass tolerance, and allowing only 1 missing cleavage. (B) Probability based mowse score. Ions score is $-10 \cdot \log(P)$, where P is the probability that the observed match is a random event. Protein scores greater than 64 are significant ($p < 0.05$). (C) Root mean square (RMS) error graph. (D) Peptides matched with the sequence of acidic calponin and their molecular mass are reported.

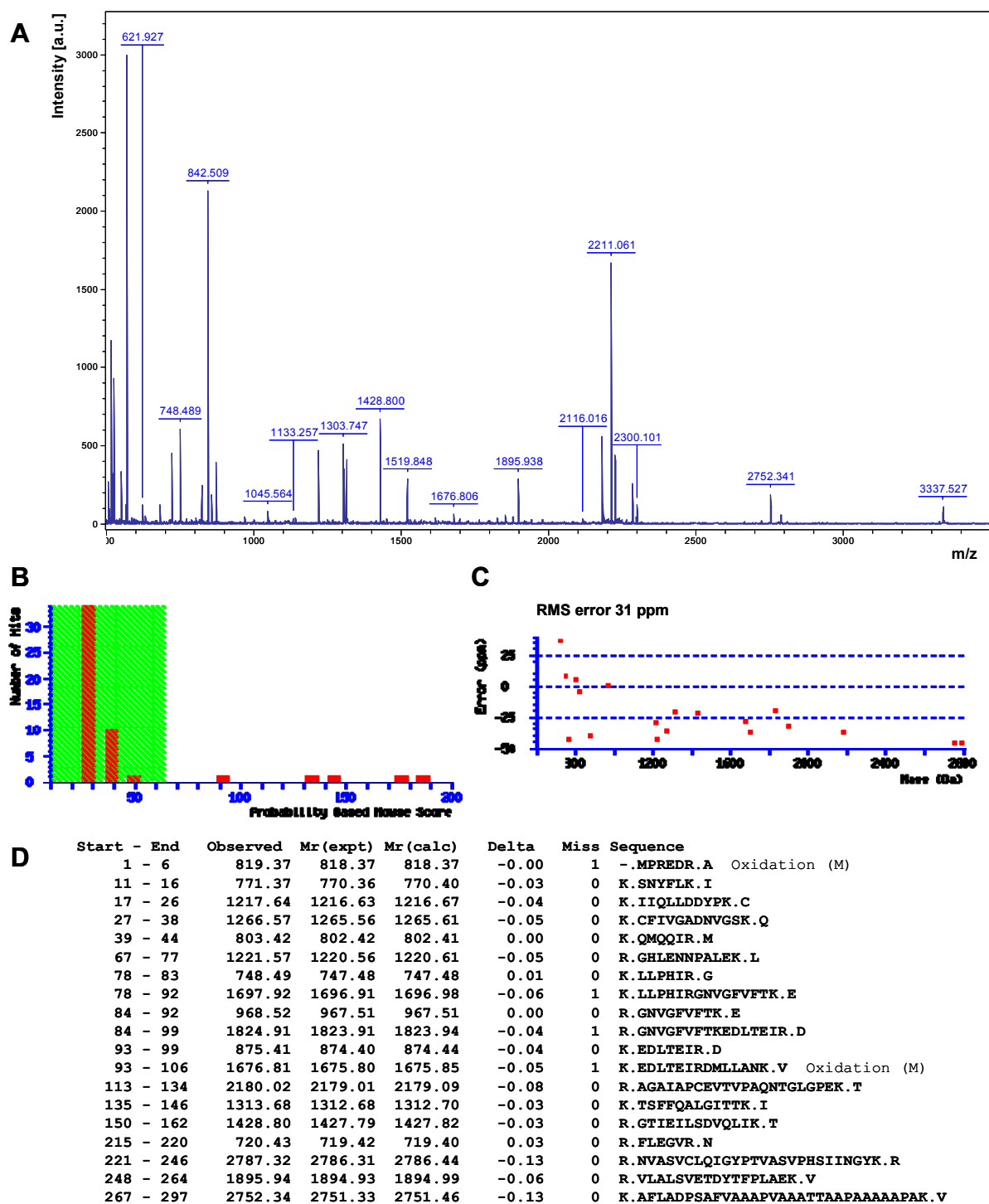


Fig. 11. Identification of spot SPH12U-1. (A) Mass spectrum of SPH12U-1 obtained after in-gel digestion and MALDI-TOF analysis. (B-D) Protein identification results obtained by database search on MASCOT server. Identifications were obtained after internal recalibration of the mass spectrum using peaks deriving from autoproteolysis of trypsin, with 50 ppm, as mass tolerance, and allowing only 1 missing cleavage. (B) Probability based mowse score. Ions score is $-10 \cdot \log(P)$, where P is the probability that the observed match is a random event. Protein scores greater than 64 are significant ($p < 0.05$). (C) Root mean square (RMS) error graph (D) Peptides matched with the sequence of acidic ribosomal protein P0 and their molecular mass are reported.

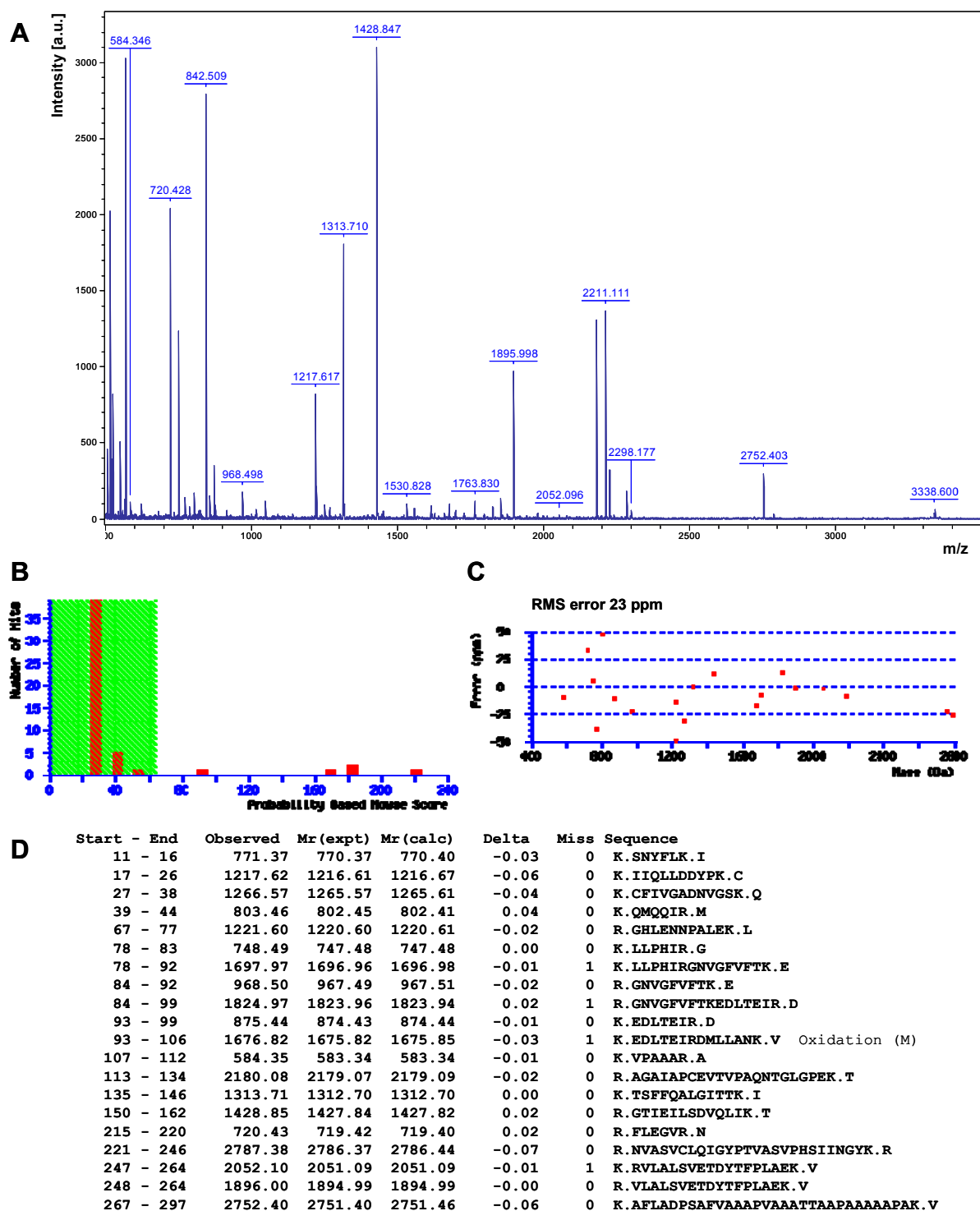


Fig. 12. Identification of spot SPH12U-2. (A) Mass spectrum of SPH12U-2 obtained after in-gel digestion and MALDI-TOF analysis. (B-D) Protein identification results obtained by database search on MASCOT server. Identifications were obtained after internal recalibration of the mass spectrum using peaks deriving from autoproteolysis of trypsin, with 50 ppm, as mass tolerance, and allowing only 1 missing cleavage. (B) Probability based mowse score. Ions score is $-10 \cdot \log(P)$, where P is the probability that the observed match is a random event. Protein scores greater than 64 are significant ($p < 0.05$). (C) Root mean square (RMS) error graph. (D) Peptides matched with the sequence of acidic ribosomal protein P0 and their molecular mass are reported.

3.2. Chemotherapy of colorectal cancer – Detection of proteins associated with chemoresistance against 5-FU

The incidence of chemoresistance is a major hindrance for the classical treatment of colorectal cancer. Therefore, the investigation of chemoresistance is an important objective. In this thesis the detection of proteins associated with acquired chemoresistance against 5-FU was performed by comparison of the expression profiles of sensitive low passage colon cancer cells and the corresponding resistant sublines by 2D electrophoresis. For this purpose, resistant sublines of the low passage colon cancer cells were established.

3.2.1. Determination of 5-FU concentrations required for reduction of proliferation of selected low passage colon cancer cells

For the investigation of acquired chemoresistance the cell lines forming multicellular spheroids were used, i.e. COGA-12, COGA-5 and COGA-5L. First, the 5-FU concentrations were determined that significantly reduced proliferation of each cell line. The proliferation of the 5-FU-treated cell lines was investigated by the Hoechst 33258 proliferation assay. However, prior the use of this method its reliability was verified. For this purpose, COGA-12 cells were harvested by treatment with trypsin/EDTA solution and cell concentration was determined. Different cell numbers were then transferred to Eppendorf tubes and centrifuged at 500 rpm. The cell pellets were used for the performing of the Hoechst 33258 proliferation assay directly in the Eppendorf tubes as described in materials and methods. For measurement the whole content of the tubes was transferred to black 96 well-plates. **Fig. 13** demonstrates that the Hoechst 33258-based proliferation assay is reliable for cell numbers ranging from 1×10^3 to 7×10^4 .

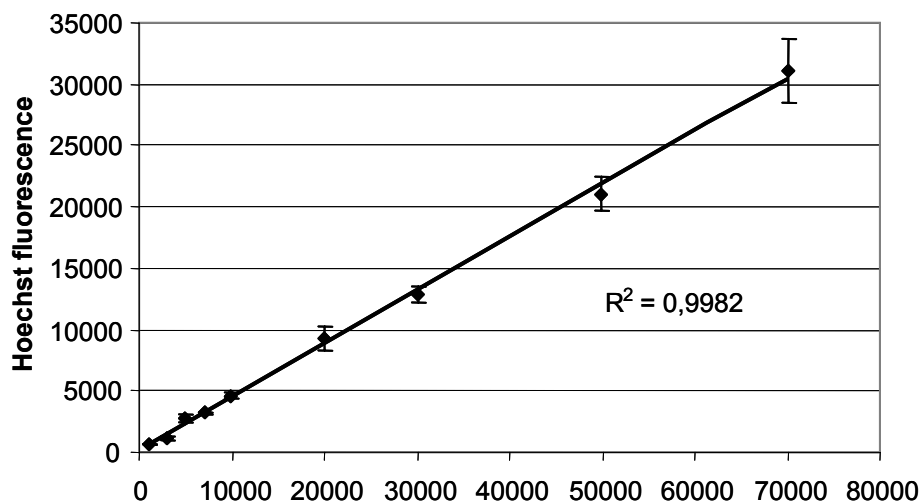


Fig. 13. Validation of the Hoechst 33258-based proliferation assay. COGA-12 cells were harvested with trypsin/EDTA and the assay was performed by incubating 1×10^3 - 7×10^4 cells with $100 \mu\text{l}$ H_2O at 37°C for 1 hour, following one freeze/thaw cycle. After adding of $100 \mu\text{l}$ $2\times$ TNE buffer containing Hoechst 33258, fluorescence was determined at 465 nm in a SPECTRAFluor Plus plate reader (excitation: 360 nm). Values are means \pm SE of triplicates.

To determine the optimal 5-FU concentration range for further experiments both cell lines COGA-12 and COGA-5L were treated with different concentrations of 5-FU ranging from $2.5 \mu\text{M}$ to $500 \mu\text{M}$. The level of cell proliferation was determined from 1 to 6 days after beginning of the treatment by using the Hoechst 33258-based proliferation assay. The results demonstrated that already after two to three days a significant reduction of cell proliferation was observed already at low 5-FU concentrations of $2.5 \mu\text{M}$ – $10 \mu\text{M}$ (Fig. 14).

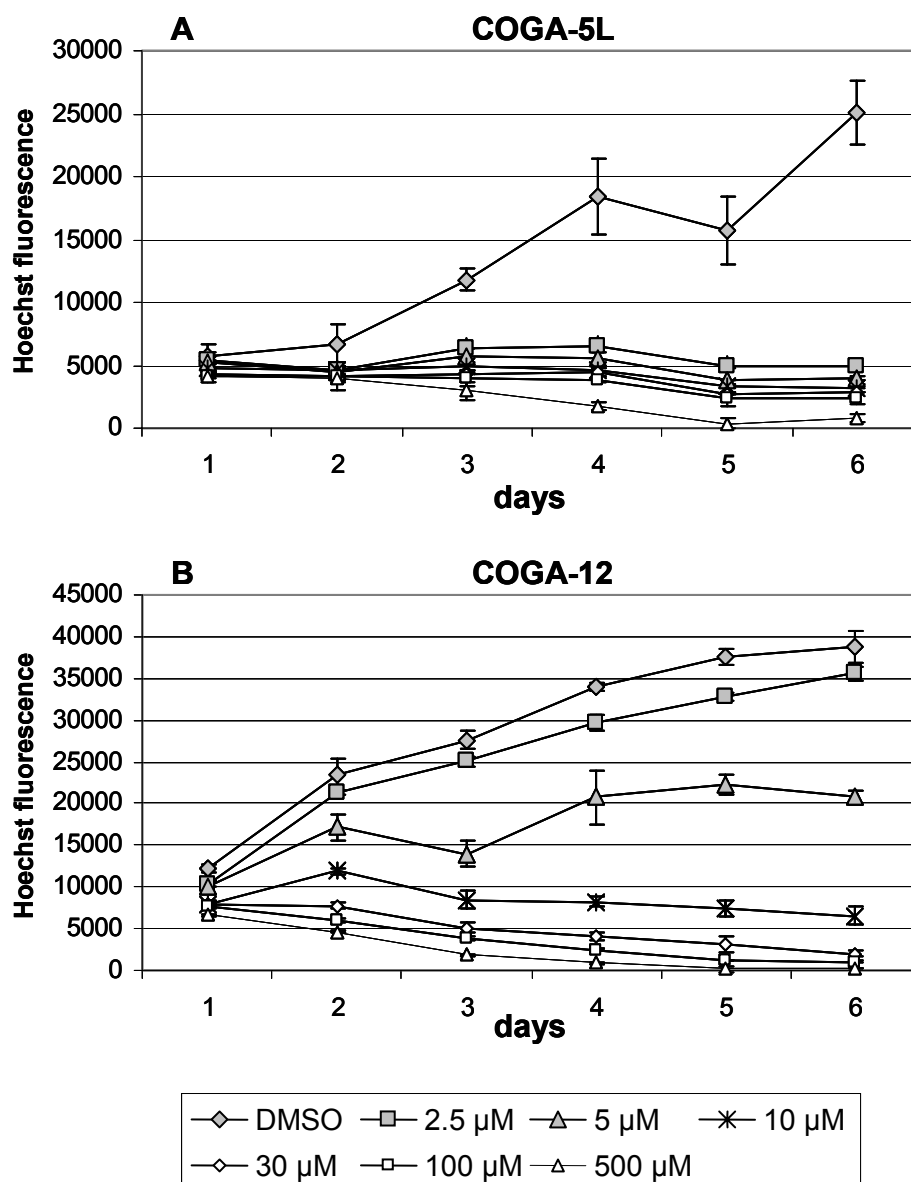


Fig. 14. Kinetics of 5-FU treatment of COGA-5L (A) and COGA-12 (B) cells. 1.5×10^4 cells/well were treated from 1 to 6 days with different concentrations of 5-FU. Growth medium was exchanged every day. Cell proliferation was determined with the Hoechst 33258-based proliferation assay. Values are means \pm SE of triplicates.

The further experiments to determine the 5-FU concentrations required for reduction of proliferation of the cell lines COGA-12, COGA-5 and COGA-5L were therefore performed in a concentration range of 2.5 μ M to 10 μ M 5-FU. Cell proliferation was determined after two and three days of treatment again by the Hoechst 33258-based proliferation assay (**Fig. 15**). In all tested cell lines the reduction of cell proliferation by 5-FU was more pronounced at day three after beginning of the treatment compared to day two. After three days the DNA amount of 5 μ M 5-FU-treated COGA-

5L and COGA-12 cells was 49 % and 44 % compared to the respective untreated cells (**Fig. 15**). Increasing of the 5-FU concentration to 10 μM further reduced the proliferation of COGA-12 cells down to 25 % compared to untreated cells. In COGA-5 cells 5 μM 5-FU and 10 μM 5-FU reduced proliferation to 73 % and 62 % of the proliferation of untreated cells, respectively (**Fig. 15**).

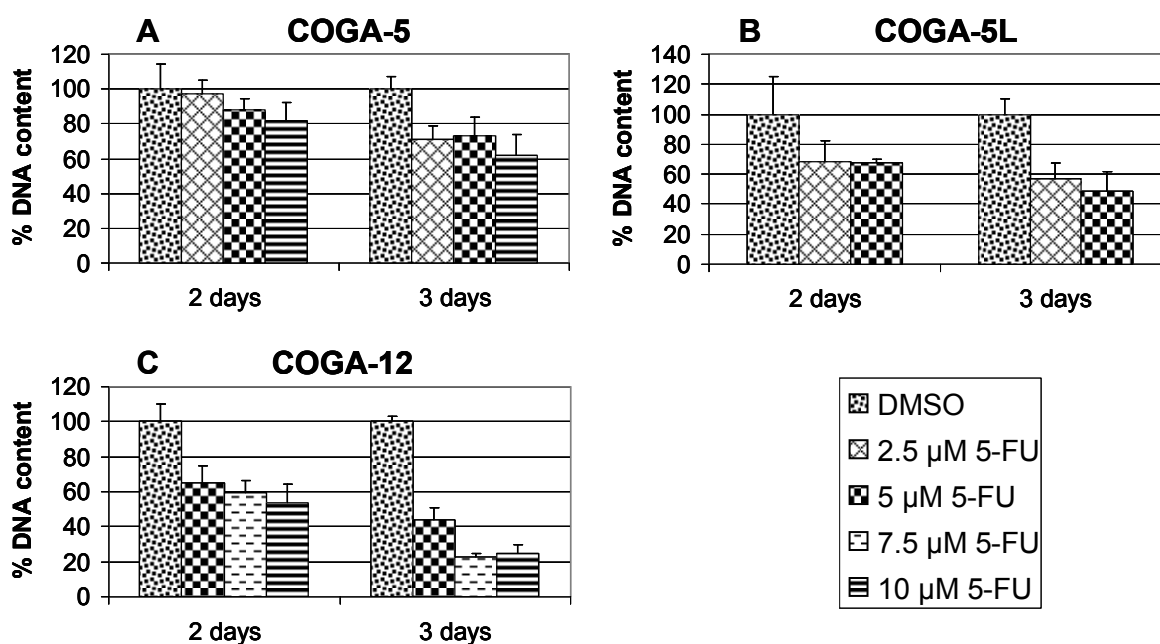


Fig. 15. Determination of 5-FU concentrations required for reduction of proliferation of COGA-5 (A), COGA-5L (B) and COGA-12 (C) cells. 1.5×10^4 COGA-5L or COGA-12 cells/well and 0.4×10^4 COGA-5 cells/well were treated for 2 and 3 days with different concentrations of 5-FU. Growth medium was exchanged every day. Cell proliferation was determined with the Hoechst 33258-based proliferation assay. Proliferation levels are shown as the percentage of proliferation levels of the respective untreated cells. The values are means \pm SE of triplicates of 2 - 3 independent experiments.

3.2.2. Long-term 5-FU treatment of selected low passage colon cancer cells

In order to obtain chemoresistant sublines COGA-12, COGA-5 and COGA-5L cells were treated continuously with 5-FU. First, all cell lines were treated for one month with 10 μM 5-FU. In a separate experiment, COGA-5 cells were additionally incubated with 5 μM 5-FU. Growth medium containing 5-FU was replaced three times per week to ensure constant 5-FU concentrations. COGA-5 cells did not survive the treatment with 5 μM or 10 μM 5-FU for one month. Concentrations of 5-FU lower than 5 μM , however, did not reduce proliferation of COGA-5 cells. Therefore, no chemoresistant sublines of COGA-5 could be established. For COGA-12 and COGA-5L cells the concentration of 5-FU was doubled after one month and cells were

incubated for another two months with continuously 5-FU-containing growth medium exchange three times a week. After total 5-FU treatment for three months the 5-FU containing medium was removed and the cell lines were propagated in 5-FU free medium.

3.2.3. Effect of 5-FU on proliferation of the long-term 5-FU-pretreated sublines

In order to test whether the long-term 5-FU-pretreated sublines of COGA-5L and COGA-12 (referred to as COGA-12/G6) developed resistance against 5-FU, the effect of 5-FU on their proliferation was compared to the parental not 5-FU-pretreated cell lines. Proliferation of COGA-12/G6 cells was only reduced to 73 % and 56 % of the proliferation of untreated COGA-12/G6 cells after treatment with 5 μ M and 10 μ M 5-FU for three days (**Fig. 16**). Therefore, COGA-12/G6 cells were more resistant against 5-FU than the parental COGA-12 cells, where proliferation was reduced to 37 % and 24 % compared to untreated COGA-12 cells by three-day treatment with 5 μ M and 10 μ M 5-FU in parallel experiments (**Fig. 16**). The long-term 5-FU pretreated COGA-5L subline did not demonstrate an enhanced proliferation level when retreated with 5-FU in comparison to parental COGA-5L cell line (data not shown). Thus, no COGA-5L chemoresistant subline could be established.

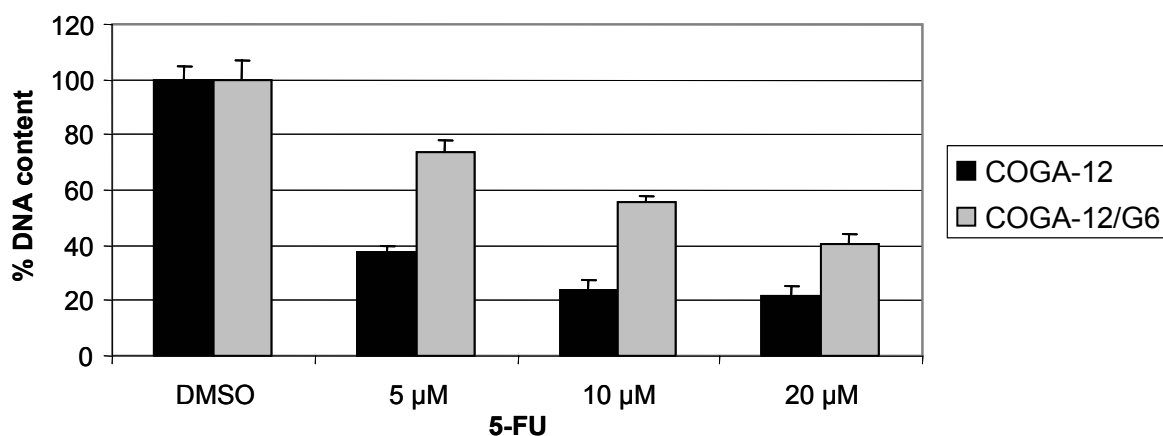


Fig. 16. Proliferation levels of three months 5-FU-pretreated COGA-12 cells (referred to as COGA-12/G6) and parental COGA-12 cells (not 5-FU-pretreated) after incubation with different concentrations of 5-FU for three days. Growth medium was exchanged every day. Cell proliferation was determined with the Hoechst 33258-based proliferation assay. Proliferation levels are shown as the percentage of the proliferation levels of the respective untreated cells. The values are means \pm SE of triplicates in two independent experiments.

3.2.4. Effect of 5-FU on the induction of apoptosis in the long-term 5-FU pretreated subline COGA-12/G6

Next, it was investigated if in addition to the enhanced proliferation despite of the presence of 5-FU also the percentage of 5-FU-induced apoptosis is lower in the chemoresistant subline COGA-12/G6 compared to the parental COGA-12 cell line. Therefore, both cell lines were treated for three days with 20 μ M 5-FU. Afterwards, the level of apoptosis and necrosis in 5-FU treated cells was determined after staining with annexin V-FITC and propidium iodide (PI), and subsequent flow cytometric analysis. Thereby, PI fluorescence was determined at a wavelength of 575 nm after excitation at 488 nm. However, also autofluorescence of 5-FU-treated COGA-12 cells (and not of untreated cells) was detected under these conditions (data not shown). Therefore, the flow cytometric analysis was modified. PI was excited at a wavelength of 356 nm and the emission was detected using a 700 \pm 20 nm bandpass filter thereby excluding the autofluorescence of 5-FU treated cells (data not shown).

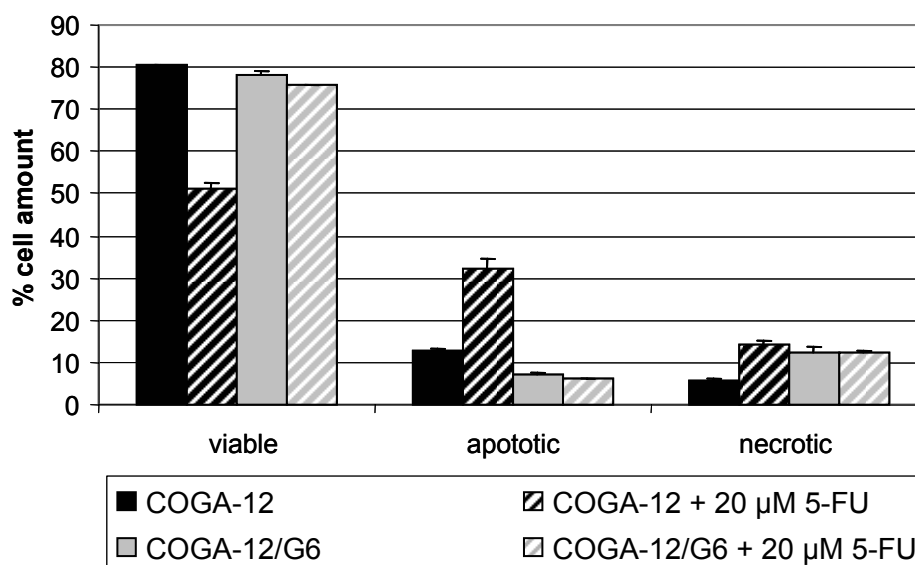


Fig. 17. Percentage of apoptotic cells in 5-FU treated chemoresistant COGA-12/G6 cells and parental COGA-12 cells. 2.8×10^5 cells per well were incubated with 20 μ M 5-FU for three days. Growth medium was exchanged every day. Necrotic cells were detected after staining with propidium iodide and apoptotic cells after staining with annexin V and subsequent flow cytometry. The values are representative means \pm SE of duplicates in two independent experiments.

As shown in **Fig. 17** the modified flow cytometric analysis revealed that 20 μ M 5-FU induced 32 % apoptotic and 14 % necrotic cells within the parental COGA-12 cells three days after beginning of the treatment, whereas in resistant COGA-12/G6 cells

the levels of apoptotic and necrotic cells were only 6 % and 12 %, respectively. It is noteworthy that the percentages of apoptotic and necrotic cells in COGA-12/G6 cells treated with 20 μ M 5-FU did not differ from control levels of untreated COGA-12/G6 cells (7 % apoptotic and 12 % necrotic cells).

Thus, COGA-12/G6 cells pretreated with 5-FU for three months were resistant against both 5-FU-induced apoptosis and inhibition of proliferation. Moreover, the morphology of the resistant COGA-12/G6 cells was slightly different compared to the parental COGA-12 cells (**Fig. 18**), and they did not form multicellular spheroids.

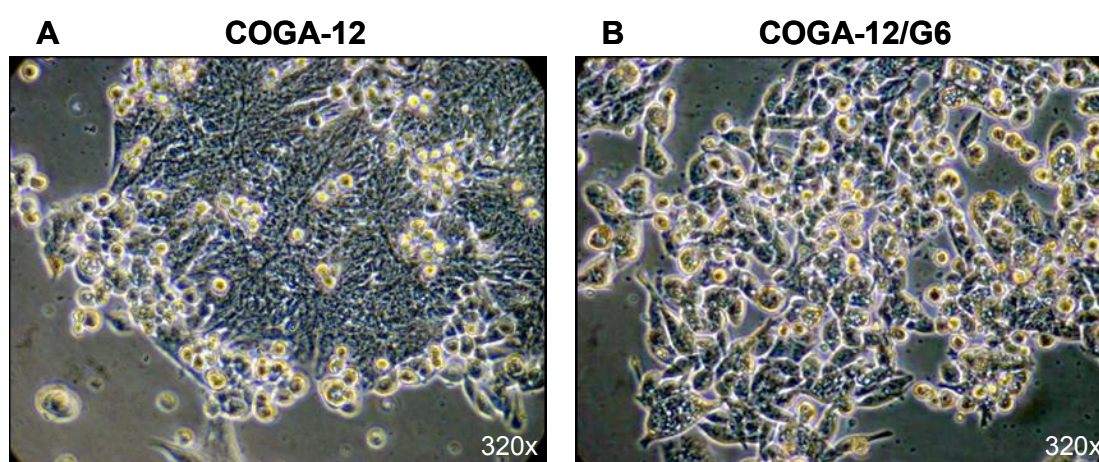


Fig. 18. Morphologies of parental COGA-12 (A) and 5-FU resistant COGA-12/G6 cells (B). Respective magnifications of transmission light microscopy are indicated.

3.2.5. Effect of 5-FU on proliferation and apoptosis in long-term propagated COGA-12 cells

Since the resistant COGA-12/G6 cells were cultured long term, it was investigated if already the long culture time of this cells has changed their response to 5-FU. To this end, parental COGA-12 cells were cultivated for the same time as COGA-12/G6 cells, but in the absence of 5-FU treatment. These high passage cells (referred to as COGA-12/NO) also demonstrated altered morphology when compared with the parental low passage COGA-12 cells as shown in **Fig. 19**, and they also were not able to form multicellular spheroids.

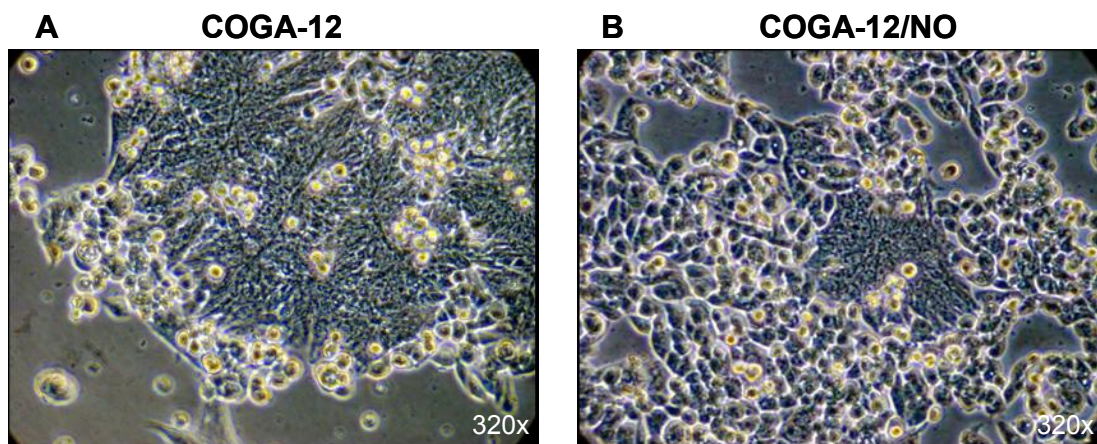


Fig. 19. Morphologies of low (A) and high (B) passage COGA-12 cells. High passage COGA-12 cells are referred to as COGA-12/NO. Respective magnifications of transmission light microscopy are indicated.

The effect of 5-FU on proliferation of COGA-12/NO cells was investigated similar as described before. The COGA-12/NO cells exhibited comparable sensitivity to 5-FU-induced reduction of proliferation as the parental short term cultivated COGA-12 cells (**Fig. 20**).

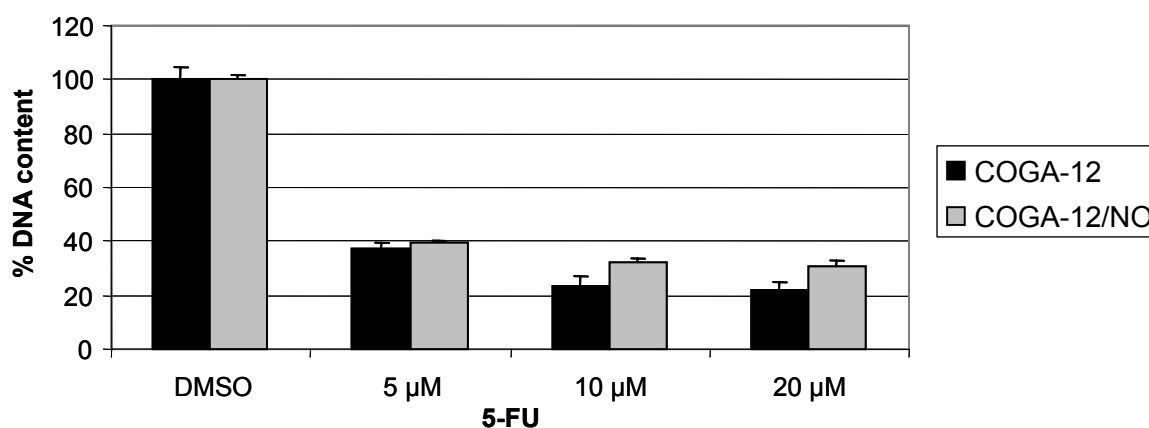


Fig. 20. Proliferation levels of low and high passage COGA-12 cells after incubation with different concentrations of 5-FU for three days. High passage COGA-12 cells are referred to as COGA-12/NO. Growth medium was exchanged every day. Cell proliferation was determined with the Hoechst 33258-based proliferation assay. Proliferation levels are shown as the percentage of proliferation levels of the respective untreated cells. The values are means \pm SE of triplicates.

Next, the level of 5-FU induced apoptosis of COGA-12/NO cells was investigated (**Fig. 21**). Surprisingly, after 5-FU treatment the percentage of apoptotic COGA-12/NO cells was as low as in the 5-FU resistant COGA-12/G6 cells (7%). This result suggested that the COGA-12/NO cells also developed resistance against 5-FU-induced apoptosis, because of changes attributed to their long term cultivation. However, they did not develop resistance against 5-FU-induced inhibition of proliferation.

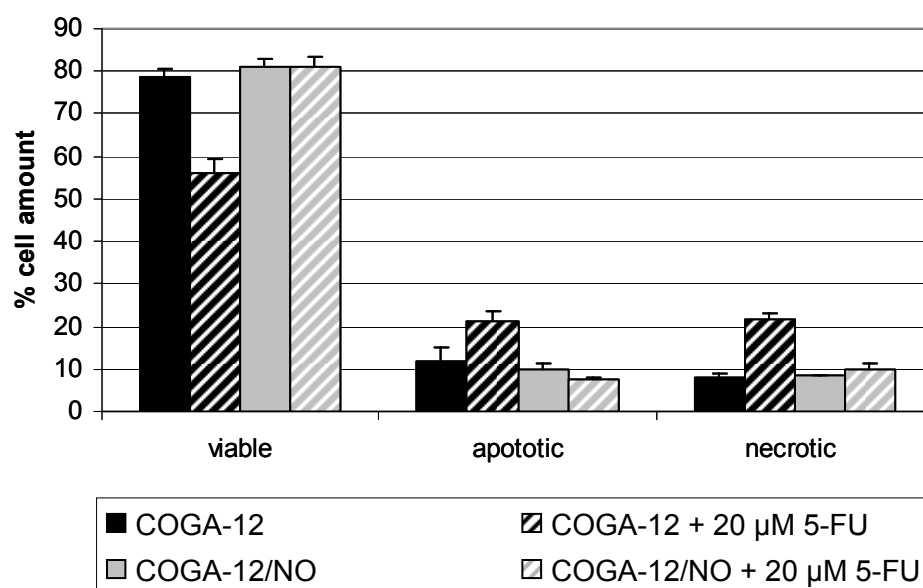


Fig. 21. Percentage of apoptotic cells in 5-FU treated low and high passage COGA-12 cells. 2.8×10^5 cells per well were incubated with 20 μ M 5-FU for three days. Growth medium was exchanged every day. Necrotic cells were detected after staining with propidium iodide and apoptotic cells after staining with annexin V and subsequent flow cytometry. The values are representative means \pm SE of duplicates in two independent experiments.

3.2.6. Differences in the expression profiles of chemoresistant cells compared to corresponding chemosensitive cells

To discover changes in the expression profile that are responsible for mediating the above described chemoresistance, the expression profile of the chemoresistant subline COGA-12/G6 was compared with the expression profile of the corresponding 5-FU sensitive parental cell line COGA-12 by 2D electrophoresis. 2D electrophoresis was performed with 200 μ g total protein of sensitive COGA-12 cells and resistant COGA-12/G6 cells. In addition, 2D electrophoresis was also performed with COGA-12/NO cells, which were resistant against 5-FU-induced apoptosis as consequence of long-term cultivation without 5-FU treatment, to distinguish between changes in the expression profile due to long-term 5-FU treatment or long-term propagation alone.

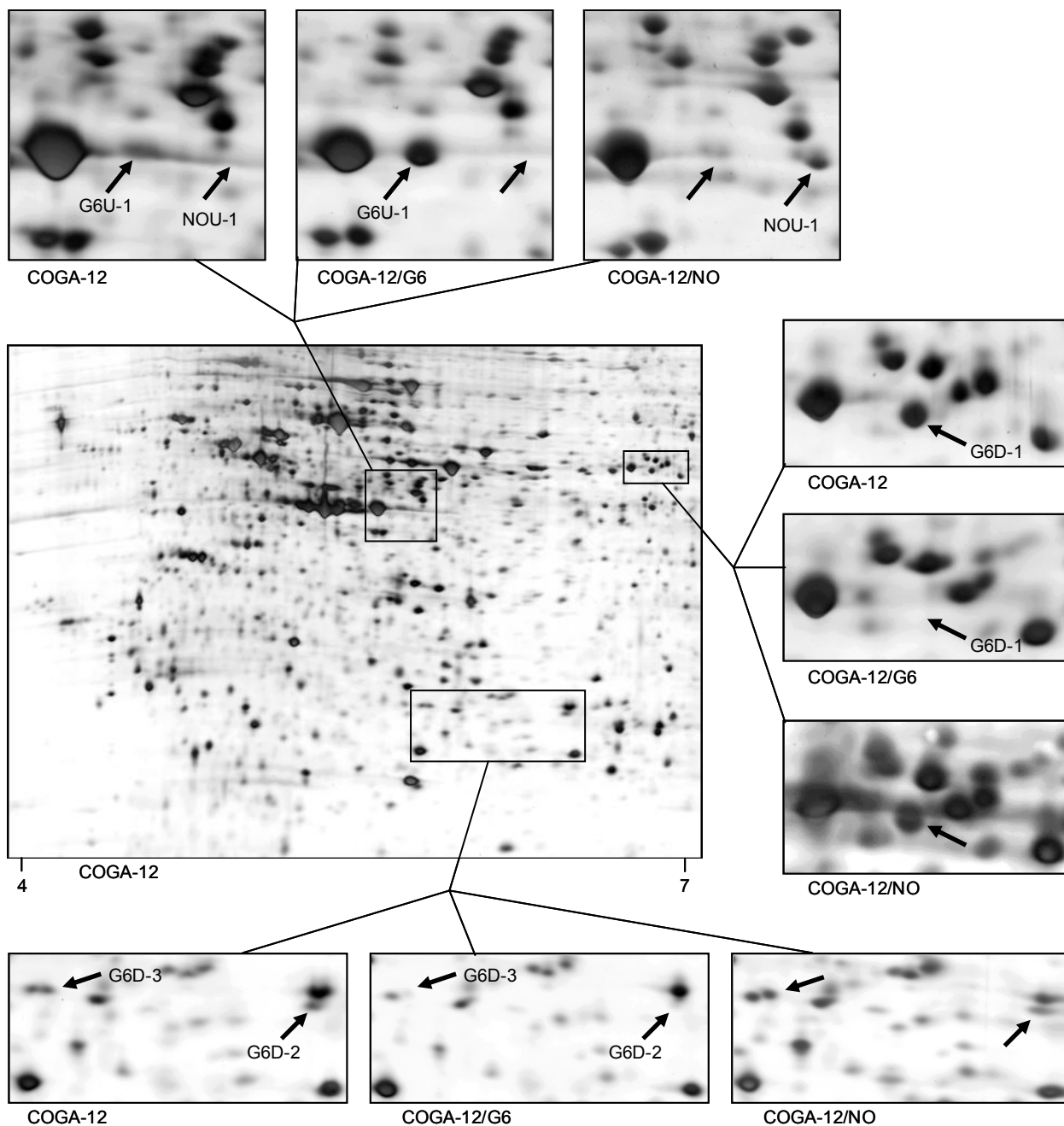


Fig. 22. Differences in the expression profiles of COGA-12, COGA-12/G6 and COGA-12/NO cells obtained by 2D electrophoresis. 2D electrophoresis was performed with IPG dry strips pH 4 - 7 in the first dimension and 11 % SDS-polyacrylamide gels in the second dimension. Representative silver stained gels are shown. Differences in the expression profiles are marked with an arrow. The respective spot intensities are listed in Table 6 and corresponding proteins identified by MALDI-TOF mass spectrometry are listed in Table 7. Respective abbreviations for numbering of spots: e.g. G6D-1: COGA-12/G6 cells, down-regulated spot number 1.

As shown in **Fig. 22** the performance of 2D electrophoresis revealed four spots that were differentially expressed between parental COGA-12 and chemoresistant COGA-12/G6 cells. One of them was up-regulated and the other three were down-regulated in the chemoresistant subline. All four changes were found exclusively in COGA-12/G6 cells but not in COGA-12/NO cells when compared to COGA-12 cells. It is important to note that one spot was detected that was exclusively differentially expressed between COGA-12/NO and COGA-12 cells as shown in **Fig. 22** (up-regulated in COGA-12/NO). The average intensities of all regulated proteins between COGA-12 cells and chemoresistant COGA-12/G6 or long-term cultivated COGA-12/NO cells are shown in **Table 6**.

The proteins that belong to the differentially expressed spots were identified by MALDI-TOF mass spectrometry and subsequent peptide mass fingerprinting. To achieve sufficient sensitivity for mass spectrometry, spots of preparative 2D gels with the total protein amount of 10×10^6 cells were used as described above. The identified proteins are shown in **Table 7**. Corresponding mass spectra and protein identifications results are shown in **Fig. 23 - 27**. The up-regulated protein in chemoresistant COGA-12/G6 cells was identified as cytokeratin 18. Two of the down-regulated proteins were identified as the same protein, namely heat shock protein (HSP) 27. The two proteins represent most likely two different posttranslational modifications (PTMs) of HSP27. The other down-regulated protein in COGA-12/G6 cells was identified as aldehyde dehydrogenase 1B1. The spot differentially expressed in long-term cultivated COGA-12/NO cells was identified as maspin (**Table 7**).

Spot number	Average intensity in COGA-12 cells	Average intensity in COGA-12/G6 cells or COGA-12/NO cells	Ratio COGA-12/G6 / COGA-12 cells or COGA-12/NO / COGA-12 cells
G6U-1	0.756 ± 0.214	2.057 ± 0.312	2.72
G6D-1	0.710 ± 0.065	---	not expressed in COGA-12/G6
G6D-2	0.762 ± 0.111	---	not expressed in COGA-12/G6
G6D-3	0.410 ± 0.109	0.111 ± 0.016	0.27
NOU-1	---	0.506 ± 0.070	only expressed in COGA-12/NO

Table 6. Average intensities of the protein spots altered between 2D gels of COGA-12 cells and 5-FU resistant COGA-12/G6 cells or long-term cultivated COGA-12/NO cells. The respective normalized average intensities ± SE of at least three separate 2D gels analyzed with the Proteomweaver software are listed.

Spot number	Protein name identified by MALDI-TOF mass spectrometry	Regulation in COGA-12/G6 or COGA-12/NO cells
G6U-1	Cytokeratin 18	up
G6D-1	Aldehyde Dehydrogenase 1B1	down
G6D-2	Heat shock protein 27	down
G6D-3	Heat shock protein 27	down
NOU-1	Maspin	up

Table 7. Proteins differentially expressed between parental COGA-12 cells and 5-FU resistant COGA-12/G6 or long-term cultivated COGA-12/NO cells

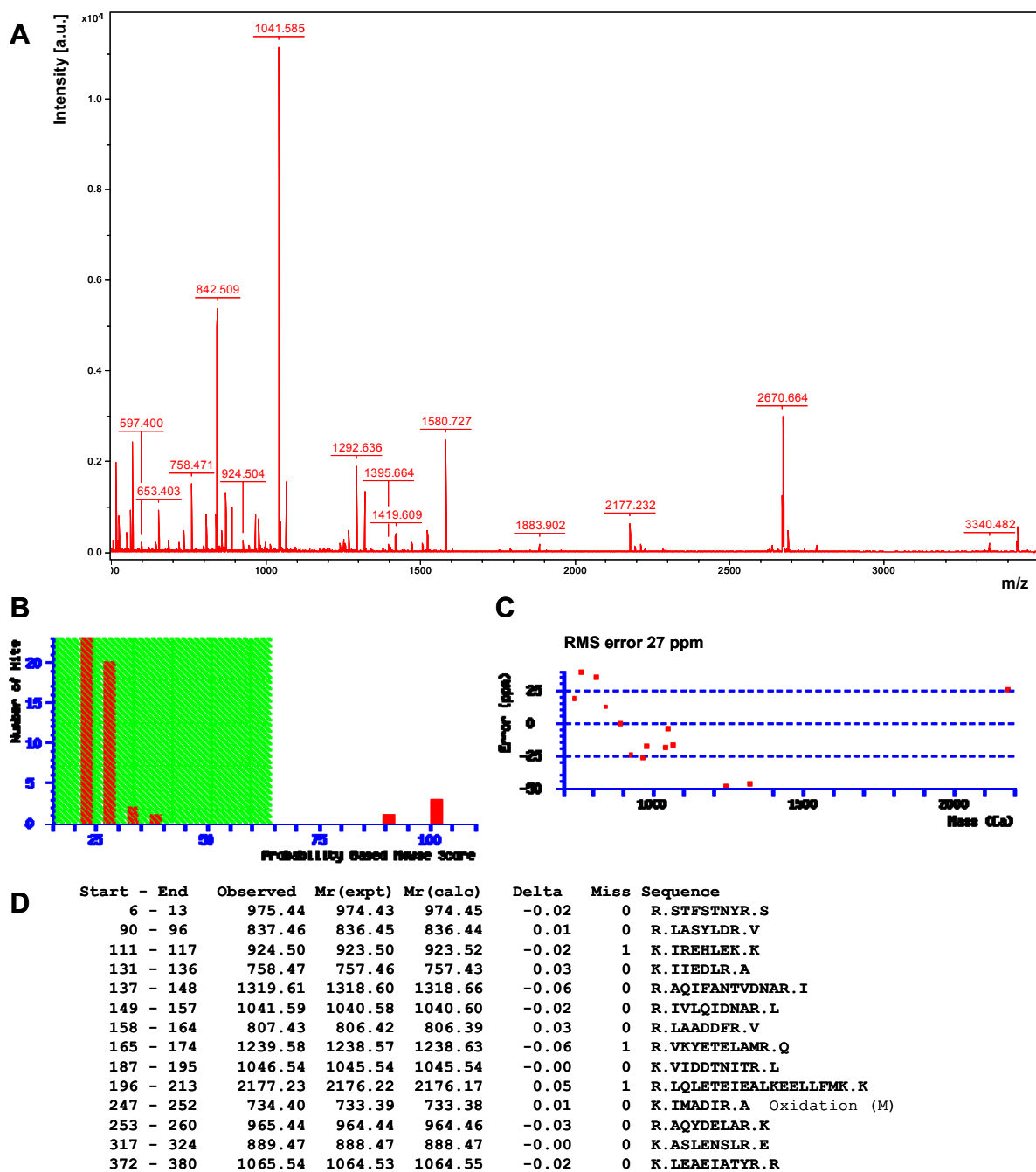


Fig. 23. Identification of spot G6U-1. (A) Mass spectrum of G6U-1 obtained after in-gel digestion and MALDI-TOF analysis. (B-D) Protein identification results obtained by database search on MASCOT server. Identifications were obtained after internal recalibration of the mass spectrum using peaks deriving from autoprolysis of trypsin, with 50 ppm, as mass tolerance, and allowing only 1 missing cleavage. (B) Probability based mowse score. Ions score is $-10 \cdot \log(P)$, where P is the probability that the observed match is a random event. Protein scores greater than 64 are significant ($p < 0.05$). (C) Root mean square (RMS) error graph. (D) Peptides matched with the sequence of cytokeratin 18 and their molecular mass are reported.

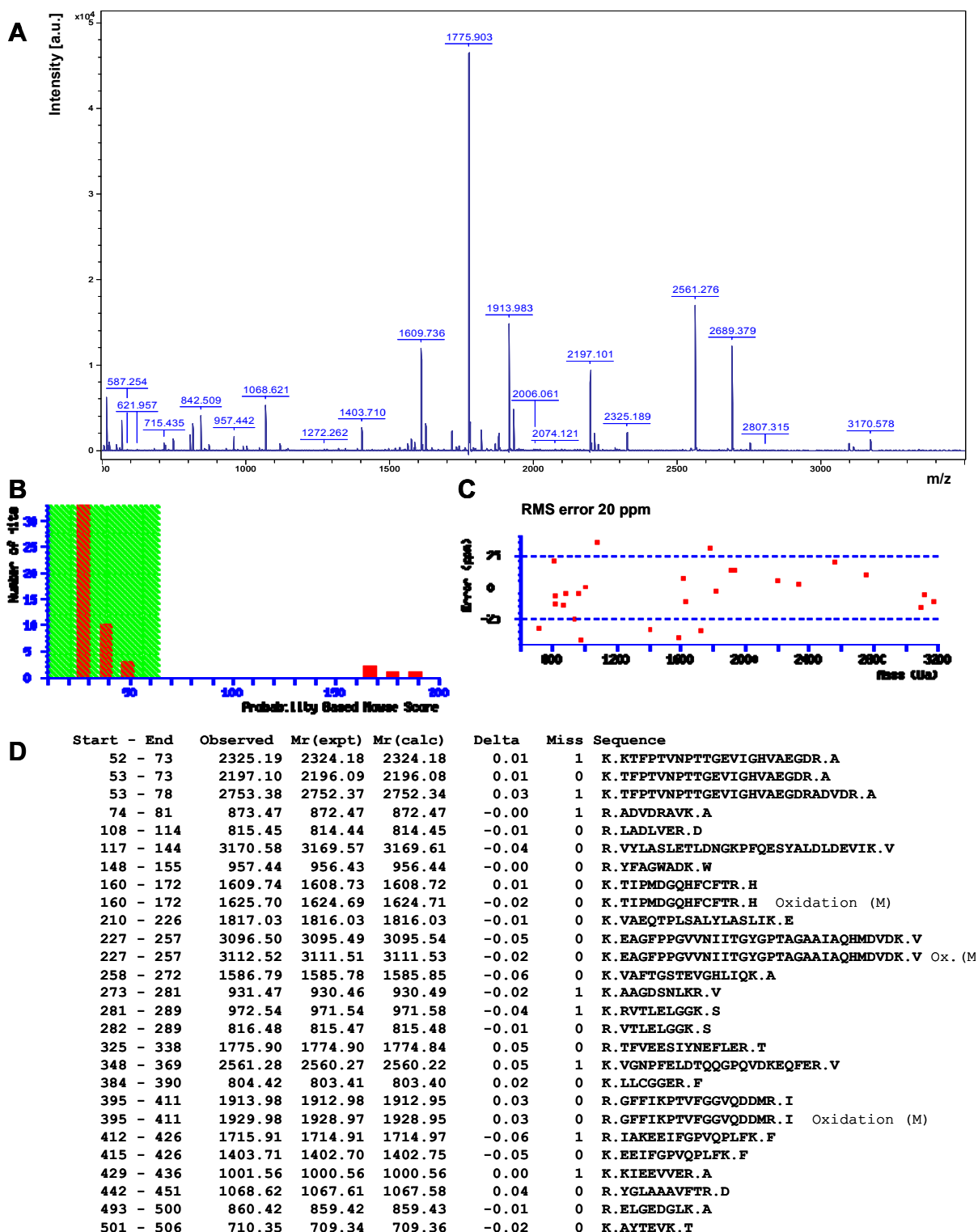


Fig. 24. Identification of spot G6D-1. (A) Mass spectrum of G6D-1 obtained after in-gel digestion and MALDI-TOF analysis. (B-D) Protein identification results obtained by database search on MASCOT server. Identifications were obtained after internal recalibration of the mass spectrum using peaks deriving from autolysis of trypsin, with 50 ppm, as mass tolerance, and allowing only 1 missing cleavage. (B) Probability based mowse score. Ions score is $-10 \cdot \log(P)$, where P is the probability that the observed match is a random event. Protein scores greater than 64 are significant ($p < 0.05$). (C) Root mean square (RMS) error graph. (D) Peptides matched with the sequence of aldehyde dehydrogenase 1B1 and their molecular mass are reported.

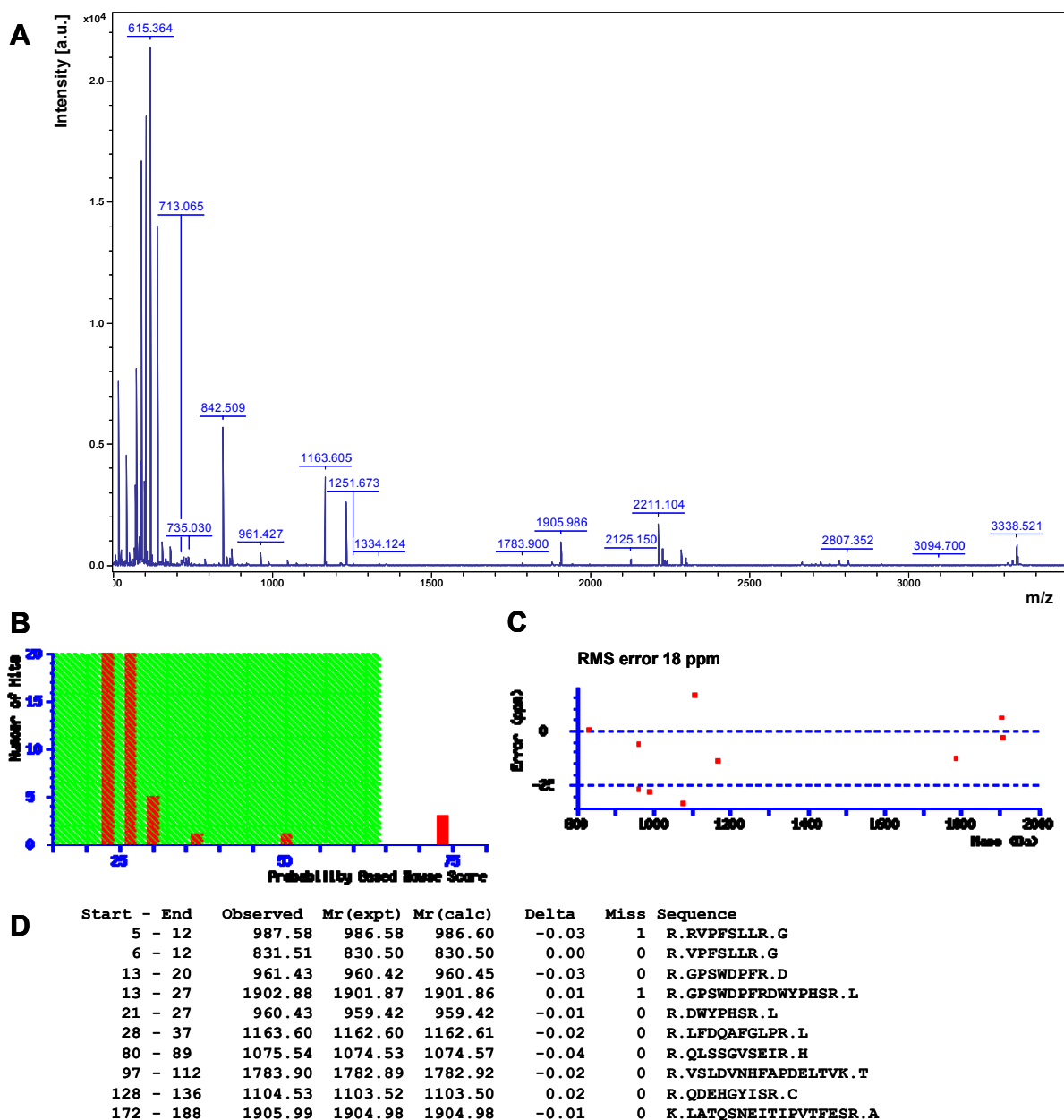


Fig. 25. Identification of spot G6D-2. (A) Mass spectrum of G6D-2 obtained after in-gel digestion and MALDI-TOF analysis. (B-D) Protein identification results obtained by database search on MASCOT server. Identifications were obtained after internal recalibration of the mass spectrum using peaks deriving from autoproteolysis of trypsin, with 50 ppm, as mass tolerance, and allowing only 1 missing cleavage. (B) Probability based mowse score. Ions score is $-10 \cdot \log(P)$, where P is the probability that the observed match is a random event. Protein scores greater than 64 are significant ($p < 0.05$). (C) Root mean square (RMS) error graph. (D) Peptides matched with the sequence of heat shock protein 27 and their molecular mass are reported.

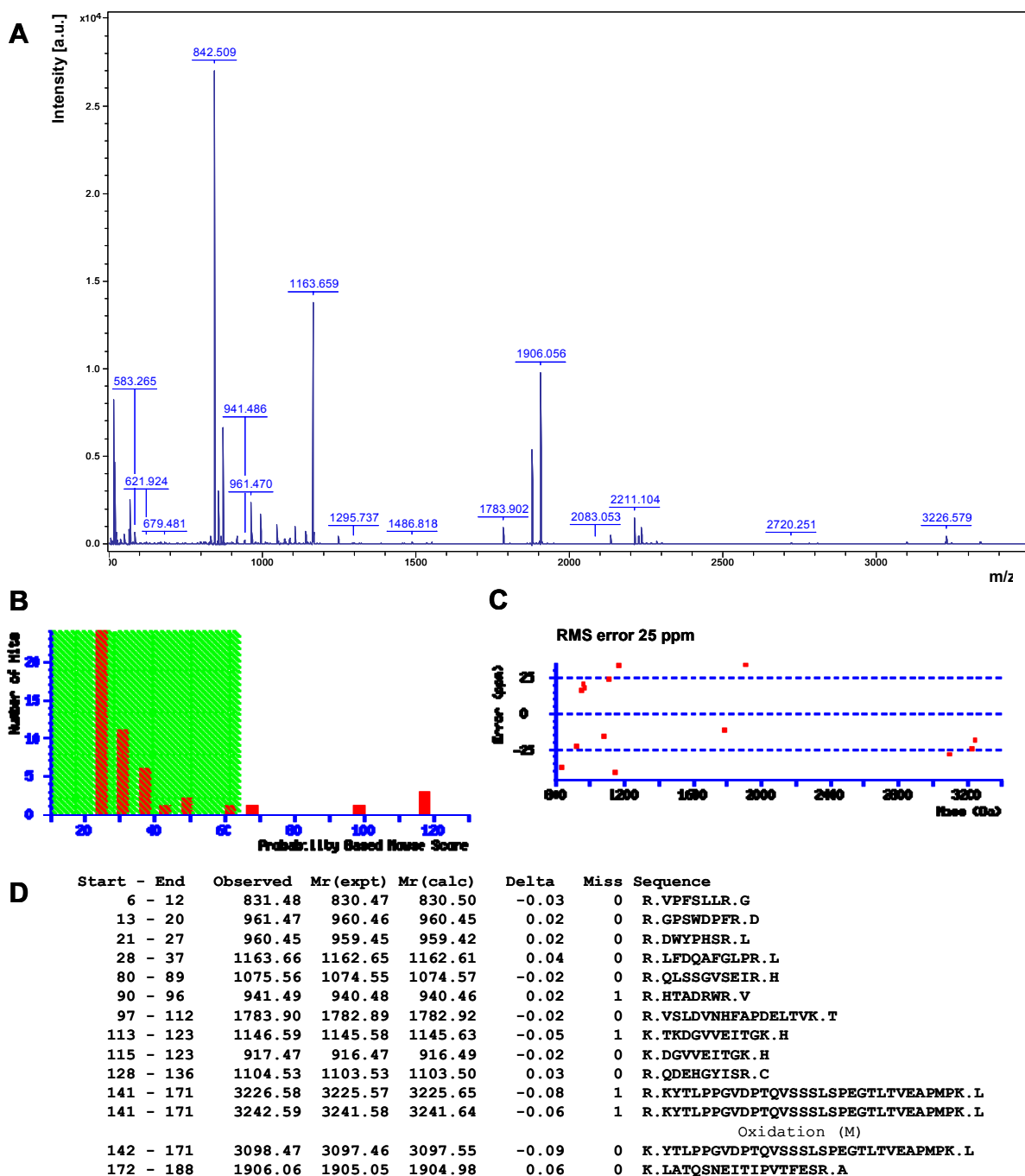


Fig. 26. Identification of spot G6D-3. (A) Mass spectrum of G6D-3 obtained after in-gel digestion and MALDI-TOF analysis. (B-D) Protein identification results obtained by database search on MASCOT server. Identifications were obtained after internal recalibration of the mass spectrum using peaks deriving from autolysis of trypsin, with 50 ppm, as mass tolerance, and allowing only 1 missing cleavage. (B) Probability based mowse score. Ions score is $-10 \cdot \log(P)$, where P is the probability that the observed match is a random event. Protein scores greater than 64 are significant ($p < 0.05$). (C) Root mean square (RMS) error graph. (D) Peptides matched with the sequence of heat shock protein 27 and their molecular mass are reported.

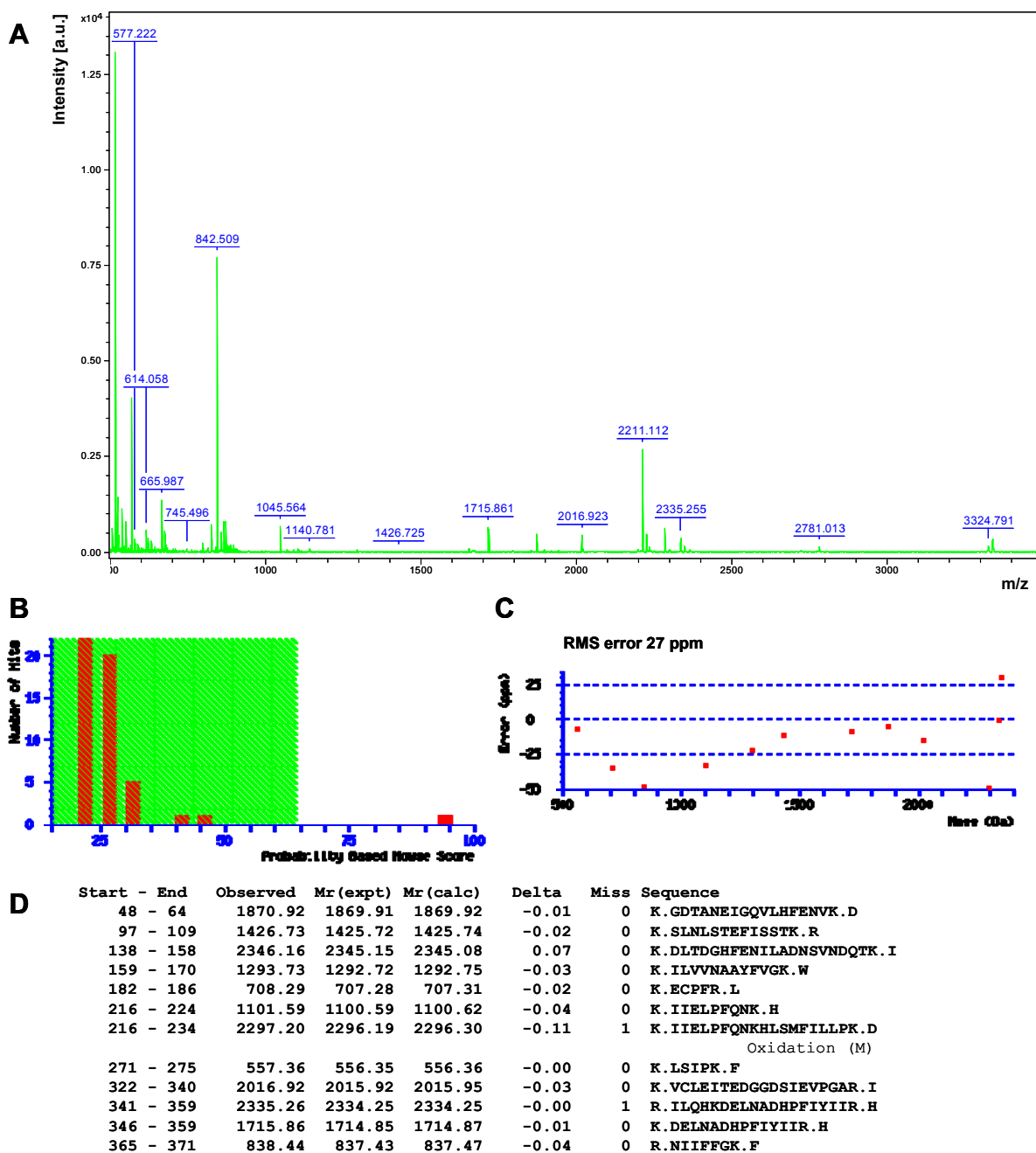


Fig. 27. Identification of spot NOU-1. (A) Mass spectrum of NOU-1 obtained after in-gel digestion and MALDI-TOF analysis. (B-D) Protein identification results obtained by database search on MASCOT server. Identifications were obtained after internal recalibration of the mass spectrum using peaks deriving from autoproteolysis of trypsin, with 50 ppm, as mass tolerance, and allowing only 1 missing cleavage. (B) Probability based mowse score. Ions score is $-10 \cdot \log(P)$, where P is the probability that the observed match is a random event. Protein scores greater than 64 are significant ($p < 0.05$). (C) Root mean square (RMS) error graph. (D) Peptides matched with the sequence of maspin and their molecular mass are reported.

3.3. Gene therapy of colorectal cancer

Gene therapy presents an encouraging alternative option for the treatment of colorectal cancers. The concept, however, is technically limited by insufficient efficiency of gene transfer and insufficient tumor specificity. In this thesis the novel cellular model systems were applied for the development and optimization of a novel gene therapy concept for colorectal cancers. First, nonviral gene transfer was optimized by generation of novel lipopolyplex formulations and comparison to lipoplex and polyplex formulations. These experiments were performed in collaboration with Dr. Jaroslav Pelisek. Second, the artificial promoter CTP4 was evaluated for transcriptional targeting of colorectal cancer cells. And third, therapeutic gene constructs for the expression of the immune stimulatory IL-2 gene, optionally in combination with the cytopathic rhinovirus protease 2A gene, were tested and optimized. The investigations were carried out with the low passage colon cancer cell lines and as control SW480 (standard colorectal cell line) and HeLa (non-colorectal) cells were used. In addition to traditional monolayer cultures, also multicellular spheroids of the low passage cell lines were used for some investigations.

3.3.1. Optimization of nonviral gene transfer to colorectal cancer cells

It was already reported that the combination of cationic lipids and polycations to form lipopolyplexes significantly improved gene transfer in different cell lines (Lampela et al., 2002; Lampela et al., 2003; Lampela et al., 2004; Lee et al., 2003). In this thesis different polycations (PLL18, PEI22lin, PEI25br, PEI2k) and cationic lipids (DOCSPER, DOSPER, DOTAP) were used to form various lipoplex, polyplex and lipopolyplex formulations to find the most adequate formulation that is promising for a successful *in vivo* application. For this purpose, it is necessary that the complexes do not aggregate and retain small particle size under physiological conditions, but are still efficient in mediating gene transfer.

3.3.1.1. Generation and biophysical properties of nonviral gene transfer formulations

Nonviral DNA formulations were generated as described in materials and methods. In short, lipopolyplexes and polyplexes were prepared by mixing plasmid DNA with

cationic lipids or polycations, respectively. For the preparation of lipopolyplexes plasmid DNA was precomplexed with polycations and subsequently mixed with cationic lipids. PEIs were used at an optimized N/P ratio (describes the molar ratio of PEI nitrogen to DNA phosphate) of 8/1 and PLL18 at an optimized charge ratio of 5/1 (Pelisek et al., 2005). Cationic lipids were used at following optimized ratios: DOCSPER/DNA at w/w ratio 10/1; DOSPER/DNA at w/w ratio 8/1 and DOTAP/DNA at w/w ratio 4/1 (Pelisek et al., 2005). The sizes of the different lipoplex, polyplex, and lipopolyplex formulations generated at low or physiological ionic strength were measured using dynamic laser-light scattering (**Fig. 28**).

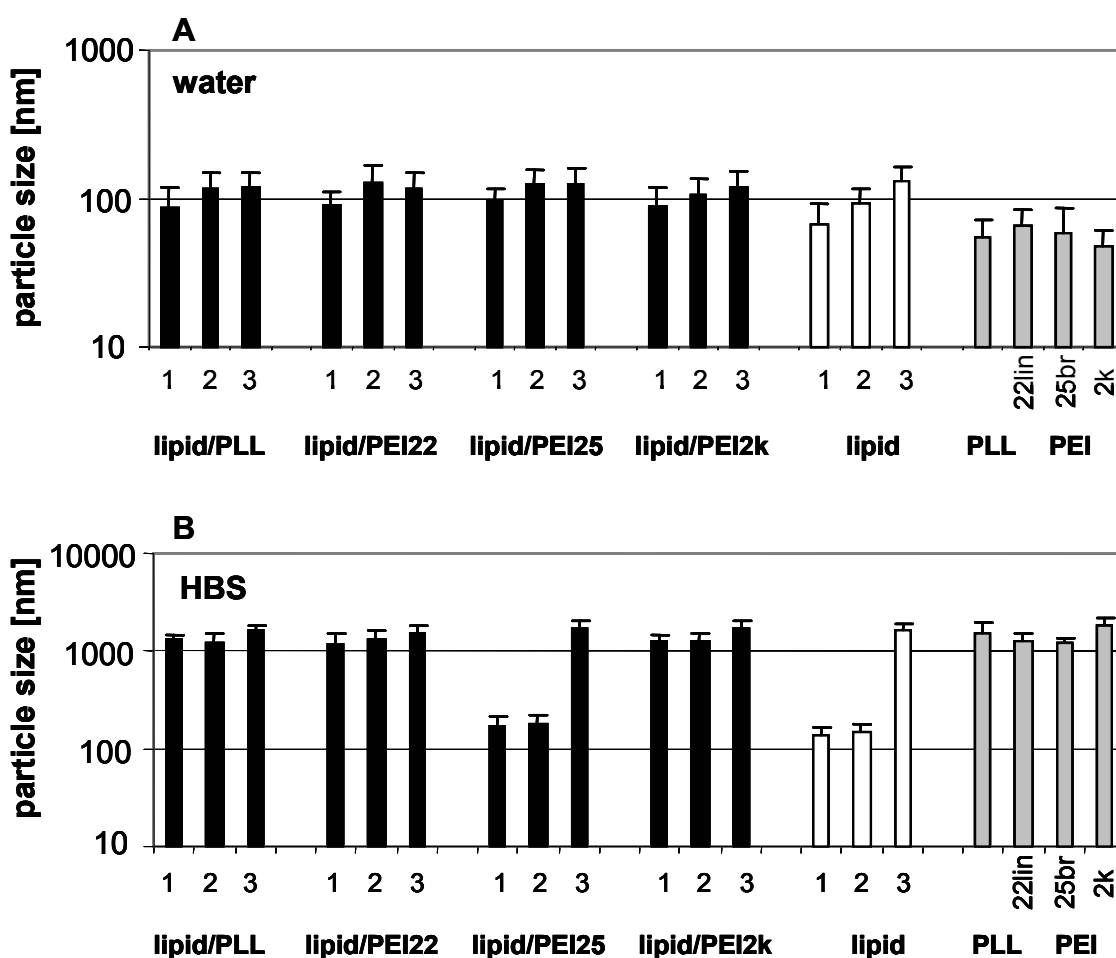


Fig. 28. Size of different lipopolyplex, lipoplex, and polyplex formulations generated at low (A) or physiological (B) ionic strength. Plasmid DNA (pCMV-Luc) was complexed in 1 ml of water (A) or HBS (B) using 5 μ g DNA and different cationic lipids (1: DOCSPER, 2: DOSPER, 3: DOTAP), different polycations (PLL18, PEI22lin, PEI25br, PEI2k), or polycation/cationic lipid combinations. The values are the means \pm SE of triplicates in two independent experiments. Experiments were performed by Dr. Jaroslav Pelisek.

At low ionic strength polyplexes, lipoplexes and lipopolyplexes were stable in particle size within a range of 50-130 nm at room temperature (**Fig. 28A**). At physiological ionic strength (HBS, pH 7.4), lipoplexes of DOTAP and polyplexes of PLL18, PEI22lin, PEI25br and PEI2k aggregated at high salt, achieving particle size distributions of 1 to 2 μm (**Fig. 28B**). Lipopolyplexes combined of DOTAP and PLL18, PEI22lin, PEI25br and PEI2k formed also large aggregates of over 1 μm at high ionic strength conditions (**Fig. 28B**). In contrast, lipoplexes of DOCSPER or DOSPER and their respective lipopolyplexes with PEI25br were stable to aggregation in high salt (140 - 220 nm) (**Fig. 28B**). Therefore, these particular lipopolyplex formulations were selected for the further experiments. The zeta-potential of all formulations had a positive charge of +20 to +40 mV.

3.3.1.2. Determination of the efficiencies of the most adequate formulations in gene transfer

The PEI25 lipopolyplex formulations which were stable in physiological salt (DOSPER/PEI25br/DNA and DOCSPER/PEI25br/DNA) were tested for their efficiency in gene transfer on one representative of each morphological category of the low passage colon cancer cell lines, namely COGA-5 (epithelial-like), COGA-12 (piled-up) and COGA-3 (rounded-up), and in addition on two control cell lines, SW480 (standard colorectal cell line) and HeLa (non-colorectal). The efficiency of the lipopolyplexes was compared to the corresponding lipoplexes and polyplexes. The luciferase activities of these formulations on HeLa, SW480, and COGA-3, -5, and 12 cells are shown in **Fig. 29**. Both lipopolyplexes significantly enhanced gene transfer (up to 400-fold) compared to the corresponding lipoplexes or polyplexes (**Fig. 29**). The gene transfer was demonstrated to depend on the presence or absence of serum in the transfer medium. When performing gene transfer in serum-free medium the level of luciferase gene expression was up to 220-fold higher using lipopolyplexes compared to corresponding lipoplexes and 110-fold higher compared to the corresponding polyplexes (**Fig. 29**). In the presence of serum the enhancement of gene transfer of lipopolyplexes compared to corresponding lipoplexes was up to 400-fold and compared to the corresponding polyplexes up to 170-fold (**Fig. 29**). Gene transfer efficiencies of lipopolyplexes were 2 to 20-fold lower in the presence of serum compared to incubation in serum-free medium (**Fig. 29**). Lipoplexes were

more affected by the presence of serum, with an up to 100-fold decrease in transfer efficiency. For polyplexes, the gene transfer in the presence of serum was only up to 10-fold lower compared to polyplexes in serum-free medium.

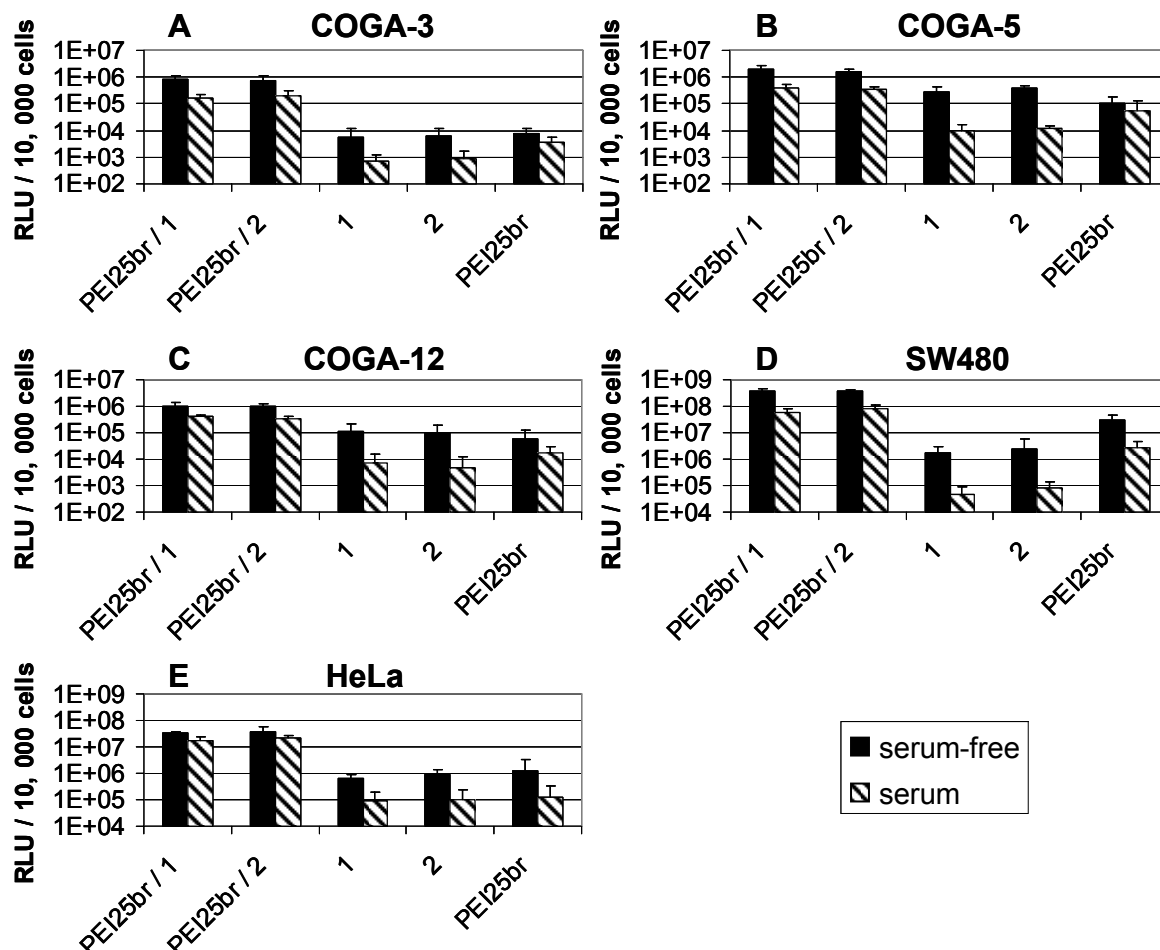


Fig. 29. Gene transfer efficiencies of lipopolyplexes in comparison to the corresponding lipopolyplexes and polyplexes in Coga-3 (A), Coga-5 (B), Coga-12 (C), HeLa (D) and SW480 (E) cells. For transfections $0.1 \mu\text{g}$ pCMV-Luc per 1×10^4 cells were used. Complexes were formed in HBS. Gene transfer was performed either in serum-free medium or in medium containing 10 % serum. 1: DOCSPER, 2: DOSPER. The values are means \pm SE of triplicates in three independent experiments. Experiments were performed in collaboration with Dr. Jaroslav Pelisek.

As the salt stable lipopolyplex formulations of PEI25br and DOCSPER or DOSPER significantly enhanced gene transfer, these formulations were used for all further experiments. Moreover, only the cationic lipid DOSPER was used, as DOCSPER and DOSPER provided comparable results.

It is known that sedimentation of large complexes may be helpful for *in vitro* transfection. Therefore, the transfection efficiency of DOSPER/PEI25br/DNA lipopolyplexes (which are stable against aggregation in physiological salt) was also

compared to DOSPER/PEI22lin/DNA lipopolyplexes (which form large aggregates). The aggregated DOSPER/PEI22lin/DNA lipopolyplex formulation displayed nearly the same gene transfer efficiency in HeLa and SW480 cells, and only slightly (up to 3-fold) higher efficiency in the COGA cells as compared to the stable DOSPER/PEI25br/DNA lipopolyplexes (Fig. 30).

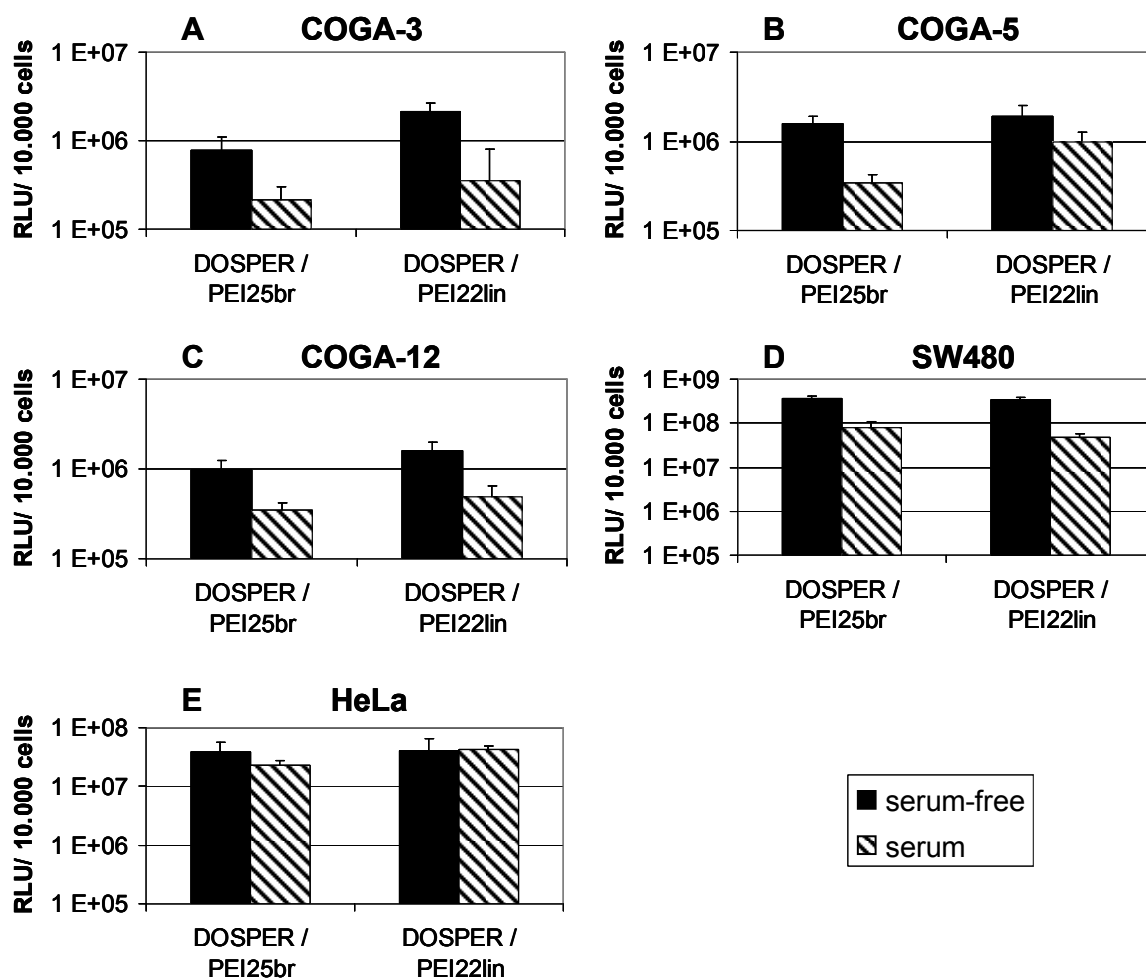


Fig. 30. Gene transfer efficiencies of salt stable DOSPER/PEI25br/DNA lipopolyplexes in comparison to DOSPER/PEI22lin/DNA lipopolyplexes aggregating in physiological salt in COGA-3 (A), COGA-5 (B), COGA-12 (C), SW480 (D) and HeLa (E) cells. 0.1 μg of pCMV-Luc per 1×10^4 cells were used for transfection. Gene transfer was performed either in serum-free medium or in medium containing 10 % serum. Values are means \pm SE of triplicates. Experiments were performed in collaboration with Dr. Jaroslav Pelisek.

3.3.1.3. Transfection of multicellular spheroids with lipopolyplexes

Furthermore, it was investigated whether lipopolyplexes also enable a sufficient transfection of multicellular spheroids. Multicellular spheroids are model systems that mimic the three-dimensional structure of *in vivo* tumors in contrast to traditional monolayers. The lipopolyplex formulation was the only formulation that was used for

gene transfer, because this formulation resulted in the highest transfection efficiencies in the previous cell culture experiment. Multicellular spheroids of cell line COGA-12 were chosen for these investigations. They were grown in medium containing 2 % or 10 % serum. Forty-eight or 96 hours after their formation multicellular spheroids were transfected with 0.1 μg , 0.25 μg , 0.5 μg , 1 μg and 2 μg of pEGFP-N1 plasmid by using lipopolyplexes for gene transfer. Forty-eight hours after transfection (96 or 144 hours after multicellular spheroid formation) the amount of EGFP positive cells was estimated by epifluorescence microscopy. Significant EGFP expression could be observed (**Fig. 31**). However, only the upper, accessible part of the multicellular spheroids exposed to the growth medium exhibited EGFP fluorescence (**Fig. 31A**), while the lower part facing the agarose coating on the bottom of the culture plate did not (**Fig. 31B**).

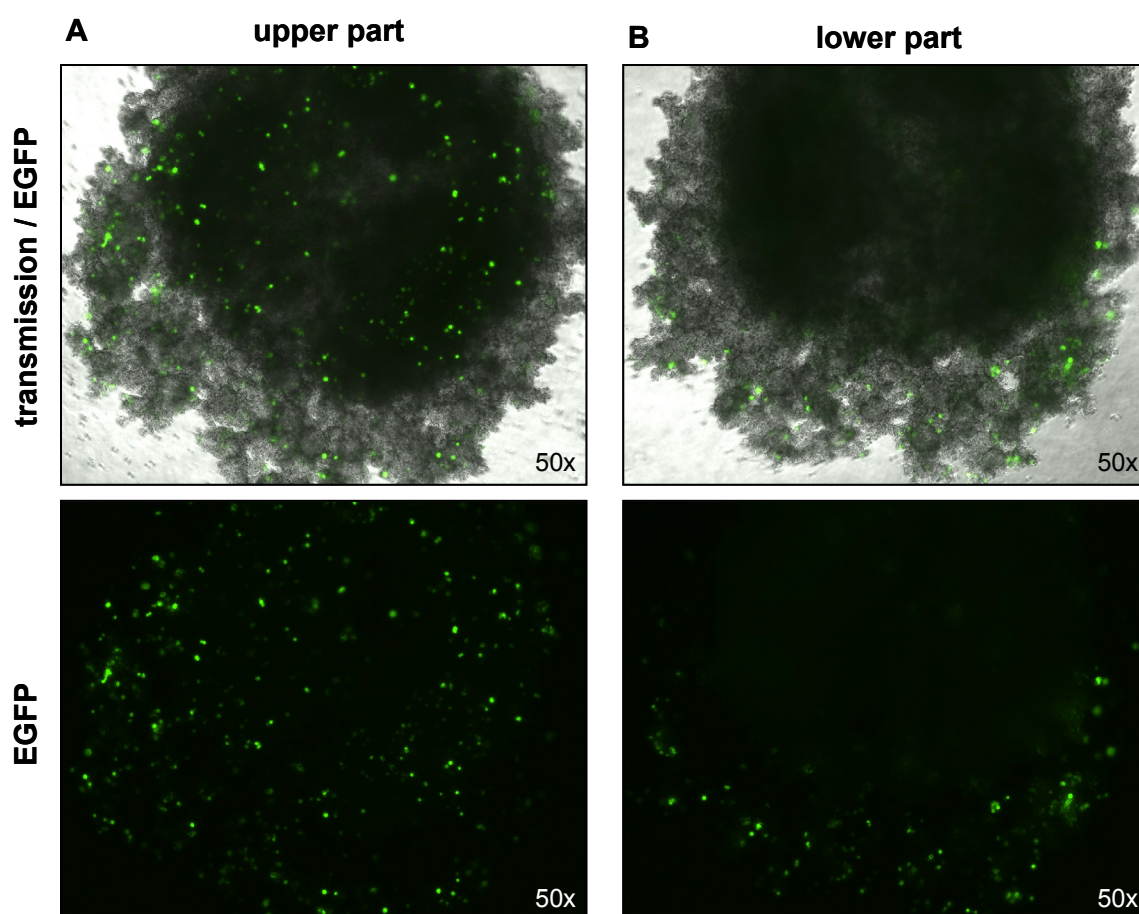


Fig. 31. EGFP expression after transfection of multicellular spheroids using lipopolyplexes for gene transfer. Multicellular spheroids of COGA-12 cells grown in medium containing 2 % serum were transfected with 0.25 μg pEGFP-N1 48 h after multicellular spheroid formation. Forty-eight hours after transfection epifluorescence microscopy was performed. Shown are overlays of transmission light and epifluorescence images (top panels) and the respective epifluorescence images (lower panels) of the upper part (A) and lower part (B) of the same multicellular spheroid.

In general, the amount of transfected COGA-12 cells was higher in medium containing 2 % serum compared to medium containing 10 % serum, while it didn't make a visual difference if multicellular spheroids were transfected 48 h or 96 h after multicellular spheroid formation. The highest number of transfected cells was obtained with 0.25 μg and 0.5 μg DNA. No visual difference in the amount of EGFP positive cells could be detected between these both concentrations. Confocal laser scanning microscopy of DAPI (4',6-Diamidino-2-phenylindole) counterstained, EGFP-transfected multicellular spheroids revealed that predominantly cells located between the surface and about 60 μm depth were transfected (**Fig. 32A**). DAPI also stained only the outer cell layers of the multicellular spheroids. As the depth of penetration of confocal laser scanning microscopy is limited, additionally cryosections of the transfected multicellular spheroids were prepared. These confirmed that only cells at the surface of the multicellular spheroids exhibited EGFP fluorescence (**Fig. 32B**).

In summary, lipopolyplexes are not only efficient in gene transfer to monolayers, but also in gene transfer to tumor-like three-dimensional model systems.

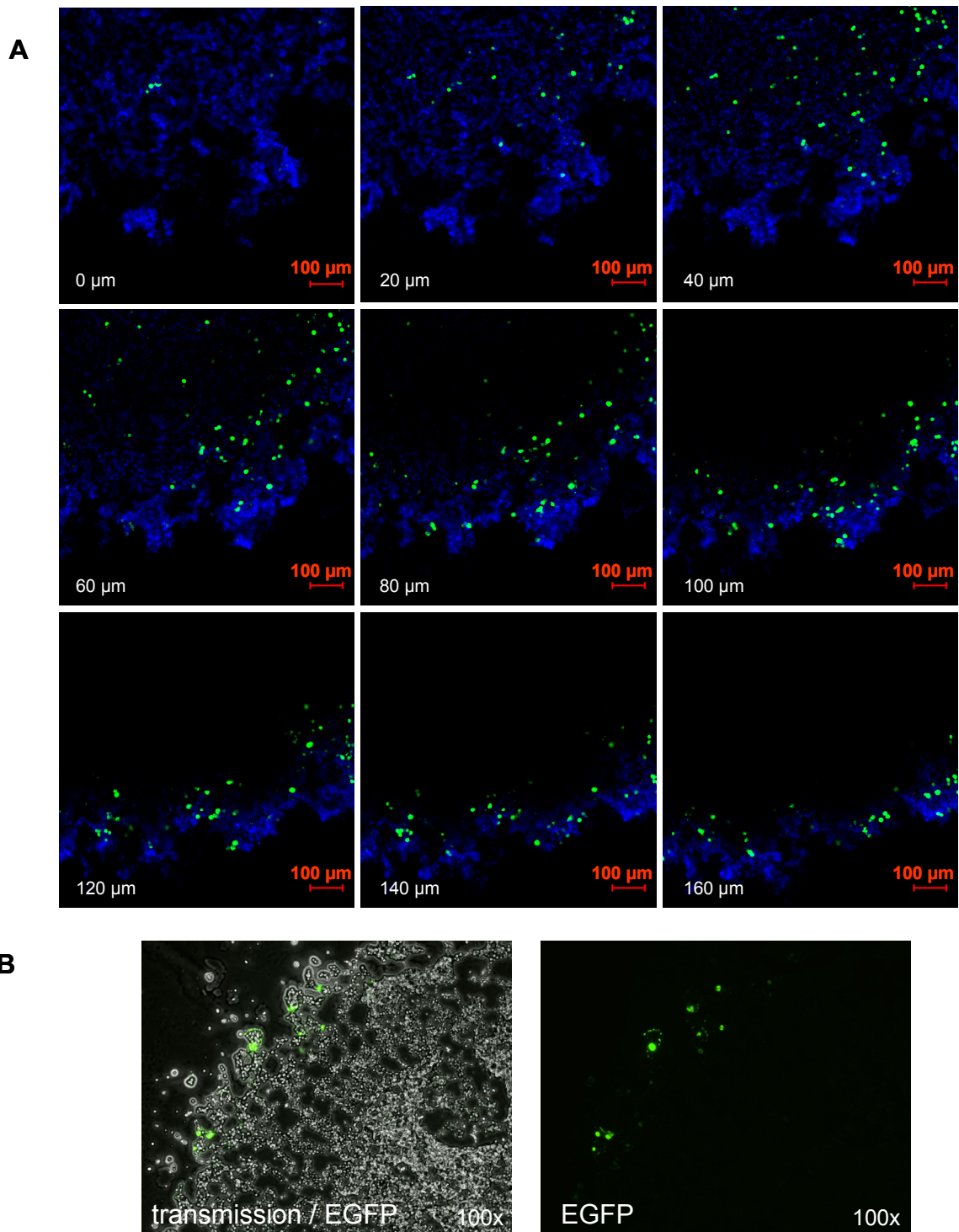


Fig. 32. Distribution of EGFP transfected cells within a multicellular spheroid of COGA-12 cells using lipopolyplexes for gene transfer. Multicellular spheroids grown in medium containing 2 % serum were transfected with 0.25 μg pEGFP-N1 48 h after spheroid formation. Forty-eight hours after transfection multicellular spheroids were fixed in 4 % PFA. (A) For confocal laser scanning microscopy cells of the multicellular spheroid were counterstained with DAPI. Confocal laser scanning microscopy stack images were taken every 20 μm moving from the outside to the inside of the spheroid. Thereby DAPI stained cell layers indicate the surface of the multicellular spheroid. Overlays of EGFP and DAPI fluorescence images are shown. (B) 10 μm cryosections of the transfected multicellular spheroids were analyzed by epifluorescence microscopy: An overlay of transmission light and epifluorescence images (left) and the respective epifluorescence image (right) are shown.

3.3.2. Transcriptional targeting of colorectal cancer cells

For therapeutic application, it is furthermore necessary that the high efficient gene transfer formulation developed in this thesis is also highly specific for colorectal tumor cells. The targeting of colorectal cancer cells was accomplished by the very promising artificial tumor specific promoter CTP4. The efficiency and specificity of this promoter was investigated in comparison to the strong but unspecific CMV promoter in the following experiments.

3.3.2.1. Gene expression levels after transcriptional targeting in various low passage colon cancer cell lines

Firstly, the relative efficiency of the CTP4 promoter and the CMV promoter was compared in transfection experiments with seven low passage colon cancer cell lines using the luciferase gene expression plasmids pCTP4-Luc or pCMV-Luc and Lipofectamine 2000 for gene transfer (**Fig. 33**). The low passage colon cancer cell lines demonstrate widely heterogeneous morphologies and large diversity regarding for example oncogenic and tumor-suppressive mutations. COGA-1, COGA-5 and COGA-10 are representatives for epithelial-like morphology, COGA-5L and COGA-12 for piled-up and COGA-2 and COGA-3 for rounded-up morphology. SW480 (standard colorectal cell line) and HeLa (non-colorectal) cells were used as controls. In the colorectal standard cell line SW480 and in the rounded-up cell lines COGA-2 and COGA-3 the luciferase expression levels driven by the colon cancer specific promoter CTP4 were even higher than the CMV-driven expression levels (in SW480 cells 5.5-fold, in COGA-2 cells 2.8-fold and in COGA-3 cells 3.7-fold increased expression) (**Fig. 33F-H**). In the piled-up cell line COGA-12 the CTP4-driven expression level was even 30-fold higher than the CMV-driven, while in cell line COGA-5L the colon cancer specific expression was slightly reduced (2-fold), but still in a high range ($> 3 \times 10^5$ RLU/well) (**Fig. 33D-E**). In the cell lines with epithelial-like morphology COGA-1, COGA-5 and COGA-10 the CTP4-driven luciferase expression level was similar (COGA-1) or slightly lower compared to the CMV-driven luciferase expression level (in COGA-5 cells a 2.5-fold and in COGA-10 cells a 5-fold reduction) (**Fig. 33A-C**). In contrast, in non-colorectal control HeLa cells with normal β -catenin levels, a 2300-fold lower expression of luciferase was detected with the CTP4

promoter compared to the CMV promoter (Fig. 33I). This clearly confirms the published high specificity of the CTP4 promoter for colorectal cancer cells.

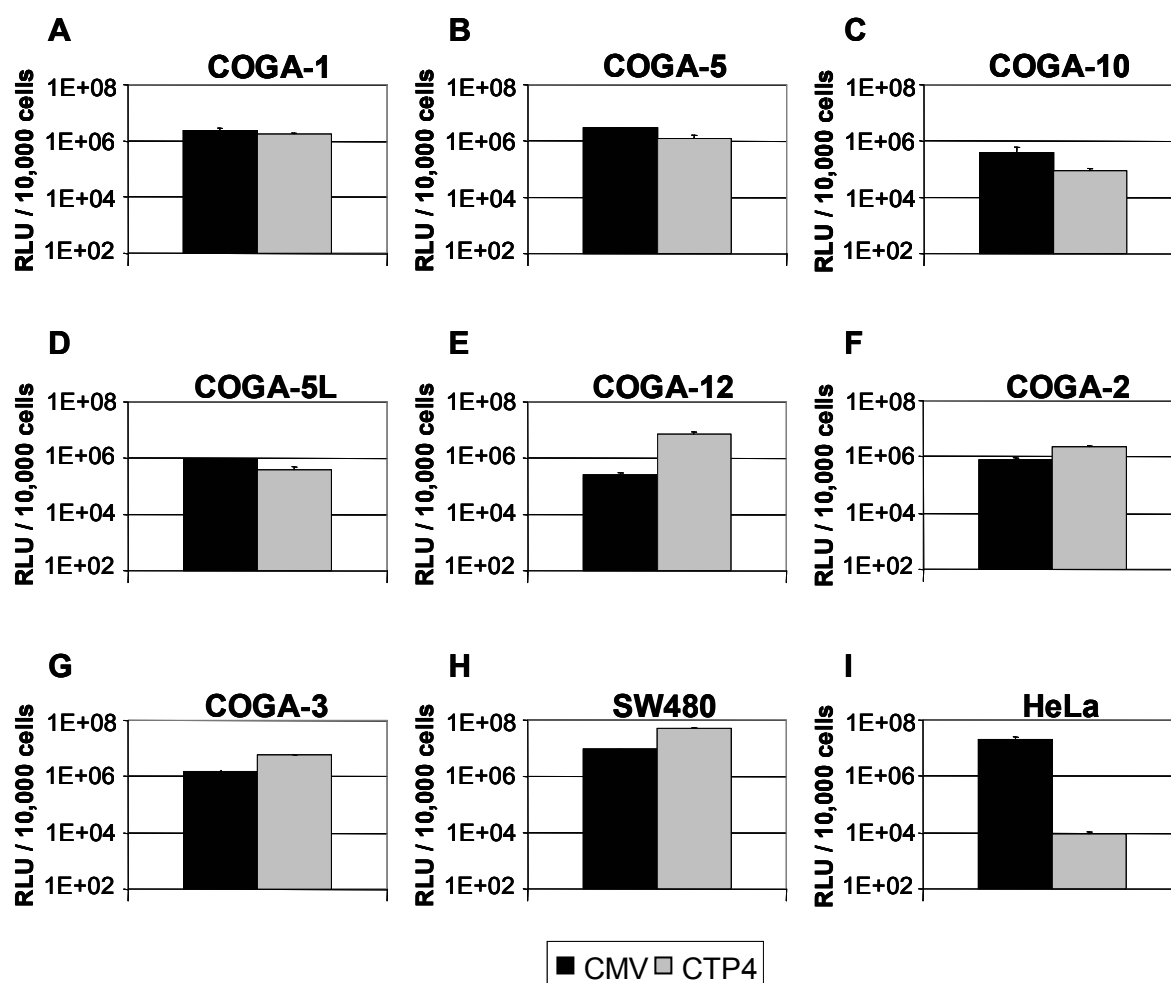


Fig. 33. Luciferase expression by the CTP4 promoter in comparison to the CMV promoter in various low passage colon cancer cell lines of different morphologies. COGA-1 (A), COGA-5 (B) and COGA-10 (C) cells are representatives for epithelial-like morphology, COGA-5L (D) and COGA-12 (E) cells for piled-up and COGA-2 (F) and COGA-3 (G) cells for rounded-up morphology. SW480 (standard colorectal cell line) (H) and HeLa (non-colorectal) (I) cells were used as control. 0.05 μ g of pCMV-Luc or pCTP4-Luc were used for transfection of 1×10^4 cells with Lipofectamine 2000. Gene transfer was performed in serum-free medium. The values are representative means \pm SE of triplicates of at least two independent experiments.

The results above demonstrate the potential of the novel artificial CTP4 promoter to serve as a powerful promoter for cell specific gene therapy. This CTP4 promoter is highly efficient in all low passage colon cancer cell lines tested despite their broad heterogeneity and, in addition, exhibits a very high specificity for colon carcinoma cells.

3.3.2.2. Transfection of selected low passage colon cancer cell lines with transcriptionally targeted lipopolyplexes

Next, the efficiency of the CTP4 promoter was investigated using the optimized lipopolyplex formulation of DOSPER and PEI25br for gene transfer (transcriptionally targeted lipopolyplexes). In addition, the results were compared with the corresponding lipoplex and polyplex formulations. The investigations were performed on the low passage colon cancer cell lines COGA-3, COGA-5 and COGA-12, each representing one morphological category, and on the two control cell lines SW480 and HeLa (Fig. 34).

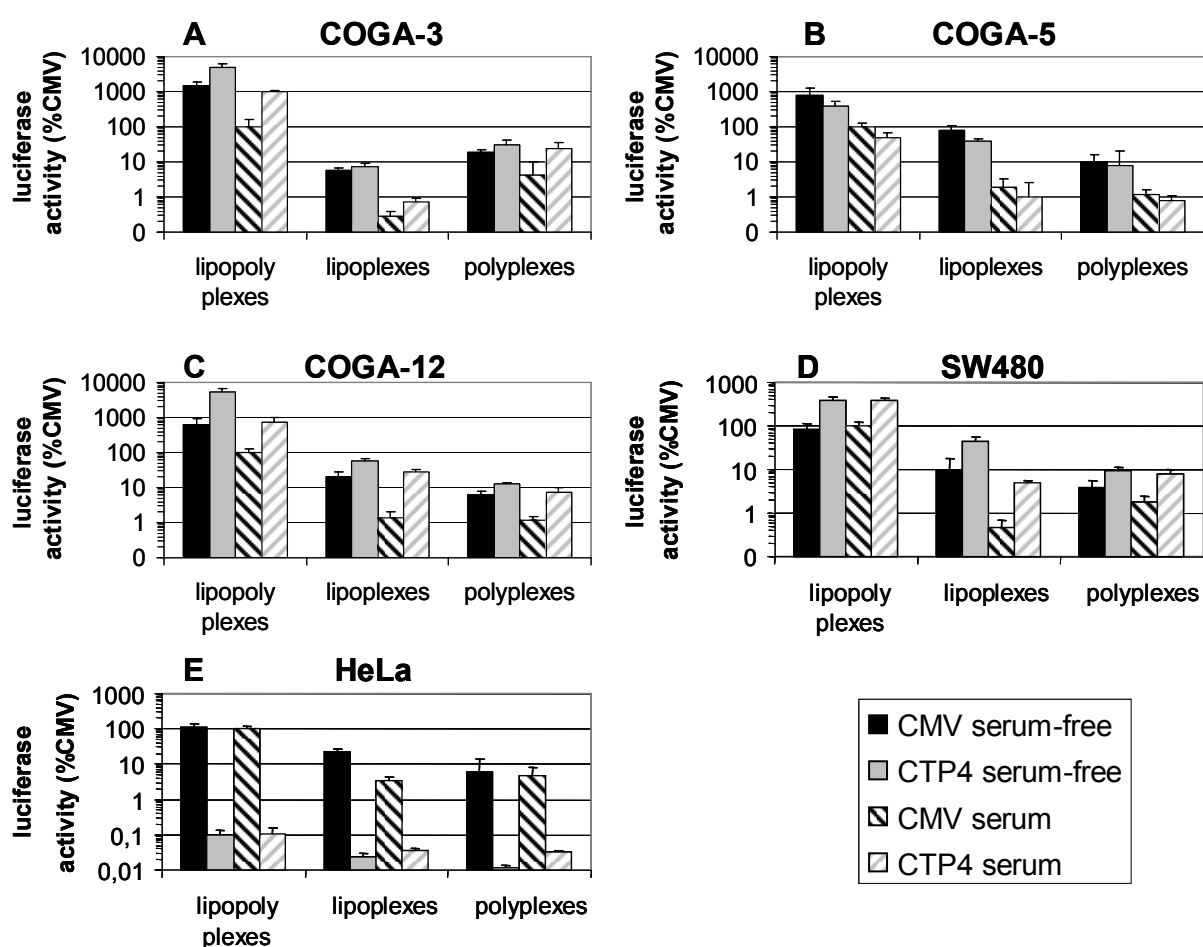


Fig. 34. Luciferase expression by the CTP4 promoter in comparison to the CMV promoter using lipopolyplex, lipoplex and polyplex formulations for gene transfer in COGA-3 (A), COGA-5 (B), COGA-12 (C), SW480 (D) and HeLa (E) cells. 0.1 μ g of pCMV-Luc or pCTP4-Luc were used for transfection of 1×10^4 cells. Gene transfer was performed either in serum-free medium or in medium containing 10 % serum. Luciferase activities in all transfections are shown as a percentage of the activity of the CMV promoter using lipopolyplexes in presence of serum. The activity of 100 % (CMV promoter in the presence of serum) corresponds to 2×10^5 RLU in COGA-3 (A) cells, to 7.2×10^5 RLU in COGA-5 (B) cells, to 6.2×10^5 RLU in COGA-12 (C) cells, to 957×10^5 RLU in SW480 (D) cells and to 42×10^5 RLU in HeLa (E) cells. Values are means \pm SE of triplicates.

In the cell lines SW480, COGA-3 and COGA-12 the CTP4 promoter resulted in significantly higher luciferase expression levels than the CMV promoter, independent of the formulation used for transfection. In SW480 cells the CTP4 promoter had up to 11-fold higher luciferase expression levels when compared with the expression levels by the CMV promoter (**Fig. 34D**). In COGA-3 cells the CTP4 promoter induced up to 10-fold (**Fig. 34A**) and in COGA-12 cells up to 20-fold increases in luciferase activity (**Fig. 34C**). Only in the COGA-5 cell line the CTP4 promoter-driven expression level of luciferase was reduced to approximately 50 % of the CMV-driven luciferase expression (**Fig. 34B**). In contrast to colon cancer cells, in the control non-colorectal cancer cell line HeLa the luciferase expression level obtained by the CTP4 promoter was up to 950-fold lower than by the CMV promoter (**Fig. 34E**).

Furthermore, the gene transfer efficiencies of lipopolyplexes were significantly enhanced compared to corresponding lipoplexes or polyplexes in all cell lines tested, also when the luciferase expression was under control of the CTP4 promoter instead of the CMV promoter (**Fig. 34**). The expression levels obtained by lipopolyplex formulations were up to 1300-fold higher compared to the corresponding lipoplexes of DOSPER and up to 430-fold higher compared to the corresponding polyplexes of PEI25br (**Fig. 34**).

To sum up, the combination of the novel lipopolyplex formulation with the novel artificial CTP4 promoter is very promising for gene therapy strategies of colorectal cancer as it enables high efficient gene transfer and both high level and high colorectal cancer specific gene expression.

3.3.2.3. Influence of plasmid DNA concentration on gene expression levels with or without transcriptional targeting

To investigate the influence of the amount of transfected DNA on CMV and CTP4 promoter-controlled luciferase expression levels, SW480 cells were transfected with 0.1 µg and 0.05 µg DNA, respectively. Again, lipopolyplex, lipoplex and polyplex formulations were used for transfections. In general, the luciferase expression levels were lower when 0.05 µg DNA were used for transfection compared to 0.1 µg DNA (**Fig. 35**). However, the range between the expression levels controlled by the CTP4 promoter and the CMV promoter was more pronounced when lower amounts of DNA

were used compared to higher DNA amounts. When 0.05 μg DNA were transfected the luciferase expression controlled by the CTP4 promoter was 10-fold higher compared to the CMV promoter using lipopolyplexes for transfection, and 85-fold and 14-fold higher using lipoplexes and polyplexes, respectively. In contrast, when using 0.1 μg DNA the range between both promoters was only 4-fold in the case of lipopolyplexes, 11-fold in the case of lipoplexes and 4-fold in the case of polyplexes (Fig. 35). The results demonstrate that the CTP4 promoter is even more efficient at lower DNA concentrations than the CMV promoter, which exposes this promoter as a promising candidate for *in vivo* applications, where the DNA amount is limited.

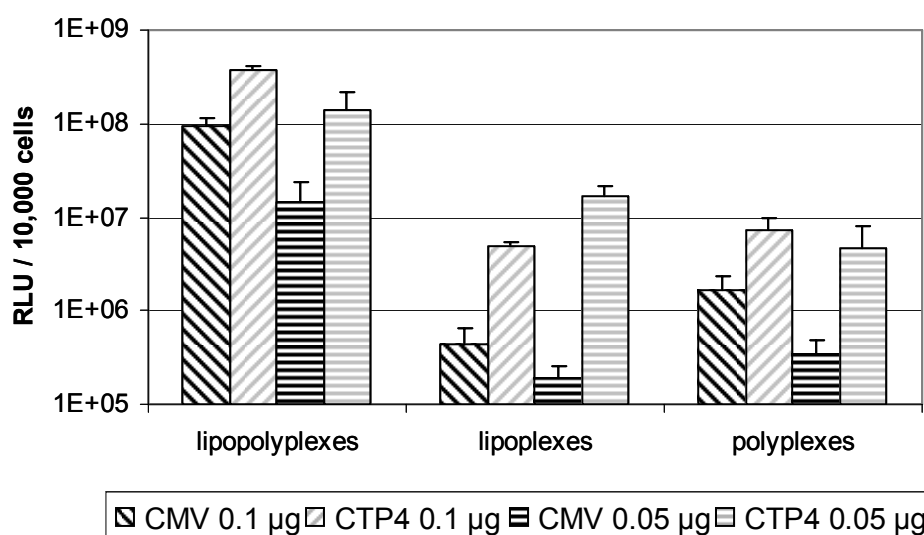


Fig. 35. Influence of the dose of transfected plasmid DNA on the CTP4 vs. CMV promoter controlled luciferase expression levels in SW480 cells. Indicated amounts of pCMV-Luc or pCTP4-Luc were used for transfection of 1×10^4 cells. Gene transfer was performed using lipopolyplex, lipoplex and polyplex formulations in medium containing 10 % serum. Values are means \pm SE of triplicates.

3.3.2.4. Percentage of transfected cells with or without transcriptionally targeted gene transfer

Next, it was investigated whether the enhanced luciferase expression using the CTP4 promoter in comparison to the CMV promoter was either the result of enhanced gene transfer efficiency or the increased protein expression per cell. For this purpose, the percentage of transfected cells and thereby the gene transfer efficiency was determined by flow cytometric analysis of EGFP expression. Since only a plasmid existed that contained the EGFP encoding gene in combination with

the CMV promoter, an analog of this plasmid was designed, which was harboring the CTP4 promoter instead of the CMV promoter. The pEGFP-LG-CTP4 vector (encoding EGFP under the control of the CTP4 promoter) was constructed by substitution of the CMV promoter of pEGFP-N1 by the CTP4 promoter of pCTP4-Luc as described in 2.2.8.

The colon cancer cell lines SW480, COGA-3, COGA-5 and COGA-12 were transfected with the plasmids containing the EGFP gene either under control of the CMV or the CTP4 promoter. Percentages of EGFP positive cells are shown in **Fig. 36**. No significant difference was detectable in the number of transfected cells obtained by the CTP4 promoter in comparison with the CMV promoter. The only discrepancy between the percentages of EGFP positive cells by both promoters was observed in COGA-5 cells transfected in absence of serum (**Fig. 36B**). This discrepancy is due to the sensitivity of the measurement. According to the luciferase data the expression levels of the CTP4 promoter were lower compared to the CMV promoter in COGA-5 cells. Hence, cells that exhibit very low EGFP expression levels driven by the CTP4 promoter can be already sorted out by flow cytometry settings, while cells with low EGFP expression levels under CMV promoter control are still included, as their expression levels are higher compared to the low EGFP expression levels driven by the CTP4 promoter. Thus, the differences in the expression levels of the EGFP gene driven by different promoters can lead to the detection of different amounts of EGFP positive cells

Again, all transfection experiments were performed with lipopolyplex, lipoplex and polyplex formulations. In presence of serum the highest percentage of transfected cells was obtained by using lipopolyplexes, resulting in up to 15 % EGFP positive cells in the human low passage colon cancer cell lines regardless of which of the two promoters was used (**Fig. 36A-C**). In the control cell line SW480 even up to 40 % of the cells were positive for EGFP when lipopolyplexes were used for transfection (**Fig. 36D**). Lower percentages of EGFP positive cells were obtained by using either lipoplexes (up to 5 % in the human low passage colon cancer cell lines and up to 7 % in SW480 cells) or polyplexes (up to 0.4 % in the human low passage colon cancer cell lines and up to 1 % in SW480 cells) for transfection in presence of serum in all cell lines (**Fig. 36**).

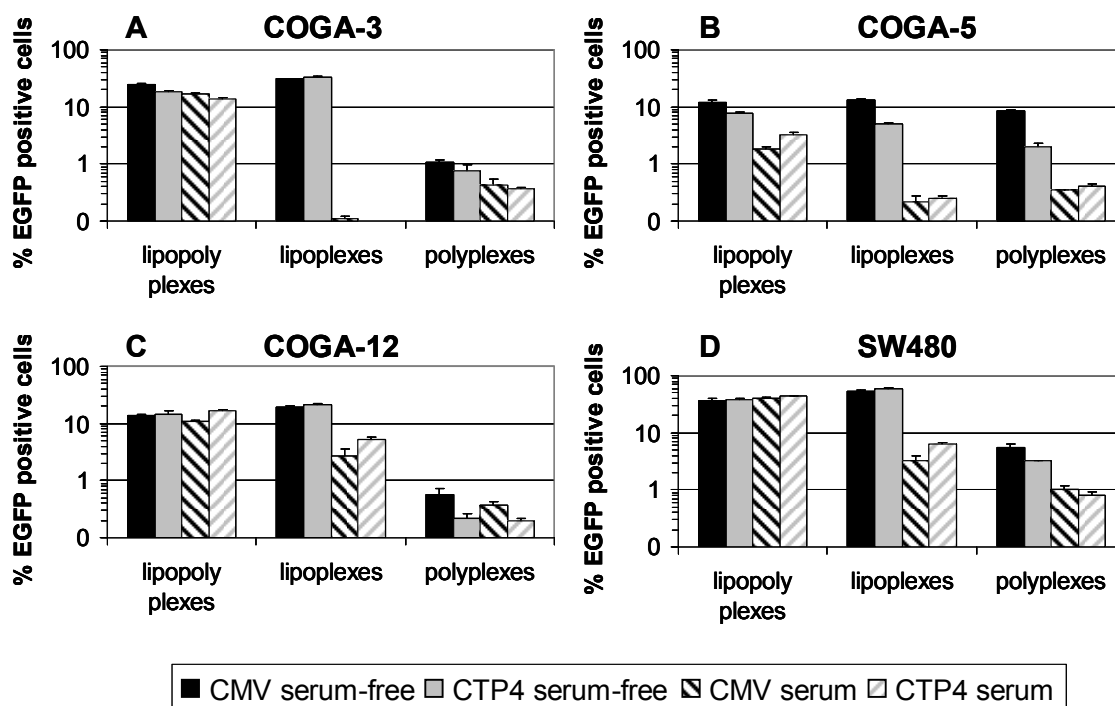


Fig. 36. Percentage of EGFP positive COGA-3 (A), COGA-5 (B), COGA-12 (C) and SW480 (D) cells following gene transfer using plasmids containing the EGFP gene under control of the CMV or CTP4 promoter. For transfection of 1×10^5 cells $0.5 \mu\text{g}$ pCMV-EGFP or pCTP4-LG-EGFP were used. EGFP expression was analyzed by flow cytometry. The mean percentages of EGFP positive cells \pm SE of duplicates are shown.

Interestingly, in contrast to transfections in the presence of serum, the transfection efficiency of lipoplex formulations was comparable with the efficiency of the corresponding lipopolyplexes in serum-free medium in all cell lines tested (Fig. 36). Polyplexes of PEI25br provided again the lowest amount of EGFP positive cells in all experiments performed in the absence of serum as shown in Fig. 36. When using lipoplexes and lipopolyplexes for transfections in the absence of serum up to 30 % of the low passage colon cancer cells were transfected (Fig. 36A-C). In the cell line SW480 up to 50 % of the cells were EGFP positive (Fig. 36D). When using polyplexes only up to 9 % of the human low passage colon cancer cells and up to 6 % of SW480 cells were EGFP positive (Fig. 36). Again, in all cases with exception of COGA-5 cells the percentage of EGFP positive cells was independent of the promoter used.

The experiments above demonstrated that the enhanced luciferase expression obtained by the CTP4 promoter compared to the CMV promoter is a result of higher gene expression attributed to the CTP4 promoter and not of enhanced gene transfer efficiency of the transcriptional targeted lipopolyplexes.

3.3.2.5. Transfection of multicellular spheroids with transcriptionally targeted lipopolyplexes

In addition, it was investigated whether the tumor specific CTP4 promoter also worked in three-dimensional cell cultures. Therefore, multicellular spheroids were transfected with lipopolyplexes harboring the EGFP gene under control of the CTP4 promoter and for comparison the CMV promoter. The use of both promoters led to significant EGFP expression (**Fig. 37**).

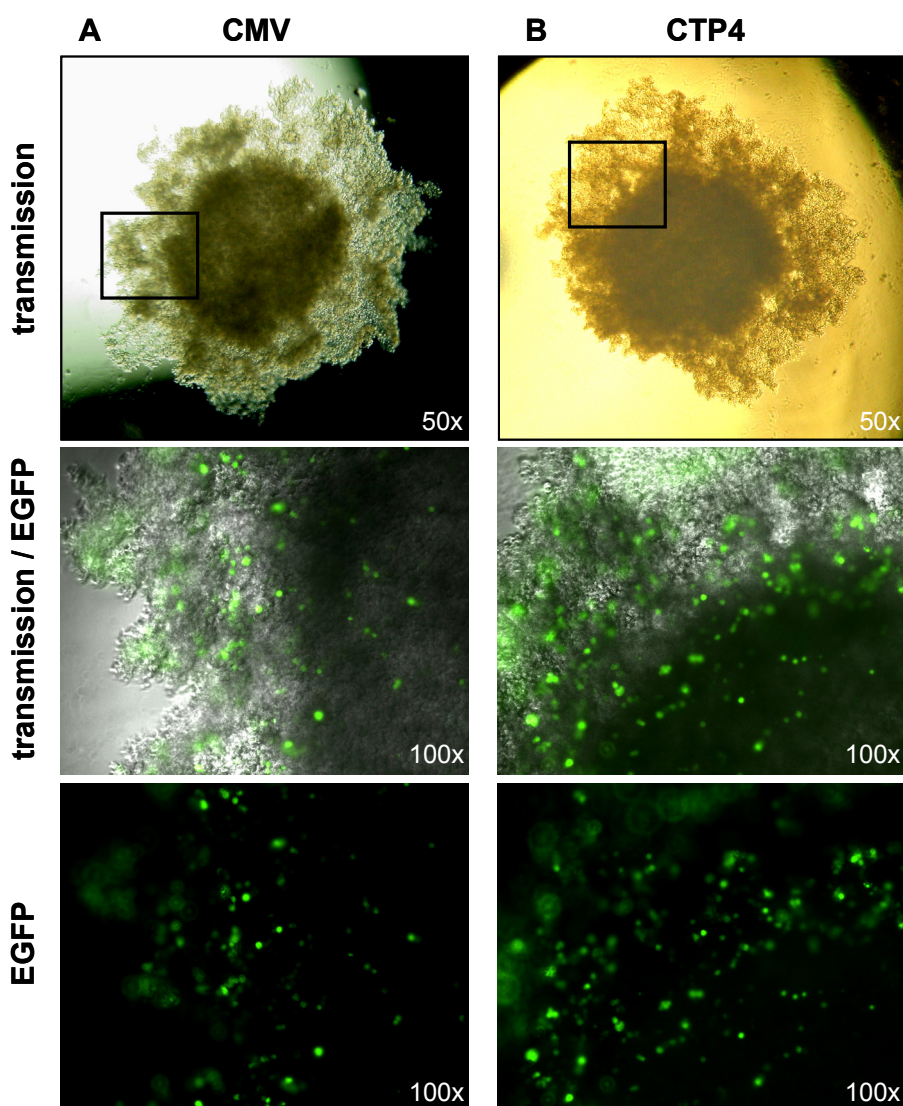


Fig. 37. Comparison of EGFP expression by the CMV (A) and the CTP4 (B) promoter in multicellular spheroids using lipopolyplexes for gene transfer. Multicellular spheroids of COGA-12 cells grown in medium containing 2 % serum were transfected with 0.25 μg pEGFP-N1 or pEGFP-LG-CTP4 96 h after multicellular spheroid formation. Forty-eight hours after transfection multicellular spheroids were fixed in 4 % PFA and analyzed by epifluorescence microscopy. The top panels show transmission light images of whole multicellular spheroids. The squares mark the respective areas of the multicellular spheroids that are displayed below as magnified overlays of transmission light and epifluorescence images (middle panels) and epifluorescence images (lower panels).

Visually, no differences in the number of EGFP positive cells and also in the intensity of EGFP expression controlled by the CTP4 promoter could be detected compared to transfections performed with the CMV promoter. This demonstrates that the CTP4 promoter is also very efficient after gene transfer by lipopolyplexes to multicellular spheroids.

3.3.3. Therapeutic strategies for treatment of colorectal cancer

Finally, two strategies for therapeutic treatment of colorectal cancer following gene transfer using lipopolyplexes were explored. First, the expression of the immune stimulatory interleukin-2 (IL-2) was investigated. Second, in a more extended concept, the expression of a cytotoxic gene coding for the rhinoviral protease 2A in addition to the expression of IL-2 was studied. The expression of these therapeutic genes was controlled by the tumor specific CTP4 promoter in comparison to the CMV promoter. Only two selected colorectal cell lines were used for the experiments below, namely COGA-12 and SW480, since both cell lines resulted generally in the highest expression levels in the previous experiments. In addition, HeLa cells were applied as non-colorectal control in some cases.

3.3.3.1. Colorectal cancer specific expression of immune stimulatory IL-2

To investigate the colorectal cancer specific expression of IL-2 after transfection of COGA-12 and SW480 cells with lipopolyplexes, plasmids containing the human IL-2 gene under the control of the CTP4 promoter were used for transfections. In addition, plasmids harboring the IL-2 gene in combination with the CMV promoter were applied for comparison. Initially, a plasmid encoding the IL-2 under the control of the CTP4 promoter (pCTP4-hIL-2) was constructed by substitution of the luciferase gene of pCTP4-Luc by the hIL-2 gene from pGShIL-2tet as described in 2.2.8.

Each plasmid was applied in two different concentrations (0.25 μg and 1 μg of plasmid DNA per 1×10^5 cells). When using 0.25 μg DNA in the absence of serum the CMV promoter led to secretion of 3.9 ng IL-2 per 10^5 COGA-12 cells, and to secretion of 0.3 ng IL-2 per 10^5 SW480 cells 48 h following transfection (**Fig. 38**). The use of the CTP4 promoter enhanced the IL-2 production up to 345-fold (95 ng IL-2 per 10^5 cells) compared to the IL-2 expression levels achieved by the CMV promoter.

The level of secreted IL-2 could be further enhanced by increasing the amount of plasmid DNA. As shown in **Fig. 38A** using 1 μg of plasmid DNA up to 27 ng IL-2 per 10^5 COGA-12 cells were detected independent of which promoter was used. In SW480 cells CMV promoter-controlled IL-2 gene also demonstrated the highest expression at 1 μg DNA (18 ng IL-2 per 10^5 cells) (**Fig. 38B**). Interestingly, when the CTP4 promoter was used in SW480 cells the maximal level of IL-2 was already achieved with 0.25 μg of DNA (95 ng IL-2 per 10^5 cells). In SW480 cells, no further enhancement was measured by higher DNA concentrations in the case of the CTP4 promoter, while in COGA-12 cells the maximal level of IL-2 was observed first using 1 μg DNA for transfection.

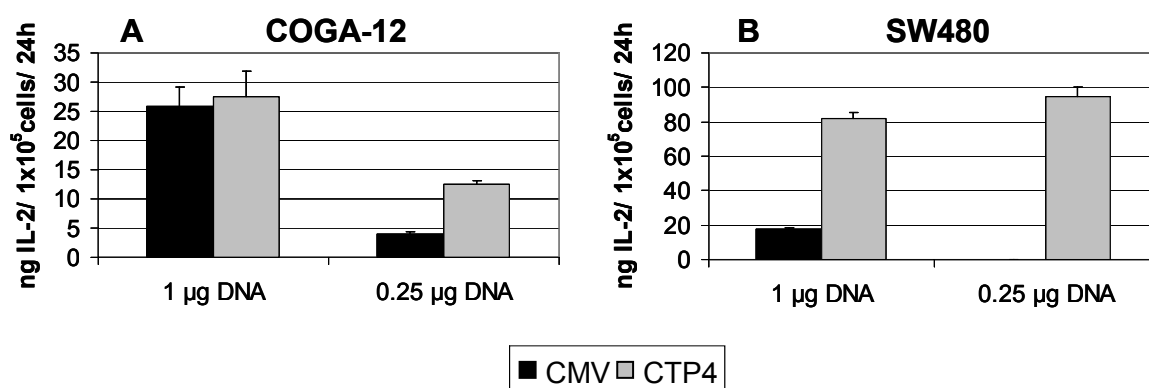


Fig. 38. Interleukin-2 (IL-2) production in COGA-12 (A) and SW480 (B) cells controlled by the CMV or CTP4 promoter using lipopolyplexes for gene transfer. Transfection was performed using 0.25 μg and 1 μg of pGShIL-2tet or pCTP4-hIL-2 per 1×10^5 cells. Twenty-four hours after transfection the growth medium was replaced by fresh medium, 48 hours following gene transfer the supernatants were collected and the level of secreted human IL-2 per 1×10^5 in 24 hours was determined using an IL-2 ELISA kit. Values are means \pm SE of duplicates.

The IL-2 expression was also investigated on multicellular spheroids. According to the optimal conditions established for EGFP expression in multicellular spheroids, COGA-12 multicellular spheroids grown in medium containing 2 % serum for 48 h were transfected with lipopolyplexes containing 0.5 μg of pGS-hIL2-tet (CMV promoter) or pCTP4-hIL-2 (CTP4 promoter). The expression of IL-2 was measured 48 h after transfection (96 h after multicellular spheroid formation) without replacement of growth medium after transfection. The use of pGS-hIL2-tet led to secretion of about 0.5 ng IL-2 per multicellular spheroid in 48 h and the use of pCTP4-hIL-2 to even about 1.4 ng IL-2 per multicellular spheroid in 48 h (**Fig. 39**).

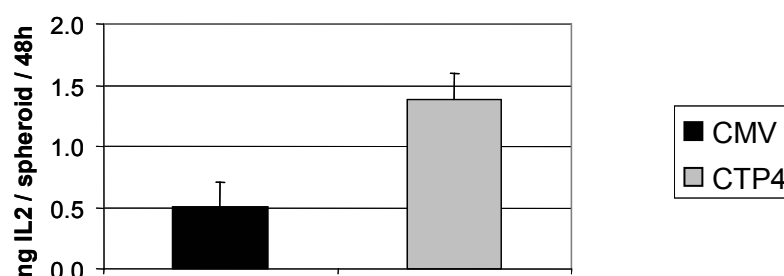


Fig. 39. Interleukin-2 (IL-2) production in COGA-12 multicellular spheroids controlled by the CMV or CTP4 promoter using lipopolyplexes for gene transfer. Multicellular spheroids were grown in medium containing 2 % serum. Transfection was performed 48 h after multicellular spheroid formation using 0.5 μ g of pGShIL-2tet or pCTP4-hIL-2 per multicellular spheroid. The growth medium was not replaced 24 hours after transfection. Forty-eight hours following gene transfer the supernatants were collected and the level of secreted human IL-2 per multicellular spheroid in 48 hours was determined using an IL-2 ELISA kit. Values are means \pm SE of duplicates.

3.3.3.2. Colorectal cancer specific coexpression of cytotoxic protease 2A and immune stimulatory IL-2

As a more extended therapeutic concept compared to the expression of IL-2 alone, a novel bicistronic construct (2A-IRES-IL2) was also evaluated for colorectal cancer specific expression with the CTP4 promoter in the low passage human colon cancer cell lines. This construct encodes both cytotoxic rhinoviral protease 2A and immune stimulatory human IL-2. The expression of protease 2A in transfected cells leads to the inability of these cells to initiate cap-dependent translation of their own cellular mRNA, leading to a reduced viability or proliferation of these cells. However, IL-2 protein synthesis, which is necessary for stimulation of the immune system, should be unaffected on the translational level. Therefore, a DNA sequence encoding a higher-ordered RNA structure known as IRES (internal ribosome entry site) is located upstream of the IL-2 sequence in the bicistronic construct 2A-IRES-IL2. This IRES allows the cap-independent initiation of translation of IL-2.

All transfections regarding the investigation of the cytotoxic effect of protease 2A and the IRES-mediated expression of IL-2 were performed using only lipopolyplexes. Furthermore, the specificity of the 2A-IRES-IL2 construct for colorectal cancer cells using the CTP4 promoter was analyzed and compared with the unspecific CMV promoter. For this purpose, a plasmid encoding the 2A-IRES-IL2 sequence under control of the CTP4 promoter (pCTP4-2A-IRES-IL2) was constructed as described in 2.2.8. Since the generated pCTP4-2A-IRES-IL2 plasmid was smaller than the p2A-

IRES-IL2 plasmid (containing the CMV promoter), a novel plasmid was created in addition that has nearly the same size as pCTP4-2A-IRES-IL2 and is harboring the 2A-IRES-IL2 sequence under control of the CMV promoter (pCMV-2A-IRES-IL2).

3.3.3.2.1. Effect of protease 2A on the overall gene expression of transfected cells

First, the effect of protease 2A on the reduction of overall cellular gene expression was tested. For this purpose, the expression levels of a cotransfected reporter gene encoding luciferase were determined. COGA-12, SW480 and HeLa cells were transfected with equal amounts of pEGFP-Luc and either pCMV-2A-IRES-IL2, pCTP4-2A-IRES-IL2 or pEGFP-N1 as a negative control. The level of luciferase expression was measured 24 and 72 hours after transfection. Twenty-four hours after transfection the expression of the CMV-driven protease 2A in COGA-12 cells led to 10-fold lower luciferase expression compared to the control transfection with pEGFP-N1 without expression of protease 2A (**Fig. 40A**). In the case of CTP4-driven protease 2A the luciferase expression was 3.6-fold lower. Seventy-two hours after transfection of COGA-12 cells reduction of luciferase expression by protease 2A was even stronger (pCMV-2A-IRES-IL2: 55-fold reduction, pCTP4-2A-IRES-IL2: 4.6-fold reduction). In SW480 cells the transfection with pCMV-2A-IRES-IL2 or pCTP4-2A-IRES-IL2 led to 14- and 18-fold lower luciferase expression compared to the control transfection 24 h after transfection (**Fig. 40B**). Seventy-two hours after transfection 24-fold and 13-fold reduction of luciferase expression were obtained in SW480 cells with pCMV-2A-IRES-IL2 and pCTP4-2A-IRES-IL2, respectively. In HeLa cells the transfection with pCMV-2A-IRES-IL2 resulted in 15-fold and 50-fold lower luciferase expression levels 24 h and 72 h after transfection compared to transfections with control plasmid (without protease 2A) (**Fig. 40C**). As expected, the transfection with pCTP4-2A-IRES-IL2 did not reduce the luciferase expression level in HeLa cells compared to the control transfection 24 h after transfection. Seventy-two hours after transfection with pCTP4-2A-IRES-IL2 the luciferase expression level of HeLa cells was about 1.5-fold lower than the expression level in the control transfection. Albeit the CTP4 promoter is highly specific for colorectal cancer cells, it still induced expression of low levels of protease 2A sufficient to slightly decrease luciferase expression. CTP4 promoter attributed expression levels in HeLa cells that were

slightly above background levels were already observed in the transfection experiments regarding the comparison of the efficiency of the CMV and CTP4 promoter (Fig. 33I).

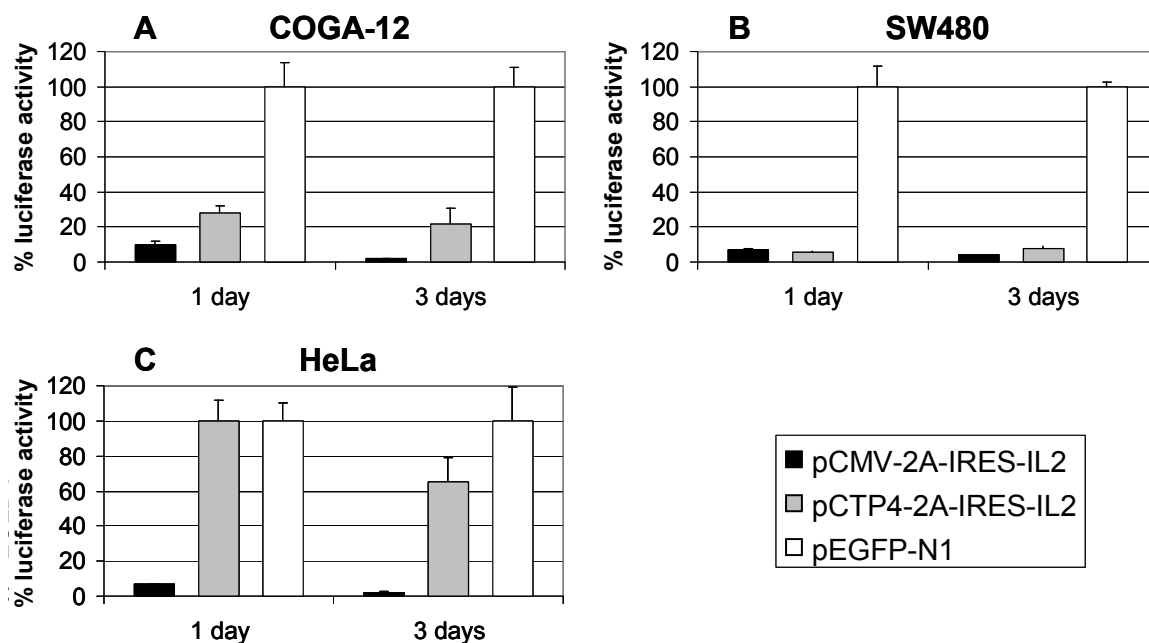


Fig. 40. Effect of protease 2A activity on the luciferase expression level of COGA-12 (A), SW480 (B) and HeLa (C) cells 24 and 72 h after transfection. For transfections $0.025 \mu\text{g}$ of pCMV-2A-IRES-IL2, pCTP4-2A-IRES-IL2 or pEGFP-N1 in combination with $0.025 \mu\text{g}$ pEGFP-Luc per 5×10^3 cells were used. Gene transfer was performed using lipopolyplexes in serum-free medium. Luciferase activities in all transfections are shown as a percentage of the activity of the respective coexpression of pEGFP-N1 and pEGFP-Luc. In COGA-12 (A) cells 100 % activity corresponds to 0.5×10^6 RLU and 0.4×10^6 RLU 24 and 72 h after transfection, respectively; in SW480 (B) cells to 2.8×10^6 RLU and 4×10^6 RLU 24 and 72 h after transfection; in HeLa (C) cells to 28×10^6 RLU and 8×10^6 RLU 24 and 72 h after transfection. Values are means \pm SE of $n = 4$.

Next, the influence of the protease 2A on the expression of the cotransfected reporter gene EGFP was investigated (Fig. 41). Similar to the experiments described above, COGA-12, SW480 and HeLa cells were transfected with equal amounts of pEGFP-N1 and either pCMV-2A-IRES-IL2, pCTP4-2A-IRES-IL2 or pEGFP-Luc as a negative control. pEGFP-Luc encodes a fusion-protein of EGFP and luciferase and was chosen for the control, as also the 2A-IRES-IL2 sequence expresses EGFP as a fusion-protein with protease 2A. Flow cytometric analysis 48 h after transfection revealed that in all cell lines the intensity of EGFP expression was lower when protease 2A was present compared to control transfections. In COGA-12 cells the intensity of EGFP expression was 1.8-fold and 1.5-fold lower attributed to CMV- and CTP4-driven expression of protease 2A compared to the control transfection without

protease 2A (**Fig. 41A**). In SW480 cells the intensity of EGFP expression was about 1.5-fold lower by CMV-driven expression of protease 2A and about 1.7-fold lower by CTP4-driven expression (**Fig. 41B**). In HeLa cells the transfection with pCMV-2A-IRES-IL2 reduced the intensity of EGFP expression even 4-fold compared to the intensity of the control transfection without protease 2A (**Fig. 41C**). In contrast to the 4-fold reduction by pCMV-2A-IRES-IL2, the intensity of EGFP expression was only 1.3-fold lower after transfection with pCTP4-2A-IRES-IL2. This slight reduction of overall gene expression in HeLa cells is again attributable to the low expression levels of protease 2A that are caused by the CTP4 promoter.

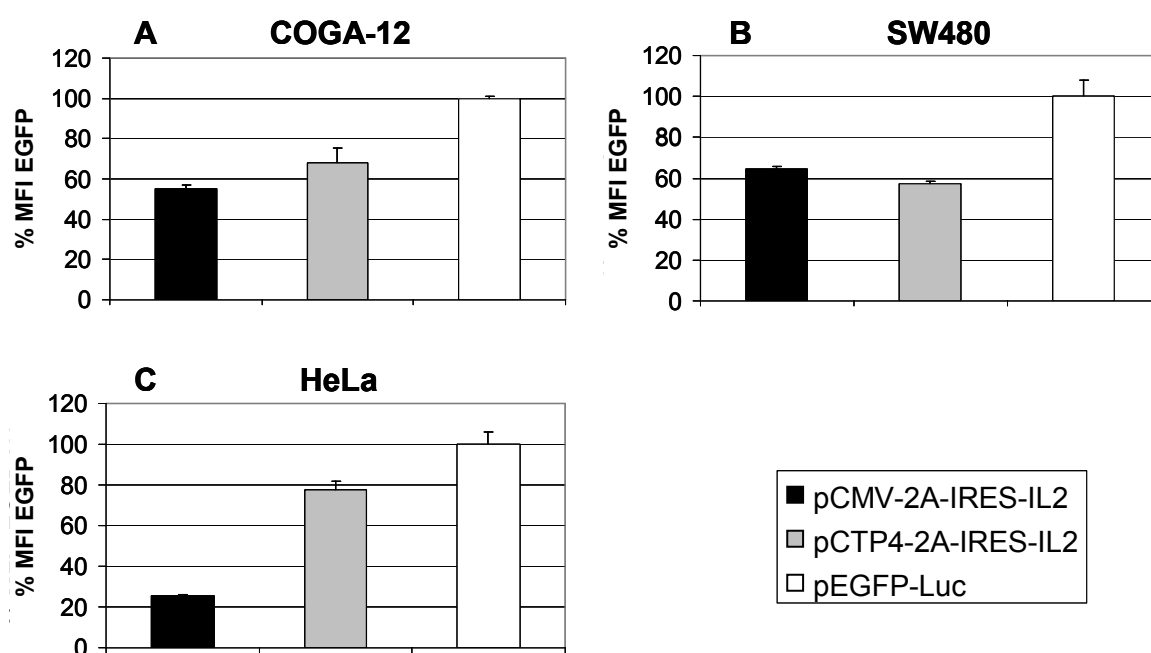


Fig. 41. Effect of protease 2A activity on the EGFP expression level of COGA-12 (A), SW480 (B) and HeLa (C) cells. For the transfections of COGA-12 and HeLa cells 0.25 μg of pCMV-2A-IRES-IL2, pCTP4-2A-IRES-IL2 or pEGFP-Luc in combination with 0.25 μg pEGFP-N1 per 0.5×10^5 cells were used. For the transfection of SW480 cells 0.5 μg of pCMV-2A-IRES-IL2, pCTP4-2A-IRES-IL2 or pEGFP-Luc in combination with 0.5 μg pEGFP-N1 per 1×10^5 cells were used. Gene transfer was performed using lipopolyplex formulation in serum-free medium. EGFP mean fluorescence intensities (MFI) were determined by flow cytometry 48 h after transfection and are shown as a percentage of the EGFP MFI of the respective coexpression of pEGFP-Luc and pEGFP-N1. Values are means \pm SE of triplicates.

3.3.3.2.2. Effect of protease 2A on the metabolic activity of transfected cells

To analyze the biological effect of protease 2A expression on cell proliferation and viability, the COGA-12, SW480 and HeLa cells were transfected with pCMV-2A-IRES-IL2 or pCTP4-2A-IRES-IL2, and as control with pEGFP-Luc. Three days after

transfection the metabolic activity of the transfected cells was measured using the MTT assay (**Fig. 42**). The metabolic activities of pCMV-2A-IRES-IL2 and pCTP4-2A-IRES-IL2 transfected cells were compared with the metabolic activity of pEGFP-Luc control transfected cells in order to exclude that reduction of metabolic activity was a result of toxicity of transfection reagents. In COGA-12 cells the metabolic activity of pCMV-2A-IRES-IL2- and pCTP4-2A-IRES-IL2-transfected cells was reduced to 76 % and 88 % compared to the metabolic activity of cells transfected with the control plasmid pEGFP-Luc (**Fig. 42A**). In SW480 cells the metabolic activity was reduced up to 60 % compared to the metabolic activity of control transfected cells, independent of the promoter used (**Fig. 42B**). In HeLa cells pCMV-2A-IRES-IL2 reduced cell proliferation up to 60 %, whereas transfection of the pCTP4-2A-IRES-IL2 plasmid did not reduce cell proliferation compared to cells transfected with the control plasmid (**Fig. 42C**).

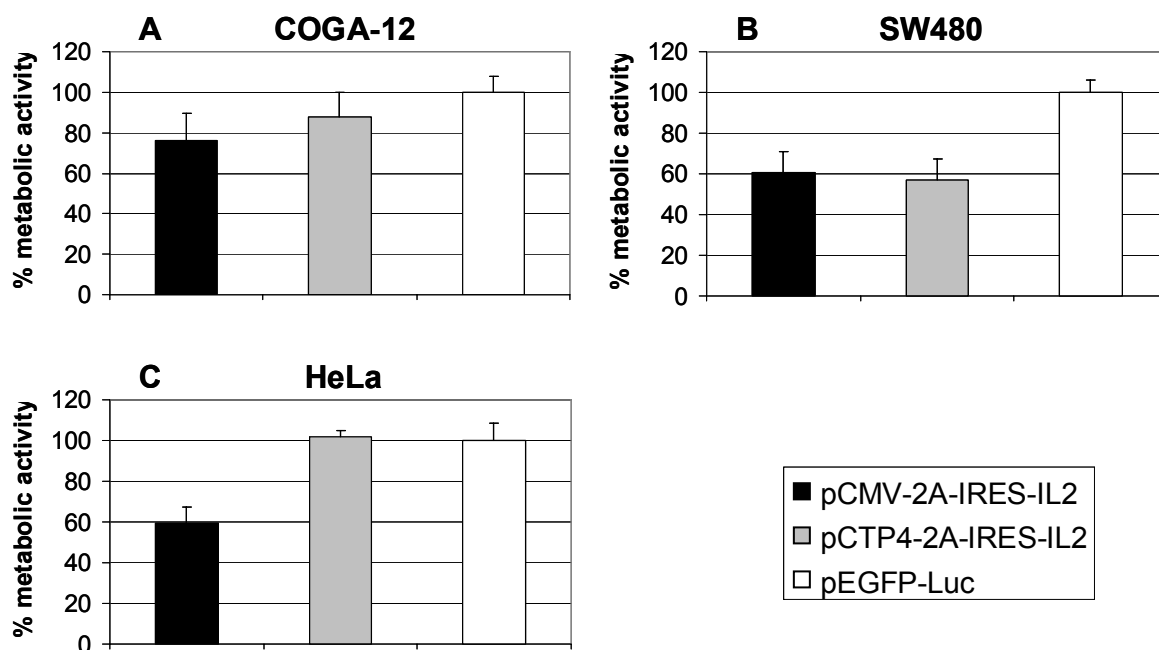


Fig. 42. Effect of protease 2A activity on the metabolic activity of COGA-12 (A) SW480 (B) and HeLa (C) cells. For transfections 0.05 μg of pCMV-2A-IRES-IL2, pCTP4-2A-IRES-IL2 or pEGFP-Luc per 5×10^3 COGA-12, SW480 or HeLa cells were used. Gene transfer was performed using lipopolyplex formulation in serum-free medium. Metabolic activity was determined 3 days after transfection by MTT assay. Metabolic activity levels are shown as a percentage of the metabolic activity of the respective pEGFP-Luc control transfections. Values are means \pm SE of $n = 5$ in 2 – 3 independent experiments.

3.3.3.2.3. Effect of protease 2A on the apoptosis rate of transfected cells

Furthermore, the possible effect of protease 2A to induce apoptosis was investigated. COGA-12 and SW480 cells were transfected with pCMV-2A-IRES-IL2, pCTP4-2A-IRES-IL2 and as control with pEGFP-Luc. Forty-eight hours after transfection the cells were incubated with annexin V and propidium iodide to distinguish between living, apoptotic and necrotic cells. Subsequently, the extent of apoptotic and necrotic cells was measured by flow cytometry. Neither cells transfected with pCMV-2A-IRES-IL2 nor pCTP4-2A-IRES-IL2 exposed a higher rate of apoptosis or necrosis compared to control cells transfected without the cytotoxic gene (**Fig. 43**).

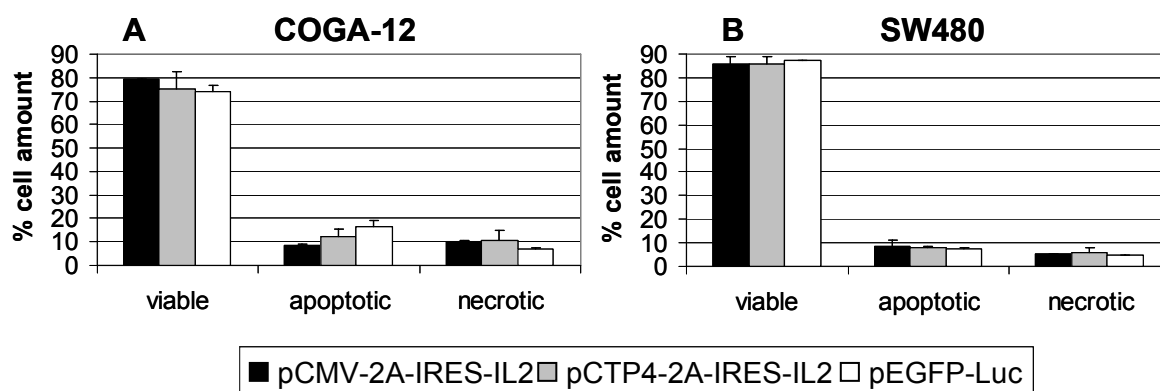


Fig. 43. Effect of protease 2A activity on the percentage of apoptotic COGA-12 (A) and SW480 (B) cells. For transfections $1 \mu\text{g}$ of pCMV-2A-IRES-IL2, pCTP4-2A-IRES-IL2 or pEGFP-Luc per 1×10^5 COGA-12 or SW480 cells were used. Gene transfer was performed using lipopolyplex formulation in serum-free medium. Apoptosis and necrosis were determined 48 h after transfection by staining with annexin V and propidium iodide and following flow cytometry. Values are representative means \pm SE of duplicates of three independent experiments.

3.3.3.2.4. IRES-mediated IL-2 expression

Finally, it was investigated, whether the 2A-IRES-IL2 constructs also enable the expression of the therapeutic gene for IL-2 in COGA-12 and SW480 cells despite the observed activity of the protease 2A. Cells were transfected with pCMV-2A-IRES-IL2 and pCTP4-2A-IRES-IL2 plasmids using lipopolyplexes. COGA-12 cells transfected with the CMV promoter containing construct secreted $1.7 \text{ ng IL-2 per } 10^5$ cells within 24 h 48 h following transfection, and SW480 cells secreted $2 \text{ ng IL-2 per } 10^5$ cells within 24 h 48 h following transfection (**Fig. 44**). The use of the CTP4 promoter led to IL-2 expression levels of $0.3 \text{ ng IL-2}/10^5$ cells/24 h in COGA-12 cells and $0.7 \text{ ng IL-2}/10^5$ cells/24 h in SW480 cells (**Fig. 44**).

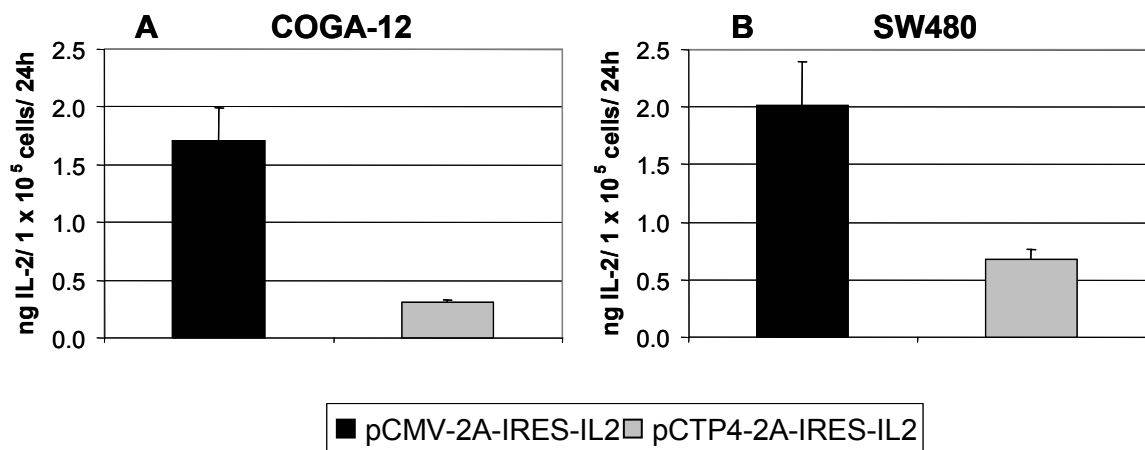


Fig. 44. IRES-mediated interleukin-2 (IL-2) production of COGA-12 (A) and SW480 (B) cells. For transfections 0.5 μ g of pCMV-2A-IRES-IL2 or pCTP4-2A-IRES-IL2 per 0.5×10^5 COGA-12 cells and 1 μ g of pCMV-2A-IRES-IL2 or pCTP4-2A-IRES-IL2 per 1×10^5 SW480 cells were used. Gene transfer was performed using lipopolyplex formulation in serum-free medium. Twenty-four hours after transfection the growth medium was replaced by fresh medium, 48 hours following gene transfer the supernatants were collected and the level of secreted human IL-2 per 1×10^5 in 24 hours was determined using an IL-2 ELISA kit. Values are means \pm SE of duplicates.

4. Discussion

4.1. Protein expression pattern in multicellular spheroids compared to monolayer cultures of low passage colon cancer cells

A major obstacle for the improvement of existing and the development of novel therapeutic strategies for the treatment of colorectal cancer is the lack of reliable model systems. Many promising therapeutic approaches that were efficient in cultured tumor cells demonstrated low or no efficiency *in vivo*, since the used *in vitro* model systems did not properly reflect the conditions *in vivo*. A major reason for this phenomenon inheres in additional mutations and alterations in the protein expression pattern of the tumor cell lines that accumulate during long-term *in vitro* cultivation. To circumvent this problem novel low passage colon cancer cell lines closely reflecting the corresponding *in vivo* tumor cells were used for all investigations in the present work. The relevance of these low passage cell lines to provide reliable model systems was confirmed in this thesis, since long-term cultivated COGA-12 cells exhibited altered properties and protein expression compared to corresponding low passage COGA-12 cells (see discussion in 4.2).

In addition to traditional monolayer cultures the low passage cell lines were cultivated as multicellular spheroids to provide a model system that better reflects the three-dimensional structure of the respective tumors *in vivo*. Very similar to the tumor *in vivo* the three-dimensional structure of cultured multicellular spheroids provides different properties compared to monolayers, in particular the spatial arrangement of the cells. In addition, the three-dimensional arrangement of cells in multicellular spheroids very likely causes alterations in the gene expression pattern compared to monolayer cultures, which again better reflects the situation in tumors *in vivo*. However, this model system does not provide the recapitulation of interactions of tumor cells with extracellular matrix (ECM) or other cell types, like for example connective tissue, which also may influence the properties and protein expression of tumor cells *in vivo* (Abbott, 2003). ECM consists of proteins like collagen, elastin and

laminin, and gives tissues their mechanical properties. Yet, the only commercially available possibility to mimic ECM is represented by Matrigel consisting of structural proteins isolated from mouse tumors. Therefore, the utilization of Matrigel is not very suitable for human tumor cells. In contrast, generating own human custom matrices is very time-consuming, expensive and the properties of these custom-made ECMs vary from batch to batch (Abbott, 2003). The absence of other cell types besides the low passage cancer cells in the multicellular spheroids used in this work provides the advantage of exclusively investigating the protein expression of the tumor cells, because contamination with proteins derived from other cell types is prevented. Therefore, multicellular spheroids represent one of the most potential, easy-to-handle alternative *in vitro* model systems for the investigation of cancers available at present in comparison to conventional monolayer cultures.

To confirm and characterize differences between multicellular spheroids of the low passage colon cancer cell lines and corresponding monolayers the expression profiles of both model systems were compared by 2D electrophoresis in this thesis. This method enables the investigation of nearly all expressed proteins and, in addition, their post translational modifications. In contrast, investigations on the level of mRNA do not display post translational modifications, and it is not clear if the respective mRNAs are translated to proteins. First, multicellular spheroids of the low passage colon cancer cell lines COGA-5, COGA-5L and COGA-12 were established (**Fig. 4**). The other tested low passage colon cancer cell lines (COGA-2, COGA-3, COGA-10) failed to form multicellular spheroids and only formed multicellular aggregates. Multicellular aggregates clearly differ from multicellular spheroids since they expose a lower degree of compaction. It was reported previously that a certain degree of compaction enabling cell-to-cell interactions is required for the development of the altered properties of multicellular spheroids compared to monolayer cultures (Mayer et al., 2001). Accordingly, multicellular aggregates do not exhibit altered properties. Whether a certain cell line forms multicellular spheroids cannot be predicted. The cell lines COGA-5L and COGA-12 formed partly compact spheroids, while the cell line COGA-5 developed fully compact spheroids (**Fig. 4**). The comparison of the protein expression profiles of the particular low passage cells cultivated as multicellular spheroids or monolayers by 2D electrophoresis revealed

several differences (**Fig. 5-7**). In multicellular spheroids of the cell line COGA-5 the expression of five proteins was found to be up-regulated and one protein was down-regulated compared to monolayers. In both, COGA-5L and COGA-12 multicellular spheroids, four proteins were found up-regulated compared to the respective monolayers (**Table 4**). All expression profiles were analyzed 96 h after formation of the multicellular spheroids. The differential expression of these proteins was highly reproducible, since differential regulation of the respective proteins was confirmed by 2D electrophoresis of protein extracts of at least three independent experiments. The identified proteins were most likely not the only differentially expressed proteins when comparing both culture conditions. Discovery of further differences in protein expression, however, was limited for the following reasons: First, proteins were only considered as differentially expressed when the differences in the spot intensities were at least two-fold. Thus, minor variations that originated from the different handling of the separate 2D gels could be excluded. Second, alterations in the expression of proteins with low abundance cannot be analyzed by 2D electrophoresis, if their expression level is beneath the detection limit of this method (lower than 1 ng). Furthermore, only proteins with an isoelectric point in the range of pH 4 – 7 were analyzed. Proteins with a more basic isoelectric point cannot be easily analyzed by 2D electrophoresis.

MALDI-TOF mass spectrometry and following peptide mass fingerprinting allowed identification of three of the differentially expressed proteins in COGA-5 and two in COGA-12 multicellular spheroids (**Table 5**). The proteins regulated in COGA-5L multicellular spheroids could not be identified. The identification failed because the amount of protein harvested from the gels was insufficient for proper analysis with MALDI-TOF mass spectrometry. Furthermore, only proteins that have been characterized before by peptide mass fingerprinting can be identified with this method.

The protein down-regulated in COGA-5 multicellular spheroids was identified as the acidic isoform of calponin (**Table 4 and 5**). Calponins are actin-associated proteins and besides acidic calponin two other isoforms are known, namely basic and neutral calponins (Applegate et al., 1994; Jin et al., 2003). Basic calponin is the best studied isoform. It is expressed exclusively in smooth muscle cells where it plays a role in the

regulation of contraction (Winder and Walsh, 1990). Less is known about acidic calponin. It is expressed in smooth muscle tissues and in a wide variety of other tissues, including heart, brain, placenta, lung, liver, skeletal muscle, kidney, pancreas, spleen, thymus, prostate, testis, ovary, small intestine, aorta, and also the colon (Maguchi et al., 1995). Acidic calponin is not involved in contraction (Fujii et al., 2002) but may play a role in cytoskeletal organization, since it binds to actin (Applegate et al., 1994; Yoshimoto et al., 2000). The different expression pattern of calponin in multicellular spheroids implies that the cytoskeleton is differentially organized in monolayer cells compared to multicellular spheroids.

One of the proteins up-regulated in multicellular spheroids of COGA-5 cells was identified as LMNA protein (**Table 4 and 5**). The database used for peptide mass fingerprinting indicated a molecular weight of 53 kDa for the LMNA protein. Surprisingly, the spot that was identified here as LMNA protein possesses a much lower molecular weight according to its location on the 2D gels of multicellular spheroids of COGA-5 cells (**Fig. 5**). It is remarkable that MALDI-TOF mass spectrometry only revealed peptides that could be ascribed to the first 216 amino acids or the last 98 amino acids of the LMNA protein (**Fig. 9D**). No peptides were obtained that fit to a sequence of about 150 amino acids located in the middle between these amino acid sequences (as shown in **Fig. 45**). Therefore, the identified protein is most likely a yet unknown variant of the LMNA protein that is generated by alternative splicing. A protein with the 150 amino acid truncation would be about 18 kDa smaller than the entire LMNA protein. The amino acid sequence of LMNA protein is identical to that of lamin C besides a deletion of 107 amino acids (amino acids 448 – 554 of lamin C) as shown in **Fig. 45**. Lamin C is encoded by the same gene as lamin A by different splicing. Two more splice variants of this gene have been described suggesting the likely identification of further splice variants (Moir and Spann, 2001). Therefore, it is likely that both the LMNA protein and the supposed 18 kDa smaller variant found in COGA-5 multicellular spheroids are also splice variants of this gene. In addition to these splice variants two other lamins are known in humans, namely lamin B1 and B2 that are encoded by two separate genes (Moir and Spann, 2001).

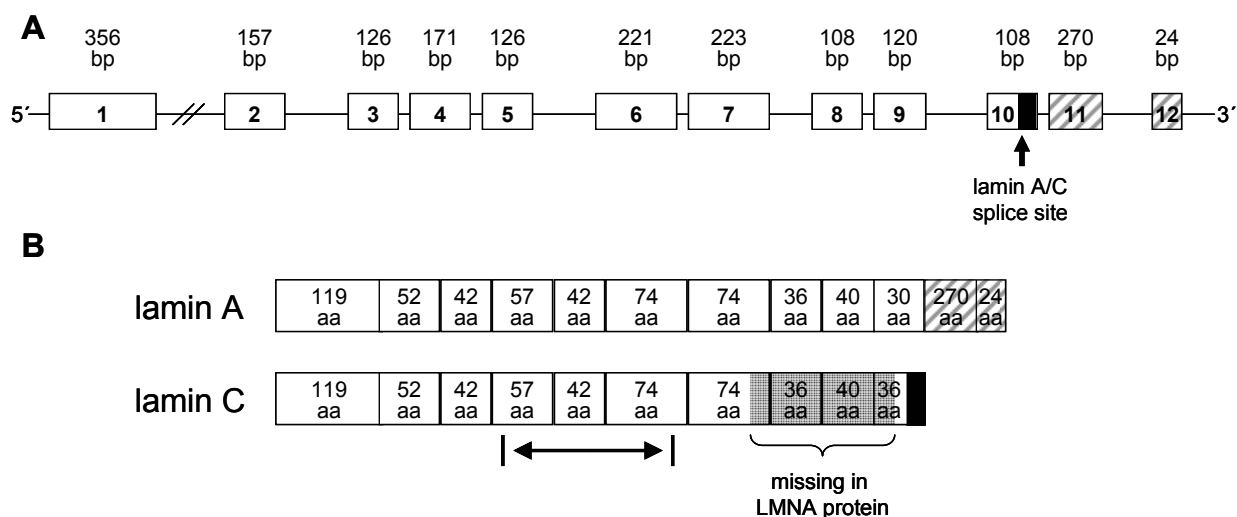


Fig. 45. Schematic illustration of the human lamin A/C gene and its gene products. White coloration indicates sequences identical for both lamin A and C, black coloration indicates the sequence specific for lamin C and vertical stripes the sequence specific for lamin A. (A) Arrangement of the exons in the lamin A/C gene (Lin and Worman, 1993). The splice site enabling the generation of lamin A and lamin C is indicated. (B) Schematic diagram of lamin A and C proteins. The grey highlighted area in lamin C indicates the amino acids missing in the LMNA protein. The approximate array missing in an assumedly 18 kDA smaller LMNA protein isotype found in COGA-5 multicellular spheroids is indicated by an arrow.

The lamins are the major proteins forming the nuclear lamina that is connecting the inner nuclear envelope membrane with chromatin (Shumaker et al., 2003). They play an important role for the assembly and shape of the nucleus. Furthermore, it has been suggested that lamins are also involved in DNA replication and transcription (Moir and Spann, 2001; Shumaker et al., 2003). The role of the up-regulated novel variant of the LMNA protein in COGA-5 multicellular spheroids remains to be clarified. However, altered cell and nucleus shape as a consequence of changes in cytoskeletal elements and nuclear structure is a hallmark of cancer cells that contribute to altered properties compared to normal cells (Konety and Getzenberg, 1999). It is likely that cells in multicellular spheroids mimic these alterations of *in vivo* tumor cells better than monolayer cells. This hypothesis is further supported by the fact that not only the nucleoskeletal LMNA protein but also the cytoskeleton-associated calponin are differentially regulated in COGA-5 multicellular spheroids compared to the corresponding monolayers.

Another protein that was up-regulated in multicellular spheroids of COGA-5 cells was identified as 15-hydroxyprostaglandin dehydrogenase (15-PGDH) (Table 4 and 5). 15-PGDH is responsible for the degradation of prostaglandins (Tai et al., 2002) and

therefore antagonizes the effect of cyclooxygenase 2 (COX-2), a prostaglandin-synthesizing enzyme (Badawi, 2000). According to the literature, prostaglandins promote growth factor signaling and antagonize apoptosis (Badawi, 2000). Therefore, 15-PGDH is considered to expose tumor suppressor activity, whereas COX-2 may exert tumor promoting activities. Moreover, it was demonstrated that 15-PGDH is down-regulated in colorectal cancers compared to normal colonic epithelial cells (Yan et al., 2004; Backlund et al., 2005). The up-regulation of 15-PGDH detected here in COGA-5 multicellular spheroids was in contrast to these previous findings and its up-regulation was therefore unexpected. However, Tong and Tai recently demonstrated that IL-6 induces the expression of 15-PGDH in prostate cancer cells (Tong and Tai, 2004). In this case 15-PGDH was supposed to be up-regulated to antagonize the effect COX-2 as a defensive regulatory mechanism or to inactivate lipoxins, which are potent inhibitors of cell proliferation (Claria et al., 1996).

Finally, two protein spots up-regulated in COGA-12 multicellular spheroids, were identified as the same protein, i.e. acidic ribosomal protein P0 (**Table 4 and 5**). This protein appears at two neighboring positions on the 2D gel most likely as a result of different posttranslational modifications (PTMs). This conclusion is supported by the fact that both proteins are located at approximately the same height on the 2D gel (implying the same molecular weight) and only differ in their isoelectric points (**Fig. 7**). P0 forms the lateral stalk of the 60S ribosomal subunit together with two hetero- or homo-dimers of acidic ribosomal proteins P1 and P2; P0 functions as ribosomal core protein for the anchorage of P1 and P2 (Uchiumi et al., 1987; Tchorzewski et al., 2000). This stalk is located at the active site of the ribosome particle, where interactions between mRNAs, tRNAs and translation factors take place during protein synthesis.

The P-proteins can be phosphorylated by casein kinase II at the serine closest to the carboxy-terminus (Hasler et al., 1991). Furthermore, PK60, RAPI, RAPII and RAPIII kinases are able to phosphorylate the stalk proteins (reviewed in Ballesta et al., 1999). However, the state of phosphorylation of the P-proteins does not affect the overall translating activity of the ribosome, but it has been suggested that phosphorylation influences the preferential translation of certain mRNAs with a specific secondary structure (Rodriguez-Gabriel et al., 1998). More recently, Wu and

Storey reported that the expression of P0, which is highly conserved in vertebrates, was regulated by oxygen levels in wood frog (*Rana sylvatica*) brain tissue suggesting a role of P0 in anoxia resistance (Wu and Storey, 2005). The function of P0 up-regulation under anoxia, however, remains unclear. Hence, P0 might be up-regulated in COGA-12 multicellular spheroids as a consequence of the lower oxygen supply in the inner layers of the spheroids. It was demonstrated previously that mRNA levels of P0 were increased in hepatocellular and colon carcinoma in accordance with cancer progression and biological aggressiveness (Barnard et al., 1992; Kondoh et al., 1999). Hence, P0 expression pattern in multicellular spheroids demonstrated that this three-dimensional culture system was superior compared to traditional monolayer cultures to reflect the expression pattern of *in vivo* tumors.

In summary, the investigation of the protein expression pattern of multicellular spheroids of the low passage colon cancer cells by 2D electrophoresis revealed a panel of alterations in comparison to monolayers affecting a wide variety of cellular functions regarding most likely growth signaling, protein biosynthesis and regulation of the cyto- or nucleoskeleton, respectively. Some of these alterations were also demonstrated in tumors *in vivo*. Thus, in comparison to monolayer cell cultures, multicellular spheroids represent a suitable model that recapitulates not only the three-dimensional structure but very likely also the protein expression of *in vivo* tumors. Therefore, the analysis of the expression pattern of multicellular spheroids may further contribute to better understanding of cancer.

It is important to note that acidic ribosomal protein P0 as well as lamins and the neutral isoform of calponin have been identified to be apoptosis-associated proteins (Brockstedt et al., 1998; Holubec et al., 2005). Therefore, it must be taken into consideration that the observed alterations could also be attributed to apoptosis occurring in the center of multicellular spheroids.

4.2. Regulation of cytoskeleton- and mitochondria-associated proteins related to chemoresistance against 5-FU

Surgery combined with 5-FU chemotherapy is the standard treatment of colorectal cancer. A major problem of such treatment is the resistance of colorectal cancer cells against 5-FU that frequently develops during chemotherapy. Chemoresistant sublines of the low passage colon cancer cell lines represent potential model systems for the identification of alterations involved in acquired 5-FU chemoresistance. Hence, the cell lines that were already investigated regarding their altered expression profile as a consequence of multicellular spheroid formation, i.e. COGA-5, COGA-5L and COGA-12 were used for the generation of chemoresistant sublines. However, it was not possible to generate resistant sublines of the cell lines COGA-5 and COGA-5L. COGA-5 cells required 10 μ M 5-FU for a reduction of proliferation by nearly 50 % but did not survive treatment with 5-FU longer than one month. COGA-5L cells required 5 μ M 5-FU for a 50 % decrease of proliferation but did not develop increased 5-FU resistance despite long-term treatment with 5-FU for three months. During the whole term of 5-FU treatment the cells exhibited the same reduced proliferation as 5-FU-treated parental COGA-5L cells. COGA-5L cells originate from the same patient as COGA-5 cells, but COGA-5 cells were isolated from the primary tumor, whereas COGA-5L cells were derived from the respective lymph node metastasis (Vecsey-Semjen et al., 2002). Hence, alterations must have occurred in the lymph node metastasis COGA-5L compared to COGA-5 cells, which are responsible for the distinct response to 5-FU between both cell lines.

In contrast, long-term (three months) pretreated COGA-12 cells exhibited enhanced proliferation in the presence of 5-FU compared to non-pretreated parental COGA-12 cells (**Fig. 16**). A concentration of 5 μ M 5-FU reduced proliferation of the long-term 5-FU pretreated cells, termed as COGA-12/G6, to approximately 75 % of the proliferation of untreated cells whereas non-pretreated cells exhibited a more pronounced reduction of proliferation, i.e. 50 %. Thus, COGA-12/G6 cells were considered chemoresistant against 5-FU. Control COGA-12 cells that were propagated long-term in absence of 5-FU, termed as COGA-12/NO, exhibited no resistance against 5-FU in the proliferation assay (**Fig. 20**). The COGA-12/G6 cells were also resistant against 5-FU induced apoptosis (**Fig. 17**). Surprisingly, the long-

term cultivated COGA-12/NO cells exhibited a similar reduced apoptosis level like COGA-12/G6 cells compared to parental low passage COGA-12 cells (**Fig. 21**). This phenomenon can be ascribed to alterations that result from the long-term propagation. This finding reveals the relevance of low passage numbers of cell lines for maintaining biological properties of the original tumor cells. It is important to note that the development of 5-FU chemoresistance through long-term cultivation or 5-FU pretreatment was associated with the regulation of different proteins (see below).

The investigation of the expression profile of the chemoresistant COGA-12/G6 cells by 2D electrophoresis revealed four proteins that were differentially regulated compared to parental sensitive COGA-12 cells (**Fig. 22**). These proteins were not altered in long-term cultivated COGA-12/NO cells. In contrast, one other protein was found to be differently expressed between the long-term cultivated COGA-12/NO and parental low passage COGA-12 cells (**Fig. 22**). Since no common alterations in the expression profiles of both sublines G6 and NO were obtained by 2D electrophoresis, it is likely that different mechanisms contribute to the same apoptosis resistance phenotype in both sublines. However, it cannot be fully excluded that the resistance against 5-FU induced apoptosis of COGA-12/G6 cells is also due to long-term propagation and not due to 5-FU treatment, although the protein expression pattern was not identical to COGA-12/NO cells.

Three of the altered proteins in the chemoresistant subline COGA-12/G6 were down-regulated and only one was up-regulated (**Table 6**). This is consistent with previous observations, where a similar proportion of up- versus down-regulations was detected in 5-FU chemoresistant colon cancer sublines compared to the original colon cancer cells (Schmidt et al., 2004). It cannot be excluded that further alterations contribute to the chemoresistant phenotype of the subline COGA-12/G6, which, however, stay unrevealed because of the limitations of 2D electrophoresis as mentioned before. Two of the three protein spots observed to be down-regulated in the chemoresistant subline COGA-12/G6 were both identified as heat shock protein 27 (HSP27) (**Table 6 and 7**). Most likely, HSP27 appeared at two nearby positions on the 2D gel as a consequence of different posttranslational modifications (PTMs). The most common PTM of HSP27 is phosphorylation. HSP27 belongs to a group of highly conserved proteins defined as molecular chaperones that fulfill a

cytoprotective role in cells undergoing various environmental stresses like hyperthermia, oxidative stress, or even exposure to chemotherapeutic drugs. The cytoprotective action of HSP27 is based on its ability to mediate resistance against apoptosis (Samali and Cotter, 1996; Concannon et al., 2003). HSP27 inhibits apoptosis by interfering with cell death signaling triggered by death receptor stimulation or through the mitochondrial pathway (Mehlen et al., 1996; Garrido et al., 1999). HSP27 is frequently expressed at high levels in tumor cells and was already reported to be involved in mediating resistance against several chemotherapeutic drugs like cisplatin, doxorubicin and etoposide (Garrido et al., 1997; Garrido et al., 1999). A major role of HSP27 in resistance against 5-FU has not been reported before. Large oligomers of HSP27 were proposed as the active form in inhibiting cell death; but only unphosphorylated HSP27 is capable to form large oligomers (Mehlen et al., 1997; Preville et al., 1998; Garrido et al., 1999). Recently, it was reported that the assembly of HSP27 oligomers can also be regulated independently of phosphorylation by S-thiolation (Eaton et al., 2002). HSP27 oligomers efficiently decrease the intracellular level of apoptosis-inducing reactive oxygen species (ROS) in a glutathione-dependent manner (Arrigo, 1998). HSP27 increases the activity of glucose-6-phosphate dehydrogenase, glutathione reductase and glutathione transferase which altogether uphold glutathione in its reduced form thereby decreasing levels of intracellular ROS (reviewed in Arrigo, 2001; and Arrigo et al., 2005). The increased activity of these enzymes may be conferred by the chaperone properties of HSP27 (Rogalla et al., 1999). In addition, HSP27 may protect cells from oxidative damage because it presents oxidized proteins to the ubiquitin-independent 20S proteasome degradation machinery and thereby mediates their elimination (Arrigo, 2001; Arrigo et al., 2005). How ROS induce apoptosis is not well understood. ROS may modulate the mitochondrial membrane potential, resulting in the release of cytochrome c, finally leading to apoptosis (Chandra et al., 2000). Another possibility is that ROS up-regulate the expression of Fas and Fas ligand (Chandra et al., 2000). This is particularly interesting since 5-FU induces apoptosis via upregulation of Fas and Fas ligand (Petak et al., 2000; Petak and Houghton, 2001). It was proposed that this increase was mainly due to p53-mediated transcriptional upregulation of Fas (Muller et al., 1998; McDermott et al., 2005). ROS are generated after treatment with

chemotherapeutic drugs (Davis et al., 2001), and recently, it was demonstrated that also the treatment with 5-FU increased the level of ROS in mitochondria of colorectal cancers thereby promoting apoptosis (Hwang et al., 2001; Liu and Chen, 2002). The 5-FU-induced increase in ROS depends on intact p53 and therefore it is interesting to note that COGA-12 cells are expressing wildtype p53 (Vecsey-Semjen et al., 2002). After treatment with 5-FU p53 increases the level of mitochondrial ferredoxin reductase, which in turn is supposed to hinder the detoxification of ROS resulting in the lethal accumulation of ROS (Liu and Chen, 2002). Furthermore, it was demonstrated that overexpression of ferredoxin reductase also suppressed the growth of colon cancer cells (Hwang et al., 2001). Overall, the data above imply a protective role of HSP27 which is in sharp contrast to its down-regulation in 5-FU chemoresistant cells in the present study. However, the chemoresistant COGA-12/G6 cells might have developed an alternative, yet unknown mechanism for the elimination of 5-FU-induced ROS levels and in this case HSP27 may not longer be required to survive ROS-associated stress.

Yet, the disappearance of the both HSP27 spots in the chemoresistant subline COGA-12/G6 compared to the sensitive cell line may also represent the vanishing of phosphorylated isoforms of HSP27. In this case the following model may be postulated: The phosphorylation of HSP27 could be inhibited by a yet unknown mechanism in the resistant subline. Alternatively, the efficiency of HSP27 dephosphorylation could be increased. Both mechanisms would lead to the supply of an increased level of unphosphorylated HSP27 to form large oligomers preventing ROS-mediated apoptosis after 5-FU treatment. HSP27 contains three potential phosphorylation sites on Ser residues at position 15, 78 and 82 (Landry et al., 1992; Cairns et al., 1994; Gusev et al., 2002). It is predominantly phosphorylated by MAPKAP (mitogen-activated protein kinase-activated protein) kinase-2 and -3, which in turn are activated by MAP (mitogen-activated protein) kinase SAPK2 (stress-activated protein kinase-2) as a response to oxidative stress (Landry and Huot, 1999; Dalle-Donne et al., 2001). Furthermore, protein kinase D and certain isoforms of protein kinase C were found to be involved in phosphorylation of HSP27 (Maizels et al., 1998; Doppler et al., 2005). Dephosphorylation of HSP27 is accomplished amongst others by protein phosphatase 2A (Cairns et al., 1994). Whether the

regulations or activities of these enzymes are altered in the chemoresistant cell line COGA-12/G6 remains to be clarified.

Cuesta and co-workers demonstrated that HSP27 additionally functions as an inhibitor of cellular protein synthesis by interaction with the translation initiation factor eIF4G during heat shock (Cuesta et al., 2000). Along these lines, the down-regulation of HSP27 could also be the reason for the enhanced proliferation of the chemoresistant subline COGA-12/G6 despite 5-FU treatment.

HSP27 is further described as a polymerization modulator of actin, a major constituent of the cytoskeleton microfilaments. Small oligomers of phosphorylated HSP27 stabilize the actin filament network thereby preventing actin degradation in response to stress (Mounier and Arrigo, 2002). In contrast, nonphosphorylated monomeric HSP27 acts as an actin cap-binding protein thereby inhibiting actin polymerization (Benndorf et al., 1994; Mounier and Arrigo, 2002). Taken together, also a rearrangement of the cytoskeleton enabled by differential expression of the actin-modulator HSP27, may contribute to the chemoresistant phenotype of COGA-12/G6 cells. In addition, Perng and co-workers demonstrated that HSP27 was also associated with cytokeratin 18 (CK18) (Perng et al., 1999), a major constituent of the cytoskeleton intermediate filaments. This suggests a role of HSP27 also in the control of filament-filament interactions.

Interestingly, CK18 was identified to be the up-regulated protein in the chemoresistant cell line COGA-12/G6 (**Table 6 and 7**). Intermediate filaments (IFs) are one of the three structural units of the cytoskeleton besides actin-containing microfilaments and tubulin-containing microtubules. Several proteins are known that form IFs: e.g. vimentin (found in mesenchymally derived cells), desmin (found in most myogenic cells), glial fibrillary acidic protein (found in astrocytes), neurofilament proteins (found in neurons), CKs (found in epithelial cells) and hair-related keratins and, further, the three nuclear lamins (Hatzfeld and Franke, 1985; Oshima, 2002). CKs can be divided in subfamilies of type I and type II cytokeratins. The type I subfamily comprises eleven acidic CKs (CK9 - 20) and type II nine larger, more basic CKs (CK1 - 9) (Chu and Weiss, 2002). Two different CKs, one of each subfamily, form a polar coiled-coil heterodimer (**Fig. 46B**). The type I and type II cytokeratins are

arranged in parallel within this coiled-coil dimer (**Fig. 46A**). Two of these polar dimers form staggered antiparallel tetramers that in turn join together into apolar protofilaments. Two of these protofilaments associate into protofibrils which finally associate into IFs (**Fig. 46C**) (Rao et al., 1996; Fuchs and Cleveland, 1998; Owens and Lane, 2003).

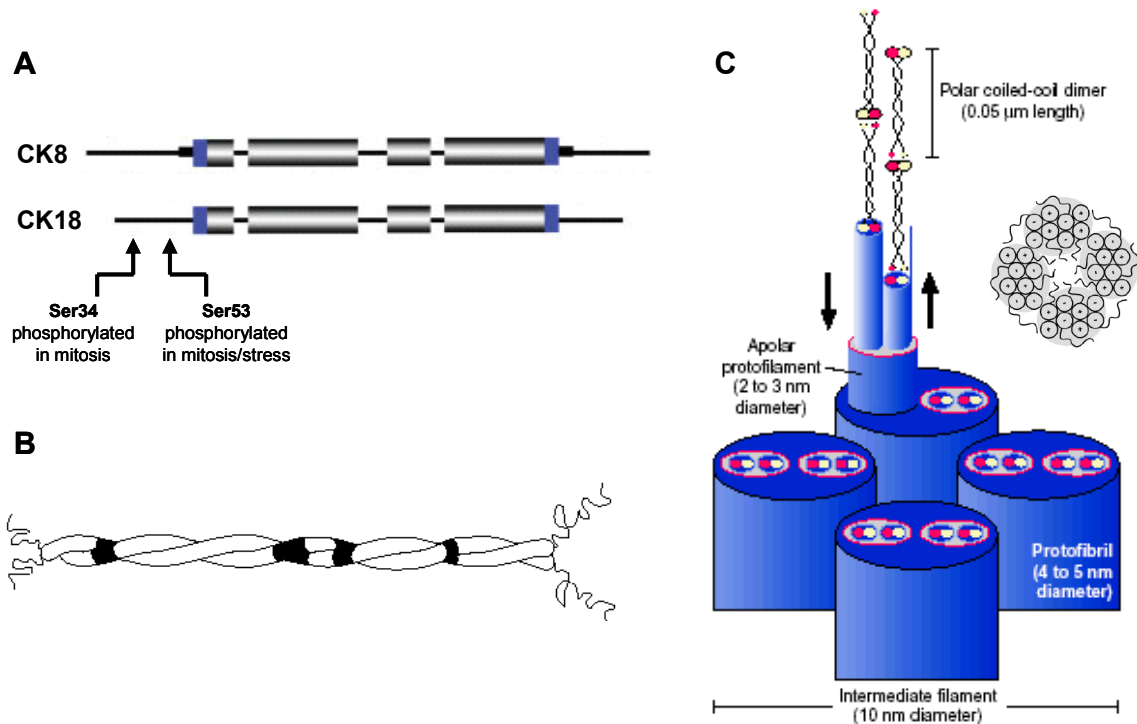


Fig. 46. Structure of intermediate filaments. (A) Cytokeratins of type I (CK18) and type II (CK8), arranged in parallel. Phosphorylation sites in CK18 are indicated (adapted from Owens and Lane, 2003) (B) Polar coiled coil heterodimer composed of a type I and type II cytokeratin (adapted from Rao et al., 1996) (C) Polar coiled coil dimers form staggered antiparallel tetramers that associate into apolar protofilaments and protofibrils. Protofibrils associate into IFs (adapted from Fuchs and Cleveland, 1998; Strelkov et al., 2003).

The type II cytokeratin partner of CK18 is CK8. Both are typically expressed in simple epithelial cells and in many adenocarcinomas (Moll et al., 1983; Chu and Weiss, 2002). The presence of CK18 has already been described previously in the cell line COGA-12 (Vecsey-Semjen et al., 2002). Thus, the observed up-regulation in chemoresistant COGA-12/G6 cells (**Fig. 22, Table 6 and 7**) may rather represent an enhanced posttranslational modification of CK18 such as phosphorylation than transcriptional regulation since CK18 expression is highly abundant in parental COGA-12 cells. CK18 possesses, for example, two phosphorylation sites (**Fig. 46A**) that are phosphorylated in mitotic or stressed cells (Owens and Lane, 2003). The differential regulation of CK18 in the subline COGA-12/G6 most likely contributed to

the chemoresistant phenotype of this cell line. CK18, besides CK8, has been described previously to mediate a resistant phenotype to five different chemotherapeutic agents, i.e. mitoxantrone, doxorubicin, melphalan, bleomycin, and mitomycin C (Anderson et al., 1996). This resistance may be attributed, in part, to a cytokeratin-conferred protection against apoptosis. A similar protection against apoptosis mediated by CK8 and CK18 was also reported for normal epithelial cells. Gilbert and co-workers demonstrated that in murine hepatocytes CK8 and CK18 provide resistance against Fas-mediated apoptosis by reducing the targeting of Fas to the cell surface (Gilbert et al., 2001). Fas protein is retained in the Golgi compartment and upon activation transferred to the surface membrane in a microtubule-dependent manner (Sodeman et al., 2000). How CK8 and CK18 influence this microtubule-dependent process that regulates the Fas density at the surface membrane has not yet been elucidated. Furthermore, actin may also be involved in this process as actin is responsible for the clustering of Fas in the surface membrane (Parlato et al., 2000).

Overall, the results obtained in this thesis strongly suggest that the cytoskeleton plays an important role for the development of acquired resistance against 5-FU in the low passage colon cancer cell line COGA-12, since CK18 and the actin-modulator HSP27 are differentially regulated. Schmidt and co-workers demonstrated, however, that colon cancer cell lines resistant against 5-FU exhibited a down-regulation of other CKs, namely CKB1, CK6, CK5, CK7 and CK19 (Schmidt et al., 2004).

Another protein that was down-regulated in the chemoresistant subline COGA-12/G6, was identified as aldehyde dehydrogenase 1B1 (ALDH1B1) by peptide mass fingerprinting (**Table 6 and 7**). Nineteen enzymes belong to the human aldehyde dehydrogenase superfamily as known so far (Vasiliou and Nebert, 2005). They catalyze the pyridine nucleotide-dependent oxidation of aldehydes to acids and are therefore involved in detoxification reactions (Sladek, 2003). ALDH1A1 and ALDH3A1, for example, catalyze the detoxification of the chemotherapeutic drug cyclophosphamide by degradation of cyclophosphamide metabolites (Sladek, 1999). ALDH3A1 is highly expressed in several tumors where it mediates chemoresistance against cyclophosphamide (Vasiliou et al., 2004). In contrast, mitochondrial

ALDH1B1 is involved in the detoxification of acetaldehydes that accumulate, for example, in the course of ethanol metabolism (Stewart et al., 1995). Besides ALDH1B1 two other ALDHs are involved in acetaldehyde degradation, namely ALDH1A1 and ALDH2 (Vasiliou and Pappa, 2000; Vasiliou et al., 2000). A role for ALDH1B1 in tumor growth, apoptosis or survival signaling has not yet been clarified (Vasiliou et al., 2004). The activity of ALDHs was demonstrated to be equally in colon cancers and respective normal tissue (Jelski et al., 2004). Another investigation implicated that the content of acetaldehyde degrading ALDHs was decreased in colon cancer tissue compared to corresponding normal tissue, though the ALDH content remained still high (Hengstler et al., 1998). Moreover, it was reported that carmofur, a derivative of 5-FU, inhibits the activity of acetaldehyde degrading ALDHs (Kan et al., 1998). In addition to the potential role of HSP27 in 5-FU chemoresistance as discussed before, the observed regulation of mitochondrial ALDH1B1 further supports the conclusion that mitochondrial mechanisms are involved in the chemoresistance against 5-FU.

According to previous work 5-FU resistance was ascribed to alterations in the (fluoro)pyrimidine metabolism (Banerjee et al., 2002). Unexpectedly, none of the differentially regulated proteins identified in this thesis was involved in (fluoro)pyrimidine metabolism. However, a recently performed comparison of the expression profiles of a colon cancer cell line and the corresponding 5-FU resistant subline via GeneChip-arrays also revealed that the regulation of enzymes of the (fluoro)pyrimidine metabolism only played a minor role in the development of 5-FU resistance in this particular subline (Schmidt et al., 2004). Yet, it has to be considered that the activity of a certain protein can be altered in chemoresistant cells whereas its expression level remains unaffected.

The protein up-regulated in the long-term cultivated subline COGA-12/NO, was identified as maspin (**Table 6 and 7**). Maspin was described as an inhibitor of serine proteases exhibiting tumor-suppressing activity in breast cancer (Maass et al., 2000). It has been suggested that maspin functions at the level of invasion and metastasis by blocking tumor cell migration and proliferation (Maass et al., 2000). Furthermore, maspin was reported to promote apoptosis through the regulation of Bcl-2 family proteins (Zhang et al., 2005). However, in thyroid carcinoma, for example, maspin

expression directly correlated with biological aggressiveness (Ito et al., 2004). Moreover, maspin overexpression correlated with poor prognosis in several other cancers of pancreas, ovary, stomach, lung, bladder and skin (Bettstetter et al., 2005). Bettstetter and co-workers further demonstrated that in colorectal cancers maspin was also overexpressed compared to benign colonic mucosa (Bettstetter et al., 2005). They further proposed that the subcellular localization of maspin in the nucleus or the cytosol affected its biological activity, although this is a matter of controversial discussions. More recently, it was demonstrated that maspin was capable to reduce ROS levels by direct interaction with glutathione S-transferase (Yin et al., 2005). This fact could explain the observation that also the long-term cultivated subline COGA-12/NO demonstrates resistance against 5-FU induced apoptosis. The overexpression of maspin could lead to decreased levels of 5-FU-induced ROS by increasing glutathione S-transferase activity that would otherwise promote apoptosis. In the chemoresistant subline COGA-12/G6 this task may be accomplished by HSP27. These findings indicate that two different alterations can provide a similar resistance against 5-FU-induced apoptosis in the chemoresistant and the long-term cultivated sublines. Furthermore, the observation that the cell line COGA-12 exhibits different response to the treatment with 5-FU after long-term cultivation again underlines the importance of using low passage colon cancer cell lines that closely reflect the properties of the corresponding *in vivo* tumors.

In conclusion, the investigation of the chemoresistant subline of the low passage colon cancer cell line COGA-12 by 2D electrophoresis revealed that alterations of the cytoskeleton may contribute to acquired chemoresistance against 5-FU. In addition, alterations in the expression of mitochondria-associated proteins seem to co-contribute to this process. Besides acquired chemoresistance also intrinsic chemoresistance plays a major role for failure of colorectal cancer chemotherapy. Intrinsic resistance differs from acquired resistance because it is present from the beginning of the treatment and does not develop in course of the treatment. Therefore, the investigation of intrinsic chemoresistance is also important. For this purpose, the multicellular spheroids of the low passage cell lines appear as a suitable model system that closely reflect the features of *in vivo* tumors. It was reported previously that multicellular spheroids demonstrated a higher resistance against

chemotherapeutic drugs than their respective monolayers (Kobayashi et al., 1993). Hence, changes in the expression profiles of multicellular spheroids of the low passage colon cancer cells compared to monolayers may contribute to clarify the phenomenon of intrinsic chemoresistance. Interestingly, some of the alterations between multicellular spheroids and monolayers of the low passage colon cancer cell lines, as identified in this work, were also related to the cytoskeleton or nucleoskeleton.

4.3. Lipopolyplexes mediate efficient gene transfer to low passage colon cancer cells

In addition to conventional chemotherapy strategies for colorectal cancer alternative therapy concepts have to be developed. Accumulating evidence demonstrates that bilateral treatment of colorectal cancer can be a promising approach since the impact of chemotherapy is enhanced by simultaneous immunotherapy with IL-2 (Gez et al., 2002; de Gast et al., 2003). However, the systemic application of IL-2 protein often exhibits severe side effects, like capillary leakage syndrome, and hepato- and nephrotoxicity (Bubenik, 2004). A promising alternative to avoid these side effects provides the application of IL-2 by gene therapy. Bishop and co-workers recently demonstrated that the antitumoral effect of the chemotherapeutic drug 5-FU could be enhanced by simultaneous IL-2 expression via gene therapy (Bishop et al., 2000). Currently, the relatively low efficiency of existing gene transfer systems represents a major problem for their broad application. Comparing the available gene delivery methods, nonviral systems provide several advantages over viral vectors, like e.g. minimal side effects and reduced immunogenicity.

A promising improvement for current nonviral gene delivery is the combination of cationic lipids and polycations to form lipopolyplexes that may significantly improve gene transfer (Gao and Huang, 1996; Lampela et al., 2002; Lampela et al., 2004). In this thesis various formulations of different polycations (PLL18, PEI22lin, PEI25br, PEI2k), cationic lipids (DOSPER, DOCSPER, DOTAP) and their combinations were therefore compared for their capability of effective gene transfer. First of all, biophysical properties of these formulations were analyzed, because the size of the transfection particles is a critical parameter influencing also their efficiency in gene

transfer. For *in vivo* applications small particles are necessary. At low ionic strength, all tested lipopolyplex formulations were small, with particle sizes in the range from 50 to 130 nm (**Fig. 28**). At physiological ionic strength, however, lipopolyplex formulations containing PLL18, PEI22lin or PEI2k aggregated rapidly. In contrast, the lipopolyplexes of PEI25br combined with DOCSPER or DOSPER retained their small size at the 4 h time point (140 to 220 nm). Although PEI25br and PEI22lin have similar molecular weight, they differ in their chemical structure (branched versus linear) and display different behavior in their ability to condense DNA and to transfect cells (Wightman et al., 2001). PEI22lin/DNA complexes aggregate already at low salt concentrations (0.5 x HBS), while PEI25br/DNA complexes generate small particles and condense DNA to a greater extent than PEI22lin under these conditions (Dunlap et al., 1997). The gene transfer efficiencies of the salt stable lipopolyplexes consisting of PEI25br and the cationic lipids DOCSPER or DOSPER were tested on the low passage colon cancer cell lines as these cells provide more relevant model systems than other available cell lines. Three candidates were chosen as representatives for the broad heterogeneity of these cell lines each representing a different phenotype, i.e. COGA-3 cells as representatives for rounded-up, COGA-5 cells for epithelial-like and COGA-12 cells for piled-up morphology. In addition, two control cell lines, HeLa and SW480, were used. The stable lipopolyplexes displayed up to 400-fold enhanced gene transfer compared to the corresponding lipopolyplexes or PEI25 polyplexes (**Fig. 29**). These experiments demonstrated that lipopolyplexes are superior to lipopolyplexes and polyplexes in gene transfer not only in the control cells HeLa and SW480 but also in the low passage colon cancer cell lines.

Large transfection particles often achieve higher *in vitro* gene transfer efficiency compared to small particles due to enhanced sedimentation onto cells and/or enhanced endosomal release (Boussif et al., 1996; Ogris et al., 1998). Interestingly, the stable DOSPER/PEI25br/DNA formulations of medium size displayed very similar gene transfer efficiency as the large aggregated (> 1 μ m) DOSPER/PEI22lin/DNA lipopolyplex formulations (**Fig. 30**). In this case the improved gene transfer efficiency of the stable PEI25 lipopolyplexes cannot be attributed to a sedimentation process.

Furthermore, experiments using EGFP as a reporter gene demonstrated that the number of EGFP positive cells was significantly higher when lipopolyplexes were

used for transfection in the presence of serum compared to the corresponding lipoplexes or polyplexes (**Fig. 36**). It is interesting to note that in the absence of serum the percentage of EGFP positive cells was almost equal independent whether lipopolyplexes or their corresponding lipoplexes were used for gene transfer. This phenomenon can be explained by the different biophysical properties of the both formulations leading to different levels and velocities of aggregation in serum-free medium. It is well known, that gene transfer efficiency *in vitro* strongly depends on the size of the particles applied (Ogris et al., 1998; Pelisek et al., 2005). Hence, rapid aggregation of a formulation leads to enhanced gene transfer efficiency.

However, despite the comparable number of transfected cells, the expression levels of luciferase were significantly lower with lipoplexes compared to lipopolyplexes also in the absence of serum (**Fig. 29**). This contradiction can be explained as follows: When using lipoplexes endosomal release and dismantling of DNA from cationic lipids occurs usually in a coordinated process thus the DNA is unprotected against degradation by cytoplasmic nucleases (Xu and Szoka, Jr., 1996). In contrast, in lipopolyplexes the polycation is believed to be still associated with the DNA following endosomal release, thus allowing better protection against degradation and greater DNA stability (Bieber et al., 2002) (see also discussion below). Therefore, less molecules of DNA will reach the nucleus in the case of lipoplexes compared to lipopolyplexes leading to lower expression levels, although the same amount of cells is transfected by both formulations (in the absence of serum).

The data obtained by transfections using the reporter genes luciferase and EGFP revealed an obvious independence between the number of transfected cells and the level of gene expression. The amount of transfected cells depends on the efficiency of cellular uptake of the gene transfer complexes. The level of gene expression, however, depends on the ability of the formulations to disrupt endosomal membrane, the stability of DNA within the cytoplasm and the efficiency of DNA to achieve the nucleus of the respective cells. This was confirmed by the fact that, for example, by using lipopolyplexes COGA-5 cells exhibited the highest level of luciferase expression among the tested low passage colon cancer cell lines (**Fig. 29**), although the lowest number of EGFP positive cells was detected in this cell line (**Fig. 36**).

The inefficiency of DNA formulations to escape the endosomolytic pathway strongly limits the efficiency of gene transfer. Free cationic lipids or PEI are able to enhance gene transfer by enhancing endosomal membrane disruption (Gao and Huang, 1996; Boeckle et al., 2004). PEI is known to possess high buffering capacity and consequently high endosomolytic activity (Boussif et al., 1995). In the case of lipopolyplex formulations, cationic lipid and PEI25br may act simultaneously in releasing DNA from endosomes, thus enhancing gene transfer. For the preparation of lipopolyplexes DNA was mixed with PEI25br first following addition of cationic lipid, because it was previously demonstrated that this order of mixing resulted in the highest transfection efficiencies (Lee et al., 2003; Pelisek et al., 2005). Therefore, cationic lipids may form an additional protective layer around the pre-condensed polycation/DNA formulations or cause partial rearrangement of these formulations where both polycation and cationic lipid work synergistic in DNA protection. Following dismantling of lipopolyplexes in the endosomes, polycations may still be associated with DNA after endosomal release, thus allowing enhanced protection of DNA against cytoplasmic nucleases.

The high potential of lipopolyplexes as an improved nonviral gene transfer system was further demonstrated by the observation that this formulation provided also the ability to efficiently transfect multicellular spheroids that mimic the three-dimensional structure of *in vivo* tumors. When using lipopolyplexes and the reporter gene for EGFP in multicellular spheroids efficient gene transfer could be observed (**Fig. 31**). Confocal microscopy and cryosectioning demonstrated that only cells located near the surface of the multicellular spheroids exhibited EGFP fluorescence and were therefore transfected (**Fig. 32**). This finding strongly suggested that the gene transfer complexes are able to diffuse only to limited distance into the compact spheroid structure. However, in contrast to multicellular spheroids *in vivo* tumors usually exhibit strong vascularisation (Auguste et al., 2005), which enables the transport of the lipopolyplexes also into the inside of the tumor.

In summary, only lipopolyplex formulations containing PEI25br and the cationic lipids DOSPER or DOCSPER generated at physiological salt conditions were stable to aggregation. These particles with medium sizes of 140-220 nm mediated efficient gene transfer in low passage colon cancer cell lines. Such formulations are therefore

promising tools for *in vitro* and potentially also *in vivo* gene transfer to colorectal cancer cells. They not only enabled efficient gene transfer in cells cultivated as traditional monolayers but also in multicellular spheroids which are more relevant with respect to *in vivo* applications.

4.4. The artificial CTP4 promoter enables high colorectal cancer specific gene expression

Besides the improvement of gene transfer efficiency, colon cancer specific gene expression is another promising strategy for the development of an efficient tumor-targeted gene therapy system. Mutations leading to β -catenin accumulation throughout the cell are found in more than 70 % of human colon tumors (Kinzler and Vogelstein, 1996). Therefore, a β -catenin/TCF-dependent promoter would be highly specific for expression in most colon cancer cells. Such a promoter, CTP1, was recently developed by Lipinski et al. (2001) and further optimized for its specificity, resulting in the artificial CTP4 promoter (Lipinski et al., 2004).

In this thesis the efficiency of this CTP4 promoter was tested in various human low passage colon cancer cell lines and as control in SW480 (standard colorectal cell line) and HeLa (non- colorectal) cells using at first Lipofectamine 2000 for gene transfer. The tumor specific promoter enabled high expression levels of luciferase in SW480 cells and all seven low passage colon cancer cell lines tested despite the broad heterogeneity of the different cell lines (**Fig. 33**). In SW480 cells and in three low passage colon cancer cell lines (COGA-2, COGA-3 and COGA-12) the expression levels by the tumor specific CTP4 promoter were even higher than expression levels achieved by the strong, but unspecific CMV promoter. In one cell line (COGA-1) the CTP4 promoter led to CMV promoter comparable expression levels and in three cell lines (COGA-5, COGA-5L and COGA-10) to slightly lower expression levels than the CMV promoter. These results clearly demonstrated that the CTP4 promoter was efficient in a broad range of heterogeneous colorectal cancer cells, however, with different degrees. Different mutations in the various cell lines may account for the observed differences in the efficiency of the CTP4 promoter in comparison to the CMV promoter. For example, it was demonstrated that in COGA-3 cells a β -catenin mutation prevented its proteasome-mediated degradation, which

resulted in accumulation of β -catenin in the nucleus (Vecsey-Semjen et al., 2002). COGA-12 cells also expose elevated levels of β -catenin (Vecsey-Semjen et al., 2002). Therefore, the high efficiency of the CTP4 promoter in both cell lines can be ascribed to elevated β -catenin levels. The lower efficiency of the CTP4 promoter in COGA-5 cells, for example, correlates with the fact that in these cells β -catenin is mainly located at cytoplasmic membranes (Vecsey-Semjen et al., 2002). Other mutations associated with the Wnt signaling pathway (Peifer, 1999) may further influence the specificity and expression level of the CTP4 promoter. For example, the APC protein that is involved in the degradation of β -catenin is truncated in the cell lines COGA-5 and COGA-12, while it is not mutated in the cell line COGA-3 (Vecsey-Semjen et al., 2002). In control experiments in non-colorectal HeLa cells the CTP4 promoter was at least 1000-fold less effective than the CMV promoter, in agreement with published results by Lipinski and co-workers (Lipinski et al., 2004). This underlines the high specificity of the CTP4 promoter for colon cancer cells with deregulated β -catenin.

More detailed analysis of the CTP4 promoter was performed using COGA-3, COGA-5 and COGA-12 cells and optimized lipopolyplexes of the cationic lipid DOSPER and the polycation PEI25br as well as their corresponding lipoplexes and polyplexes for gene transfer (**Fig. 34**). Importantly, the results demonstrated that also the transcriptionally targeted lipopolyplexes mediated an up to 1300-fold higher luciferase expression compared to the corresponding lipoplexes and polyplexes. In COGA-3, COGA-12, and control SW480 cells the CTP4 promoter had higher luciferase expression levels than the CMV promoter, similar to the results achieved with Lipofectamine 2000 above. In the cell line COGA-5, the CTP4 promoter had again lower luciferase expression levels than the CMV promoter, but the expression level was still in a high range.

Furthermore, the analysis of EGFP expression controlled by the CTP4 or the CMV promoter showed equal percentages of EGFP positive cells regardless which promoter was used (**Fig. 36**). This demonstrates that the enhanced luciferase expression levels obtained by the CTP4 promoter compared to the CMV promoter are due to higher transcriptional activity achieved by the CTP4 promoter and not attributable to differences in transfection efficiencies.

Finally, transfection of multicellular spheroids with transcriptionally targeted lipopolyplexes led also to a high quantity of EGFP positive cells (**Fig. 37**). The amount of EGFP positive cells was comparable with the amount obtained by lipopolyplexes containing the EGFP gene under control of the CMV promoter. This suggests that the transcriptionally targeted lipopolyplexes are suitable for future *in vivo* applications.

In conclusion, the use of transcriptionally targeted lipopolyplexes that combine efficient lipopolyplex formulations with tumor specific CTP4 promoter containing plasmids can be a powerful approach for the treatment of colon cancer as it combines enhanced gene transfer efficiency, high expression levels and high tumor specificity.

4.5. Transcriptionally targeted lipopolyplexes enable sufficient expression of the immune stimulatory gene IL-2

The transcriptionally targeted lipopolyplexes might be applied for a therapeutic treatment of colorectal cancer. For example, the tumor specific expression of the immune stimulatory gene IL-2 at high levels directly in tumor cells will be a very promising approach. Furthermore, combination therapy of colorectal cancers with the IL-2 gene (applied by the transcriptionally targeted lipopolyplexes) together with conventional chemotherapy is conceivable. Therefore, the expression levels of IL-2 after transfection with transcriptionally targeted lipopolyplexes in comparison to lipopolyplexes harboring the IL-2 gene under control of the CMV promoter were investigated in the colon cancer cell line SW480 and the low passage colon cancer cell line COGA-12 (**Fig. 38**). High amounts of IL-2 were expressed in the two cell lines after application of both the CMV and the CTP4 promoter (up to 95 ng IL-2 per 1×10^5 cells in 24 h). However, while large amounts of DNA (1 μ g IL-2 DNA per $1 - 1.5 \times 10^5$ cells) were necessary to obtain high IL-2 levels by utilization of the CMV promoter, already small amounts of DNA (0.25 μ g IL-2 DNA per $1 - 1.5 \times 10^5$ cells) were sufficient to obtain high levels of IL-2 by utilization of the CTP4 promoter. The CTP4 promoter directed 3-fold and even up to 350-fold higher IL-2 expression levels than the CMV promoter when low DNA amounts were used for transfection of the cell lines COGA-12 and SW480, respectively. When the amount of transfected DNA was

increased (to 1 μg DNA per $1 - 1.5 \times 10^5$ cells), equal IL-2 expression levels were obtained by both promoters in COGA-12 cells. Comparable results were achieved regarding luciferase expression levels (**Fig. 35**). Again, the differences in the luciferase expression levels were less pronounced between both promoter systems when high DNA doses were applied. A probable reason for these observations is that with increasing amounts of DNA the expression machinery of the cell is saturated which limits the maximum expression level of the exogenous gene. The benefit of the CTP4 promoter over the CMV promoter was clearly visible when using lower DNA doses, where the DNA concentration and not the expression machinery was the limiting factor. This also explains why the CTP4-driven IL-2 expression level of SW480 cells could not be further increased with high DNA amounts compared to low DNA amounts. The saturation level of protein expression was achieved already with the low DNA amount. Thus, the present investigations with IL-2 gene transfer demonstrated that if the extend of DNA transfer is high, the use of the tumor specific CTP4 promoter leads to expression levels comparable with the expression levels of the widely used, strong, but unspecific CMV promoter. However, in the case of lower gene transfer efficiency, for example after *in vivo* applications, the use of the tumor specific promoter CTP4 may lead to favorable expression levels compared to the CMV promoter expression levels. Hence, the use of the CTP4 promoter may partially compensate for low transfection efficiencies *in vivo*.

Furthermore, transfection of multicellular spheroids of COGA-12 cells with lipopolyplexes resulted also in pronounced IL-2 expression (up to 1.4 ng per multicellular spheroid) (**Fig. 39**), although only cells at the surface of the multicellular spheroids were transfected according to the EGFP expression pattern of transfected multicellular spheroids (**Fig. 32**). Again, the expression levels were higher with the CTP4 promoter than with the unspecific CMV promoter.

In summary, the transcriptional targeted lipopolyplexes developed in this thesis enabled high expression of the reporter genes luciferase and EGFP, and also high expression of the therapeutic gene IL-2 following transfection of the low passage colon cancer cells, even in multicellular spheroids.

4.6. Therapeutic potential of combined immune stimulatory and cytotoxic gene expression in colorectal cancer cells

High expression levels of immune stimulatory IL-2 after transfection of tumor cells is a promising therapeutic approach. However, an even higher impact of gene therapy may be achieved, if the expression of a cytotoxic gene would reduce viability or proliferation of the transfected cells in addition to the activation of the immune system by e.g. IL-2. The efficiency of bicistronic constructs enabling simultaneously expression of a cytotoxic and a cytokine gene for gene therapy has already been demonstrated (Kwong et al., 1997; Pizzato et al., 1998). In this thesis a novel bicistronic construct, 2A-IRES-IL2, enabling the simultaneous expression of the cytotoxic rhinoviral protease 2A and the immune stimulatory IL-2 was investigated. Protease 2A inhibits cap-dependent translation and therefore the expression of cellular proteins in general, which in turn leads to reduced viability. In contrast, despite the presence of protease 2A sufficient expression of IL-2 is enabled by an IRES-element located upstream of the IL-2 encoding sequence in the 2A-IRES-IL2 plasmid. This IRES enables the cap-independent expression of IL-2 as shown in **Fig. 47**.

Protease 2A expression by such a 2A-IRES-IL2 construct has been reported previously (Kisser, 2003). In this study successful mediated protease 2A expression was demonstrated by cleavage of translation initiation factor eIF4G, the major substrate of protease 2A. Yet, evidence for an influence of the expression of protease 2A on the viability of the treated cells was missing. In the present work, the therapeutic potential of the 2A-IRES-IL2 construct was analyzed in the low passage colon cancer cell line COGA-12, in SW480 cells, and in HeLa cells. In addition, the properties of the 2A-IRES-IL2 construct were investigated in combination with the CTP4 promoter.

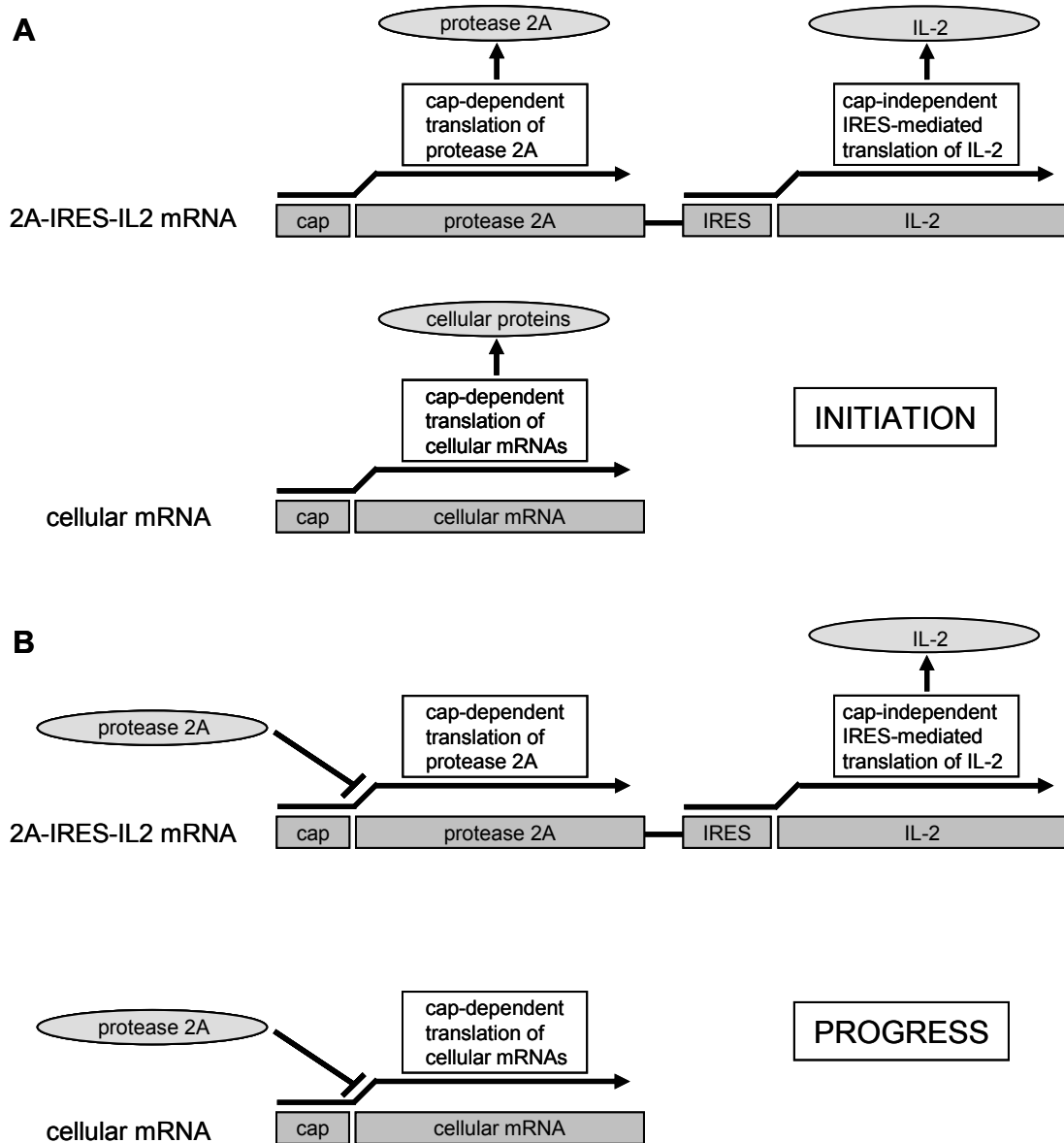


Fig. 47. Effect of protease 2A on cap-dependent or IRES-mediated cap-independent translation in cells transfected with 2A-IRES-IL2 plasmid. Examples of the 2A-IRES-IL2 mRNA and a cellular mRNA are displayed. (A) Translation processes early after initiation of 2A-IRES-IL2 transcription. (B) Translation processes at later time point when protease 2A is already expressed at high levels.

The results demonstrated that protease 2A is capable of reducing the overall gene expression of transfected cells. This was demonstrated by measuring the decrease of expression levels of the reporter genes luciferase and EGFP, which were cotransfected for this purpose (**Fig. 40 and 41**). The influence of protease 2A was considered relatively to cells transfected with appropriate control plasmids without protease 2A. In the cell lines SW480 and COGA-12 already one day after transfection the expression levels of luciferase were up to 14-fold lower in presence

of protease 2A compared to luciferase levels in control transfections independent whether the CMV or the CTP4 promoter was used (**Fig. 40**). Three days after transfection the expression of luciferase was further reduced in both cell lines. In contrast, in HeLa cells only the CMV but not the CTP4 promoter enabled sufficient expression of protease 2A that decreased the luciferase level already one day after transfection. This data confirmed again the specificity of the CTP4 promoter in colon cancer cells. Three days after transfection the CMV promoter-driven expression of protease 2A decreased luciferase levels of HeLa cells even up to 50-fold compared to control transfections, while the CTP4 promoter-driven expression of protease 2A only slightly decreased luciferase levels. Two days after transfection the mean fluorescence intensities (MFIs) of EGFP expression were about 1.8-fold lower in presence of protease 2A compared to the MFIs of EGFP expression in control transfections in the cell lines SW480 and COGA-12 (**Fig. 41**). These results were again independent of the promoter that was used for the expression of protease 2A. Accordingly, the MFI of EGFP expression in HeLa cells analyzed two days after transfection was up to 4-fold decreased by the CMV-driven protease 2A compared to the MFI of EGFP expression in control transfections. In contrast, the CTP4-driven protease 2A expression in HeLa cells was obviously negligible and therefore did not significantly decrease the MFI of EGFP expression.

Protease 2A decreased the expression of luciferase to a greater extent (14-fold in SW480 cells) than the expression of EGFP (1.8-fold in SW480 cells). Apparently, for analysis of the effect of protease 2A the luciferase reporter system is more sensitive than EGFP, because of the higher turnover rate of luciferase compared to the stably expressed EGFP. Furthermore, the higher reduction observed in the luciferase cotransfection assays was most likely the result of overall gene expression reduction and, in addition, cytotoxic effects mediated by protease 2A. In contrast, in the EGFP cotransfection assays only surviving cells were analyzed according to the flow cytometry settings. Therefore, the reduction of the MFI of EGFP expression represented only the protease 2A-mediated decrease of overall gene expression in viable cells but not in cells where protease 2A-mediated blockade of protein expression exerted strong toxicity and cell death. Nevertheless, a significant reduction of protein expression was still clearly detectable.

The expression of protease 2A reduced the viability of transfected SW480 and COGA-12 cells down to about 60 % and 80 % of control transfected cells three days after transfection, again independent of the used promoter (**Fig. 42**). In contrast, in HeLa cells the expression of protease 2A controlled by the CTP4 promoter was insufficient to influence cell viability compared to control transfections, while CMV promoter controlled expression of protease 2A reduced viability of the HeLa cells also to 60 % of control transfections. Despite the fact that protease 2A reduced the viability and proliferation of transfected cells, the enzyme did not alter their apoptosis level compared to cells transfected with a control plasmid (**Fig. 43**). This result is in contradiction to previously published data reporting enhanced apoptosis levels in cell lines that stably expressed protease 2A in an inducible manner (Goldstau et al., 2000; Calandria et al., 2004). However, for these experiments polioviral protease 2A was used in contrast to the rhinoviral protease 2A used in the present work. Nevertheless, the utilization of rhinoviral protease 2A appears as a viable strategy for the treatment of colorectal cancer since the inhibition of proliferation of cancer cells is a requisite aim of tumor therapy and the missing apoptosis allows the expression of IL-2 necessary for the activation of the immune system.

Furthermore, it was demonstrated that the IRES sequence, located upstream of the IL-2 gene in the 2A-IRES-IL2 construct, enabled significant cap-independent expression levels of IL-2 (**Fig. 44**), despite the fact that the overall cap-dependent gene expression is reduced by expression of protease 2A. Up to 2 ng IL-2 per 10^5 cells were expressed under control of the CMV promoter within 24 h after using lipopolyplexes for gene transfer to the cell lines SW480 and COGA-12. The CTP4 promoter achieved slightly lower IL-2 levels compared to the CMV promoter in both cell lines. This result is in discrepancy with former results of the present work using another construct expressing only IL-2, where the CTP4 promoter mediated significantly higher IL-2 expression levels than the CMV promoter. However, the CTP4 promoter may exhibit different efficiencies in the context of the 2A-IRES-IL2 construct. Most importantly, even in the context of the 2A-IRES-IL2 construct the CTP4 promoter provided sufficient expression levels of IL-2 that were comparable to the expression levels by the strong CMV promoter. In addition, the CTP4 promoter

expression is specific for colorectal cancer cells in contrast to the unspecific CMV promoter.

Moreover, the IL-2 expression levels were in general lower in the context of the 2A-IRES-IL2 construct compared to plasmids harboring exclusively the IL-2 gene in previous experiments, independent of the used promoter. Several reasons could be responsible for this discrepancy. Since the 2A-IRES-IL2 construct consists of two encoding sequences it is larger than the plasmid exclusively harboring the IL-2 gene. Therefore, it is likely that fewer 2A-IRES-IL2 plasmid numbers are complexed in a single lipopolyplex compared to lipopolyplexes containing the smaller IL-2 plasmid. Hence, fewer numbers of 2A-IRES-IL2 plasmid than of IL-2 plasmid may be delivered to the cells. Moreover, the quantity of mRNAs transcribed from the 2A-IRES-IL2 sequence is probably reduced as the presence of protease 2A reduces the overall gene expression of the transfected cells and thereby also the availability of components necessary for the transcription machinery. The availability of proteins required for the translation of IL-2 is most likely also reduced. Finally, the IRES-mediated translation of IL-2 may be less effective than the cap-dependent translation of IL-2. Nevertheless, the use of the novel 2A-IRES-IL2 bicistronic construct provided considerable IL-2 expression levels despite the cytotoxic properties accomplished through the protease 2A.

In conclusion, the bicistronic construct 2A-IRES-IL2 encoding the cytotoxic rhinoviral protease 2A and the therapeutic IL-2 applied by transcriptionally targeted lipopolyplexes is a promising tool for the treatment of colorectal cancer. The protease 2A significantly reduced viability not only of transfected standard cell lines but also of low passage colon cancer cells while concomitantly sufficient expression of immune stimulatory IL-2 was assured.

5. SUMMARY

The development of relevant cellular model systems for colorectal cancer is of utmost importance for an improved *in vitro* assessment of therapeutic strategies against colorectal cancer.

Recently published low passage colon cancer cell lines that closely reflect the characteristics of the respective parental *in vivo* tumor cells represent very promising cell culture models and were therefore used for the investigations in the present thesis. To provide an *in vitro* model system that also recapitulates the three-dimensional structure of *in vivo* tumors, these low passage cell lines were cultivated as multicellular spheroids. Compared to monolayer cultures the multicellular spheroids exhibited a wide variety of changes in their expression patterns. The differential expression includes proteins that are involved in growth signaling (15-hydroxyprostaglandin dehydrogenase), protein biosynthesis (acidic ribosomal protein P0), and regulation of the cyto- or nucleoskeleton (acidic calponin and LMNA protein). These proteins were identified by 2D electrophoresis and subsequent MALDI-TOF mass spectrometry. Both methods were established in the lab in the context of this work.

Chemotherapy with 5-FU represents the traditional treatment of colorectal cancer. However, in many patients the efficiency of this therapeutic strategy is often limited by the development of chemoresistance against 5-FU. Therefore, it was an aim of this thesis to detect novel proteins involved in 5-FU chemoresistance that were previously not ascribed to resistance against this chemotherapeutic drug. A chemoresistant subline of a colon cancer cell line was generated by long-term treatment with 5-FU and served as a model for the investigation of 5-FU chemoresistance. This subline exhibited resistance against both 5-FU-induced inhibition of proliferation and apoptosis. Differences in the expression of cytokeratin 18, heat shock protein 27 and aldehyde dehydrogenase 1B1 between the chemoresistant subline and parental cells were detected by 2D electrophoresis. These findings imply that the cytoskeleton plays a role in the development of chemoresistance against 5-FU. Furthermore, processes located to the mitochondria

seem to be involved in this resistance, since heat shock protein 27 and aldehyde dehydrogenase 1B1 are associated with this subcellular organelle. The biological relevance of the findings made in the present PhD thesis has to be determined in further studies.

Gene therapy represents a promising alternative strategy for the treatment of colorectal cancer. A novel nonviral gene transfer system was developed by combination of DNA with the polycation PEI25br and the cationic lipids DOCSPER or DOSPER to form lipopolyplexes. These lipopolyplexes enabled enhanced gene transfer *in vitro* and are promising for *in vivo* applications, since the established lipopolyplexes preserved their small size at physiological conditions; a property essential for a successful *in vivo* application. Furthermore, the lipopolyplexes exhibited the capability to efficiently transfect three-dimensional multicellular spheroids. The potential of lipopolyplexes for therapeutic applications was further increased by the utilization of the artificial promoter CTP4 which enables highly specific gene expression in cancer cells with mutations in the Wnt signaling pathway by transcriptional targeting. In addition to its high specificity, this promoter enabled high gene expression levels that were comparable to expression levels obtained by the strong, but unspecific CMV promoter. The efficiency of the CTP4 promoter was demonstrated in seven low passage colon cancer cell lines and also in multicellular spheroids. The transcriptional targeted lipopolyplexes not only enabled high tumor specific expression of reporter genes like luciferase or EGFP but also the expression of a therapeutic gene, interleukin-2 (IL-2). Furthermore, tumor specific expression of cytotoxic protease 2A in combination with IL-2 was possible by using a novel bicistronic construct. The expression of the rhinoviral protease 2A led to efficient reduction of overall cap-dependent gene expression levels and therefore also the proliferation of the transfected cells, while continued IL-2 expression was guaranteed by an IRES element enabling cap-independent gene expression in the presence of protease 2A.

In summary, the present results provide a promising basis for the development of novel potent strategies in the treatment of colorectal cancer.

6. APPENDIX

6.1. Abbreviations

aa	amino acids
ALDH	aldehyde dehydrogenase
APC	adenomatous polyposis coli
ATP	adenosine triphosphate
bp	base pairs
BSA	bovine serum albumin
CHAPS	3-[(3-Cholamidopropyl)dimethylammonio]-1-propanesulfonate
CK18	cytokeratin 18
CMV	cytomegalovirus
COX-2	cyclooxygenase 2
CY5	cyanine-5
2D	two-dimensional
DAPI	4',6-Diamidino-2-phenylindole
DMEM	Dulbecco's Modified Eagle's Medium
DMSO	dimethyl sulfoxide
DNA	deoxyribonucleic acid
dNTP	deoxynucleotide triphosphate
DOCSPER	1,3-dioleoyloxy-2-(N-carbamoyl-spermyl)-propane)
DOSPER	1,3-dioleoyloxy-2-(6-carboxy-spermyl)-propylamide
DOTAP	N-[1-(2,3-dioleoyloxy)propyl]-N,N,N-trimethyl-ammonium methylsulfate
DTE	dithioerythritol
DTT	dithiothreitol
ECM	extracellular matrix
E.coli	Escherichia coli
EDTA	ethylenediaminetetraacetic acid

EGF	epidermal growth factor
EGFP	enhanced green fluorescent protein
ELISA	enzyme-linked immunosorbent assay
FAP	familial adenomatous polyposis
FCS	fetal calf serum
FITC	fluorescein isothiocyanate
5-FU	5-fluorouracil
g	relative centrifugal force
HBS	HEPES-buffered saline
HCl	hydrochloric acid
HEPES	N-(2-hydroxyethyl)piperazine-N'-(2-ethanesulfonic acid)
HNPCC	hereditary nonpolyposis colorectal cancer
hIL-2	human interleukin-2
HSP27	heat shock protein 27
IEF	isoelectric focusing
IF	intermediate filament
IL-2	interleukin-2
IRES	internal ribosomal entry site
kDa	kilo Dalton
Luc	luciferase
MALDI	matrix assisted laser desorption ionization
MCR	multicellular resistance
MDR	multidrug resistance
MFI	mean fluorescence intensity
MMR	mismatch repair
MSI	microsatellite instability
MS	mass spectrometry
MTT	1-(4,5-Dimethylthiazol-2-yl)-3,5-diphenylformazan
N/P ratio	molar ratio of PEI nitrogen to DNA phosphate
NA	numerical aperture
NaCl	sodium chloride

p2A-IRES-IL2	plasmid encoding for rhinoviral protease 2A and interleukin-2 under control of the CMV promoter/enhancer
PBS	phosphate-buffered saline
pCMV-2A-IRES-IL2	plasmid encoding for rhinoviral protease 2A and interleukin-2 under control of the CMV promoter/enhancer based on pEGFP-N1
pCMV-Luc	plasmid encoding for luciferase under control of the CMV promoter/enhancer
pCTP4-2A-IRES-IL2	plasmid encoding for rhinoviral protease 2A and interleukin-2 under control of the CTP4 promoter based on pEGFP-N1
pCTP4-hIL-2	plasmid encoding for interleukin-2 under control of the CTP4 promoter
pCTP4-Luc	plasmid encoding for luciferase under control of the CTP4 promoter
pEGFP-LG-CTP4	plasmid encoding for EGFP under control of the CTP4 promoter
pEGFP-Luc	plasmid encoding a fusion of EGFP and luciferase under control of the CMV promoter/enhancer
pEGFP-N1	plasmid encoding for EGFP under control of the CMV promoter/enhancer
pEGFP-N1-0	plasmid encoding for EGFP without the presence of a promoter
PEI	polyethylenimine
PEI22lin	linear PEI of 22 kDa
PEI25br	branched PEI of 25 kDa
PEI2k	branched PEI of 2 kDa
PFA	para-formaldehyde
15-PGDH	15-hydroxyprostaglandin dehydrogenase
Pgp	P-glycoprotein
pGShIL-2tet	plasmid encoding for interleukin-2 under control of the CMV promoter/enhancer
PI	propidium iodide

PLL18	poly-L-lysine with 18 lysine monomers
PTM	posttranslational modification
RLU	relative light units
RNA	ribonucleic acid
ROS	reactive oxygen species
rpm	revolutions per minute
RPMI	Roswell Park Memorial Institute medium
RT	room temperature
SDS	Sodium dodecyl sulfate
SE	standard error
TFA	trifluoroacetic acid
TGF- β	transforming growth factor β
TOF	time of flight
Tris	tris(hydroxymethyl)aminomethane
TS	thymidylate synthase
w	weight

6.2. Publications

6.2.1. Original Papers

Pelisek, J., Gaedtke, L., DeRouchey, J., Walker, G.F., Nikol, S., and Wagner, E. (2006). Optimized lipopolyplex formulations for gene transfer to human colon carcinoma cells under in vitro conditions. *J. Gene Med.* 8, 186-197.

Pelisek, J., Fuchs, A., Kuehnl, A., Tian, W., Kuhlmann, M., Rolland, P.H., Wagner, E., Mekkaoui, C., Gaedtke, L., Armenau, S., and Nikol, S. Gene transfer of C-type Natriuretic Peptide is superior over single CNP peptide administration. *J. Gene Med.*, *resubmitted*.

Gaedtke, L., Pelisek, J., Lipinski, K., Wrighton, C., and Wagner, E. Efficient and cancer specific transgene expression using lipopolyplexes and a β -catenin/TCF-dependent promoter in human low passage colon cancer cells. *Hum. Gene Ther.*, *submitted*.

Gaedtke, L., Pelisek, J., Kisser, A., Seipelt, J., and Wagner, E. Cancer specific IRES-mediated coexpression of cytotoxic and immune stimulatory molecules in human colon cancer cells, *in preparation*.

Gaedtke, L., Culmsee, C., Mayer, B., and Wagner, E. Alterations in the protein expression pattern in multicellular spheroids compared to monolayer cultures, *in preparation*.

Gaedtke, L., Culmsee, C., Ogris, M., and Wagner, E. Regulation of cytoskeleton- and mitochondria-associated proteins related to chemoresistance against 5-FU, *in preparation*.

6.2.2. Poster presentation

Gaedtke, L., Mayer, B., Wagner, E. (2003). Multicellular spheroids of human low passage colon cancer cell lines. Proteomic Forum, 14.-17. September, Munich.

7. REFERENCES

- Abbott, A. (2003). Cell culture: biology's new dimension. *Nature* 424, 870-872.
- Anderson, J. M., Heindl, L. M., Bauman, P. A., Ludi, C. W., Dalton, W. S., and Cress, A. E. (1996). Cytokeratin expression results in a drug-resistant phenotype to six different chemotherapeutic agents. *Clin. Cancer Res.* 2, 97-105.
- Applegate, D., Feng, W., Green, R. S., and Taubman, M. B. (1994). Cloning and expression of a novel acidic calponin isoform from rat aortic vascular smooth muscle. *J Biol. Chem.* 269, 10683-10690.
- Arrigo, A. P. (1998). Small stress proteins: chaperones that act as regulators of intracellular redox state and programmed cell death. *Biol. Chem.* 379, 19-26.
- Arrigo, A. P. (2001). Hsp27: novel regulator of intracellular redox state. *IUBMB. Life* 52, 303-307.
- Arrigo, A. P., Viot, S., Chaufour, S., Firdaus, W., Kretz-Remy, C., and Diaz-Latoud, C. (2005). Hsp27 consolidates intracellular redox homeostasis by upholding glutathione in its reduced form and by decreasing iron intracellular levels. *Antioxid. Redox. Signal.* 7, 414-422.
- Auguste, P., Lemièrre, S., Larrieu-Lahargue, F., and Bikfalvi, A. (2005). Molecular mechanisms of tumor vascularization. *Crit Rev. Oncol. Hematol.* 54, 53-61.
- Backlund, M. G., Mann, J. R., Holla, V. R., Buchanan, F. G., Tai, H. H., Musiek, E. S., Milne, G. L., Katkuri, S., and Dubois, R. N. (2005). 15-Hydroxyprostaglandin dehydrogenase is down-regulated in colorectal cancer. *J Biol. Chem.* 280, 3217-3223.
- Backus, H. H., Wouters, D., Ferreira, C. G., van Houten, V. M., Brakenhoff, R. H., Pinedo, H. M., and Peters, G. J. (2003). Thymidylate synthase inhibition triggers apoptosis via caspases-8 and -9 in both wild-type and mutant p53 colon cancer cell lines. *Eur. J Cancer* 39, 1310-1317.
- Badawi, A. F. (2000). The role of prostaglandin synthesis in prostate cancer. *BJU. Int.* 85, 451-462.
- Ballesta, J. P., Rodríguez-Gabriel, M. A., Bou, G., Briones, E., Zambrano, R., and Remacha, M. (1999). Phosphorylation of the yeast ribosomal stalk. Functional effects and enzymes involved in the process. *FEMS Microbiol. Rev.* 23, 537-550.

- Bally, M. B., Harvie, P., Wong, F. M., Kong, S., Wasan, E. K., and Reimer, D. L. (1999). Biological barriers to cellular delivery of lipid-based DNA carriers. *Adv. Drug Deliv. Rev.* **38**, 291-315.
- Banerjee, D., Mayer-Kuckuk, P., Capiiaux, G., Budak-Alpdogan, T., Gorlick, R., and Bertino, J. R. (2002). Novel aspects of resistance to drugs targeted to dihydrofolate reductase and thymidylate synthase. *Biochim. Biophys Acta* **1587**, 164-173.
- Barnard, G. F., Staniunas, R. J., Bao, S., Mafune, K., Steele, G. D., Jr., Gollan, J. L., and Chen, L. B. (1992). Increased expression of human ribosomal phosphoprotein P0 messenger RNA in hepatocellular carcinoma and colon carcinoma. *Cancer Res.* **52**, 3067-3072.
- Benndorf, R., Hayess, K., Ryazantsev, S., Wieske, M., Behlke, J., and Lutsch, G. (1994). Phosphorylation and supramolecular organization of murine small heat shock protein HSP25 abolish its actin polymerization-inhibiting activity. *J Biol. Chem.* **269**, 20780-20784.
- Bettstetter, M., Woenckhaus, M., Wild, P. J., Rummele, P., Blaszyk, H., Hartmann, A., Hofstadter, F., and Dietmaier, W. (2005). Elevated nuclear maspin expression is associated with microsatellite instability and high tumour grade in colorectal cancer. *J Pathol.* **205**, 606-614.
- Bieber, T., Meissner, W., Kostin, S., Niemann, A., and Elsasser, H. P. (2002). Intracellular route and transcriptional competence of polyethylenimine-DNA complexes. *J. Control Release* **82**, 441-454.
- Bienz, M. and Clevers, H. (2000). Linking colorectal cancer to Wnt signaling. *Cell* **103**, 311-320.
- Bishop, J. S., Thull, N. M., Matar, M., Quezada, A., Munger, W. E., Batten, T. L., Muller, S., and Pericle, F. (2000). Antitumoral effect of a nonviral interleukin-2 gene therapy is enhanced by combination with 5-fluorouracil. *Cancer Gene Ther* **7**, 1165-1171.
- Boeckle, S., von Gersdorff, K., van der Piepen, S., Culmsee, C., Wagner, E., and Ogris, M. (2004). Purification of polyethylenimine polyplexes highlights the role of free polycations in gene transfer. *J Gene Med* **6**, 1102-1111.
- Boussif, O., Lezoualc'h, F., Zanta, M. A., Mergny, M. D., Scherman, D., Demeneix, B., and Behr, J. P. (1995). A versatile vector for gene and oligonucleotide transfer into cells in culture and in vivo: polyethylenimine. *Proc. Natl. Acad. Sci. U. S. A* **92**, 7297-7301.
- Boussif, O., Zanta, M. A., and Behr, J. P. (1996). Optimized galenics improve in vitro gene transfer with cationic molecules up to 1000-fold. *Gene Ther* **3**, 1074-1080.

- Brockstedt, E., Rickers, A., Kostka, S., Laubersheimer, A., Dorken, B., Wittmann-Liebold, B., Bommert, K., and Otto, A. (1998). Identification of apoptosis-associated proteins in a human Burkitt lymphoma cell line. Cleavage of heterogeneous nuclear ribonucleoprotein A1 by caspase 3. *J Biol. Chem.* 273, 28057-28064.
- Bubenik, J. (2004). Interleukin-2 therapy of cancer. *Folia Biol. (Praha)* 50, 120-130.
- Buschle, M., Cotten, M., Kirlappos, H., Mechtler, K., Schaffner, G., Zauner, W., Birnstiel, M. L., and Wagner, E. (1995). Receptor-mediated gene transfer into human T lymphocytes via binding of DNA/CD3 antibody particles to the CD3 T cell receptor complex. *Hum. Gene Ther* 6, 753-761.
- Cairns, J., Qin, S., Philp, R., Tan, Y. H., and Guy, G. R. (1994). Dephosphorylation of the small heat shock protein Hsp27 in vivo by protein phosphatase 2A. *J Biol. Chem.* 269, 9176-9183.
- Calandria, C., Irurzun, A., Barco, A., and Carrasco, L. (2004). Individual expression of poliovirus 2Apro and 3Cpro induces activation of caspase-3 and PARP cleavage in HeLa cells. *Virus Res.* 104, 39-49.
- Chandra, J., Samali, A., and Orrenius, S. (2000). Triggering and modulation of apoptosis by oxidative stress. *Free Radic. Biol. Med* 29, 323-333.
- Chu, P. G. and Weiss, L. M. (2002). Keratin expression in human tissues and neoplasms. *Histopathology* 40, 403-439.
- Claria, J., Lee, M. H., and Serhan, C. N. (1996). Aspirin-triggered lipoxins (15-epi-LX) are generated by the human lung adenocarcinoma cell line (A549)-neutrophil interactions and are potent inhibitors of cell proliferation. *Mol Med* 2, 583-596.
- Concannon, C. G., Gorman, A. M., and Samali, A. (2003). On the role of Hsp27 in regulating apoptosis. *Apoptosis.* 8, 61-70.
- Cuesta, R., Laroia, G., and Schneider, R. J. (2000). Chaperone hsp27 inhibits translation during heat shock by binding eIF4G and facilitating dissociation of cap-initiation complexes. *Genes Dev.* 14, 1460-1470.
- Dalle-Donne, I., Rossi, R., Milzani, A., Di Simplicio, P., and Colombo, R. (2001). The actin cytoskeleton response to oxidants: from small heat shock protein phosphorylation to changes in the redox state of actin itself. *Free Radic. Biol. Med* 31, 1624-1632.
- Davis, W. Jr., Ronai, Z., and Tew, K. D. (2001). Cellular thiols and reactive oxygen species in drug-induced apoptosis. *J Pharmacol. Exp. Ther* 296, 1-6.

- de Gast, G. C., Batchelor, D., Kersten, M. J., Vyth-Dreese, F. A., Sein, J., van de Kastele, W. F., Nooijen, W. J., Nieweg, O. E., de Waal, M. A., and Boogerd, W. (2003). Temozolomide followed by combined immunotherapy with GM-CSF, low-dose IL2 and IFN alpha in patients with metastatic melanoma. *Br. J Cancer* *88*, 175-180.
- Desoize, B. and Jardillier, J. (2000). Multicellular resistance: a paradigm for clinical resistance? *Crit Rev. Oncol. Hematol.* *36*, 193-207.
- Doppler, H., Storz, P., Li, J., Comb, M. J., and Toker, A. (2005). A phosphorylation state-specific antibody recognizes Hsp27, a novel substrate of protein kinase D. *J Biol. Chem.* *280*, 15013-15019.
- Dunlap, D. D., Maggi, A., Soria, M. R., and Monaco, L. (1997). Nanoscopic structure of DNA condensed for gene delivery. *Nucleic Acids Res* *25*, 3095-101.
- Eaton, P., Fuller, W., and Shattock, M. J. (2002). S-thiolation of HSP27 regulates its multimeric aggregate size independently of phosphorylation. *J Biol. Chem.* *277*, 21189-21196.
- Eichhorst, S. T., Muerkoster, S., Weigand, M. A., and Krammer, P. H. (2001). The chemotherapeutic drug 5-fluorouracil induces apoptosis in mouse thymocytes in vivo via activation of the CD95(APO-1/Fas) system. *Cancer Res.* *61*, 243-248.
- Fearon, E. R. and Vogelstein, B. (1990). A genetic model for colorectal tumorigenesis. *Cell* *61*, 759-767.
- Felgner, P. L., Gadek, T. R., Holm, M., Roman, R., Chan, H. W., Wenz, M., Northrop, J. P., Ringold, G. M., and Danielsen, M. (1987). Lipofection: A highly efficient, lipid mediated DNA-transfection procedure. *Proc Natl Acad Sci U S A* *84*, 7413-7417.
- Fodde, R. (2002). The APC gene in colorectal cancer. *Eur. J Cancer* *38*, 867-871.
- Fodde, R., Kuipers, J., Rosenberg, C., Smits, R., Kielman, M., Gaspar, C., van Es, J. H., Breukel, C., Wiegant, J., Giles, R. H., and Clevers, H. (2001). Mutations in the APC tumour suppressor gene cause chromosomal instability. *Nat. Cell Biol.* *3*, 433-438.
- Friedmann, T. and Roblin, R. (1972). Gene therapy for human genetic disease? *Science* *175*, 949-955.
- Fuchs, E. and Cleveland, D. W. (1998). A structural scaffolding of intermediate filaments in health and disease. *Science* *279*, 514-519.
- Fujii, T., Yabe, S., Nakamura, K., and Koizumi, Y. (2002). Functional analysis of rat acidic calponin. *Biol. Pharm. Bull.* *25*, 573-579.

Gao, X. and Huang, L. (1996). Potentiation of cationic liposome-mediated gene delivery by polycations. *Biochemistry* **35**, 1027-1036.

Garrido, C., Bruey, J. M., Fromentin, A., Hammann, A., Arrigo, A. P., and Solary, E. (1999). HSP27 inhibits cytochrome c-dependent activation of procaspase-9. *Faseb J* **13**, 2061-2070.

Garrido, C., Ottavi, P., Fromentin, A., Hammann, A., Arrigo, A. P., Chauffert, B., and Mehlen, P. (1997). HSP27 as a mediator of confluence-dependent resistance to cell death induced by anticancer drugs. *Cancer Res.* **57**, 2661-2667.

Gez, E., Rubinov, R., Gaitini, D., Meretyk, S., Best, L. A., Native, O., Stein, A., Erlich, N., Beny, A., Zidan, J., Haim, N., and Kuten, A. (2002). Interleukin-2, interferon-alpha, 5-fluorouracil, and vinblastine in the treatment of metastatic renal cell carcinoma: a prospective phase II study: the experience of Rambam and Lin Medical Centers 1996-2000. *Cancer* **95**, 1644-1649.

Gilbert, S., Loranger, A., Daigle, N., and Marceau, N. (2001). Simple epithelium keratins 8 and 18 provide resistance to Fas-mediated apoptosis. The protection occurs through a receptor-targeting modulation. *J Cell Biol.* **154**, 763-773.

Godbey, W. T., Wu, K. K., and Mikos, A. G. (1999). Poly(ethylenimine) and its role in gene delivery
988. *J. Control Release* **60**, 149-160.

Goldstaub, D., Gradi, A., Bercovitch, Z., Grosman, Z., Nophar, Y., Luria, S., Sonenberg, N., and Kahana, C. (2000). Poliovirus 2A protease induces apoptotic cell death. *Mol Cell Biol.* **20**, 1271-1277.

Groth, D., Keil, O., Lehmann, C., Schneider, M., Rudolph, M., and Reszka, R. (1998). Preparation and characterisation of a new lipospermine for gene delivery into various cell lines. *Int J Pharmac* **162**, 143-157.

Gusev, N. B., Bogatcheva, N. V., and Marston, S. B. (2002). Structure and properties of small heat shock proteins (sHsp) and their interaction with cytoskeleton proteins. *Biochemistry (Mosc.)* **67**, 511-519.

Hasler, P., Brot, N., Weissbach, H., Parnassa, A. P., and Elkon, K. B. (1991). Ribosomal proteins P0, P1, and P2 are phosphorylated by casein kinase II at their conserved carboxyl termini. *J Biol. Chem.* **266**, 13815-13820.

Hatzfeld, M. and Franke, W. W. (1985). Pair formation and promiscuity of cytokeratins: formation in vitro of heterotypic complexes and intermediate-sized filaments by homologous and heterologous recombinations of purified polypeptides. *J Cell Biol.* **101**, 1826-1841.

- He, T. C., Sparks, A. B., Rago, C., Hermeking, H., Zawel, L., da Costa, L. T., Morin, P. J., Vogelstein, B., and Kinzler, K. W. (1998). Identification of c-MYC as a target of the APC pathway. *Science* *281*, 1509-1512.
- Henderson, B. R. (2000). Nuclear-cytoplasmic shuttling of APC regulates beta-catenin subcellular localization and turnover. *Nat. Cell Biol.* *2*, 653-660.
- Hengstler, J. G., Bottger, T., Tanner, B., Dietrich, B., Henrich, M., Knapstein, P. G., Junginger, T., and Oesch, F. (1998). Resistance factors in colon cancer tissue and the adjacent normal colon tissue: glutathione S-transferases alpha and pi, glutathione and aldehyde dehydrogenase. *Cancer Lett.* *128*, 105-112.
- Holubec, H., Payne, C. M., Bernstein, H., Dvorakova, K., Bernstein, C., Waltmire, C. N., Warneke, J. A., and Garewal, H. (2005). Assessment of apoptosis by immunohistochemical markers compared to cellular morphology in ex vivo-stressed colonic mucosa. *J Histochem. Cytochem.* *53*, 229-235.
- Huber, O., Korn, R., McLaughlin, J., Ohsugi, M., Herrmann, B. G., and Kemler, R. (1996). Nuclear localization of beta-catenin by interaction with transcription factor LEF-1. *Mech. Dev.* *59*, 3-10.
- Huland, E. and Huland, H. (1989). Local continuous high dose interleukin 2: a new therapeutic model for the treatment of advanced bladder carcinoma. *Cancer Res.* *49*, 5469-5474.
- Hutter, G. and Sinha, P. (2001). Proteomics for studying cancer cells and the development of chemoresistance. *Proteomics.* *1*, 1233-1248.
- Hwang, P. M., Bunz, F., Yu, J., Rago, C., Chan, T. A., Murphy, M. P., Kelso, G. F., Smith, R. A., Kinzler, K. W., and Vogelstein, B. (2001). Ferredoxin reductase affects p53-dependent, 5-fluorouracil-induced apoptosis in colorectal cancer cells. *Nat. Med.* *7*, 1111-1117.
- Ito, Y., Yoshida, H., Tomoda, C., Uruno, T., Takamura, Y., Miya, A., Kobayashi, K., Matsuzuka, F., Matsuura, N., Kuma, K., and Miyauchi, A. (2004). Maspin expression is directly associated with biological aggressiveness of thyroid carcinoma. *Thyroid* *14*, 13-18.
- Jelski, W., Zalewski, B., Chrostek, L., and Szmitkowski, M. (2004). The activity of class I, II, III, and IV alcohol dehydrogenase isoenzymes and aldehyde dehydrogenase in colorectal cancer. *Dig. Dis. Sci.* *49*, 977-981.
- Jin, J. P., Wu, D., Gao, J., Nigam, R., and Kwong, S. (2003). Expression and purification of the h1 and h2 isoforms of calponin. *Protein Expr. Purif.* *31*, 231-239.

- Kan, S., Moriya, F., and Ishizu, H. (1998). Effects of antineoplastics, antibiotics and antidiabetics on acetaldehyde metabolism after alcohol ingestion. *Acta Med Okayama* 52, 9-17.
- Kaplan, K. B., Burds, A. A., Swedlow, J. R., Bekir, S. S., Sorger, P. K., and Nathke, I. S. (2001). A role for the Adenomatous Polyposis Coli protein in chromosome segregation. *Nat. Cell Biol.* 3, 429-432.
- Kaufmann, S. H. and Earnshaw, W. C. (2000). Induction of apoptosis by cancer chemotherapy. *Exp. Cell Res.* 256, 42-49.
- Kerb, R., Hoffmeyer, S., and Brinkmann, U. (2001). ABC drug transporters: hereditary polymorphisms and pharmacological impact in MDR1, MRP1 and MRP2. *Pharmacogenomics.* 2, 51-64.
- Kinzler, K. W. and Vogelstein, B. (1996). Lessons from hereditary colorectal cancer. *Cell* 87, 159-170.
- Kircheis, R., Wightman, L., and Wagner, E. (2001). Design and gene delivery activity of modified polyethylenimines. *Adv. Drug Deliv. Rev.* 53, 341-358.
- Kisser, A. (2003). IRES-mediated coexpression of cytotoxic and immune modulatory molecules. Diploma Thesis, Department of Medical Biochemistry, Medical University of Vienna.
- Knudson, A. G. (1971). Mutation and cancer: statistical study of retinoblastoma. *Proc. Natl. Acad. Sci. U. S. A* 68, 820-823.
- Knudson, A. G. (1993). Antioncogenes and human cancer. *Proc. Natl. Acad. Sci. U. S. A* 90, 10914-10921.
- Kobayashi, H., Man, S., Graham, C. H., Kapitan, S. J., Teicher, B. A., and Kerbel, R. S. (1993). Acquired multicellular-mediated resistance to alkylating agents in cancer. *Proc. Natl. Acad. Sci. U. S. A* 90, 3294-3298.
- Kondoh, N., Wakatsuki, T., Ryo, A., Hada, A., Aihara, T., Horiuchi, S., Goseki, N., Matsubara, O., Takenaka, K., Shichita, M., Tanaka, K., Shuda, M., and Yamamoto, M. (1999). Identification and characterization of genes associated with human hepatocellular carcinogenesis. *Cancer Res.* 59, 4990-4996.
- Konety, B. R. and Getzenberg, R. H. (1999). Nuclear structural proteins as biomarkers of cancer. *J Cell Biochem Suppl* 32-33, 183-191.
- Koshiji, M., Adachi, Y., Taketani, S., Takeuchi, K., Hioki, K., and Ikehara, S. (1997). Mechanisms underlying apoptosis induced by combination of 5-fluorouracil and interferon-gamma. *Biochem Biophys Res. Commun.* 240, 376-381.

- Kursa, M., Walker, G. F., Roessler, V., Ogris, M., Roedl, W., Kircheis, R., and Wagner, E. (2003). Novel Shielded Transferrin-Polyethylene Glycol-Polyethylenimine/DNA Complexes for Systemic Tumor-Targeted Gene Transfer. *Bioconjug. Chem.* *14*, 222-231.
- Kwong, Y. L., Chen, S. H., Kosai, K., Finegold, M., and Woo, S. L. (1997). Combination therapy with suicide and cytokine genes for hepatic metastases of lung cancer. *Chest* *112*, 1332-1337.
- Lampela, P., Elomaa, M., Ruponen, M., Urtti, A., Mannisto, P. T., and Raasmaja, A. (2003). Different synergistic roles of small polyethylenimine and Dosper in gene delivery. *J Control Release* *88*, 173-183.
- Lampela, P., Raisanen, J., Mannisto, P. T., Yla-Herttuala, S., and Raasmaja, A. (2002). The use of low-molecular-weight PEIs as gene carriers in the monkey fibroblastoma and rabbit smooth muscle cell cultures. *J Gene Med* *4*, 205-214.
- Lampela, P., Soininen, P., Urtti, A., Mannisto, P. T., and Raasmaja, A. (2004). Synergism in gene delivery by small PEIs and three different nonviral vectors. *Int. J Pharm.* *270*, 175-184.
- Landry, J. and Huot, J. (1999). Regulation of actin dynamics by stress-activated protein kinase 2 (SAPK2)-dependent phosphorylation of heat-shock protein of 27 kDa (Hsp27). *Biochem Soc. Symp.* *64*, 79-89.
- Landry, J., Lambert, H., Zhou, M., Lavoie, J. N., Hickey, E., Weber, L. A., and Anderson, C. W. (1992). Human HSP27 is phosphorylated at serines 78 and 82 by heat shock and mitogen-activated kinases that recognize the same amino acid motif as S6 kinase II. *J Biol. Chem.* *267*, 794-803.
- Lane, D. P. (1992). Cancer. p53, guardian of the genome. *Nature* *358*, 15-16.
- Lee, C. H., Ni, Y. H., Chen, C. C., Chou, C., and Chang, F. H. (2003). Synergistic effect of polyethylenimine and cationic liposomes in nucleic acid delivery to human cancer cells. *Biochim. Biophys Acta* *1611*, 55-62.
- Leslie, A., Carey, F. A., Pratt, N. R., and Steele, R. J. (2002). The colorectal adenoma-carcinoma sequence. *Br. J Surg.* *89*, 845-860.
- Lieubeau-Teillet, B., Rak, J., Jothy, S., Iliopoulos, O., Kaelin, W., and Kerbel, R. S. (1998). von Hippel-Lindau gene-mediated growth suppression and induction of differentiation in renal cell carcinoma cells grown as multicellular tumor spheroids. *Cancer Res.* *58*, 4957-4962.
- Lin, F. and Worman, H. J. (1993). Structural organization of the human gene encoding nuclear lamin A and nuclear lamin C. *J Biol. Chem.* *268*, 16321-16326.

- Lipinski, K. S., Djeha, A. H., Ismail, T., Mountain, A., Young, L. S., and Wrighton, C. J. (2001). High-level, beta-catenin/TCF-dependent transgene expression in secondary colorectal cancer tissue. *Mol. Ther.* **4**, 365-371.
- Lipinski, K. S., Djeha, H. A., Gawn, J., Cliffe, S., Maitland, N. J., Palmer, D. H., Mountain, A., Irvine, A. S., and Wrighton, C. J. (2004). Optimization of a synthetic beta-catenin-dependent promoter for tumor-specific cancer gene therapy. *Mol. Ther.* **10**, 150-161.
- Liu, D., Ren, T., and Gao, X. (2003). Cationic transfection lipids. *Curr. Med Chem.* **10**, 1307-1315.
- Liu, F. (2001). SMAD4/DPC4 and pancreatic cancer survival. Commentary re: M. Tascilar et al., The SMAD4 protein and prognosis of pancreatic ductal adenocarcinoma. *Clin. Cancer Res.*, **7**: 4115-4121, 2001. *Clin. Cancer Res.* **7**, 3853-3856.
- Liu, G. and Chen, X. (2002). The ferredoxin reductase gene is regulated by the p53 family and sensitizes cells to oxidative stress-induced apoptosis. *Oncogene* **21**, 7195-7204.
- Lloyd, R. E., Grubman, M. J., and Ehrenfeld, E. (1988). Relationship of p220 cleavage during picornavirus infection to 2A proteinase sequencing. *J Virol.* **62**, 4216-4223.
- Longley, D. B., Harkin, D. P., and Johnston, P. G. (2003). 5-fluorouracil: mechanisms of action and clinical strategies. *Nat. Rev. Cancer* **3**, 330-338.
- Lynch, H. T. and de la Chapelle, A. (2003). Hereditary colorectal cancer. *N. Engl. J Med* **348**, 919-932.
- Maass, N., Hojo, T., Zhang, M., Sager, R., Jonat, W., and Nagasaki, K. (2000). Maspin--a novel protease inhibitor with tumor-suppressing activity in breast cancer. *Acta Oncol.* **39**, 931-934.
- Macdonald, J. S. and Astrow, A. B. (2001). Adjuvant therapy of colon cancer. *Semin. Oncol.* **28**, 30-40.
- Maguchi, M., Nishida, W., Kohara, K., Kuwano, A., Kondo, I., and Hiwada, K. (1995). Molecular cloning and gene mapping of human basic and acidic calponins. *Biochem Biophys Res. Commun.* **217**, 238-244.
- Maizels, E. T., Peters, C. A., Kline, M., Cutler, R. E., Jr., Shanmugam, M., and Hunzicker-Dunn, M. (1998). Heat-shock protein-25/27 phosphorylation by the delta isoform of protein kinase C. *Biochem J* **332** (Pt 3), 703-712.

Mayer, B., Klement, G., Kaneko, M., Man, S., Jothy, S., Rak, J., and Kerbel, R. S. (2001). Multicellular gastric cancer spheroids recapitulate growth pattern and differentiation phenotype of human gastric carcinomas. *Gastroenterology* 121, 839-852.

McDermott, U., Longley, D. B., Galligan, L., Allen, W., Wilson, T., and Johnston, P. G. (2005). Effect of p53 status and STAT1 on chemotherapy-induced, Fas-mediated apoptosis in colorectal cancer. *Cancer Res.* 65, 8951-8960.

Mehlen, P., Hickey, E., Weber, L. A., and Arrigo, A. P. (1997). Large unphosphorylated aggregates as the active form of hsp27 which controls intracellular reactive oxygen species and glutathione levels and generates a protection against TNFalpha in NIH-3T3-ras cells. *Biochem Biophys Res. Commun.* 241, 187-192.

Mehlen, P., Schulze-Osthoff, K., and Arrigo, A. P. (1996). Small stress proteins as novel regulators of apoptosis. Heat shock protein 27 blocks Fas/APO-1- and staurosporine-induced cell death. *J Biol. Chem.* 271, 16510-16514.

Miller, N. and Whelan, J. (1997). Progress in transcriptionally targeted and regulatable vectors for genetic therapy. *Hum. Gene Ther* 8, 803-815.

Miyaki, M. and Kuroki, T. (2003). Role of Smad4 (DPC4) inactivation in human cancer. *Biochem Biophys Res. Commun.* 306, 799-804.

Moir, R. D. and Spann, T. P. (2001). The structure and function of nuclear lamins: implications for disease. *Cell Mol Life Sci.* 58, 1748-1757.

Moll, R., Krepler, R., and Franke, W. W. (1983). Complex cytokeratin polypeptide patterns observed in certain human carcinomas. *Differentiation* 23, 256-269.

Moolten, F. L. (1986). Tumor chemosensitivity conferred by inserted herpes thymidine kinase genes: paradigm for a prospective cancer control strategy. *Cancer Res.* 46, 5276-5281.

Mounier, N. and Arrigo, A. P. (2002). Actin cytoskeleton and small heat shock proteins: how do they interact? *Cell Stress. Chaperones.* 7, 167-176.

Mueller-Klieser, W. (1997). Three-dimensional cell cultures: from molecular mechanisms to clinical applications. *Am. J Physiol* 273, C1109-C1123.

Mueller-Klieser, W. (2000). Tumor biology and experimental therapeutics. *Crit Rev. Oncol. Hematol.* 36, 123-139.

Muller, M., Wilder, S., Bannasch, D., Israeli, D., Lehlbach, K., Li-Weber, M., Friedman, S. L., Galle, P. R., Stremmel, W., Oren, M., and Krammer, P. H. (1998). p53 activates the CD95 (APO-1/Fas) gene in response to DNA damage by anticancer drugs. *J Exp. Med* 188, 2033-2045.

- Nettelbeck, D. M., Jerome, V., and Muller, R. (1998). A strategy for enhancing the transcriptional activity of weak cell type-specific promoters. *Gene Ther* 5, 1656-1664.
- Ogris, M., Carlisle, R. C., Bettinger, T., and Seymour, L. W. (2001). Melittin enables efficient vesicular escape and enhanced nuclear access of nonviral gene delivery vectors. *J Biol Chem* 276, 47550-47555.
- Ogris, M., Steinlein, P., Kursa, M., Mechtler, K., Kircheis, R., and Wagner, E. (1998). The size of DNA/transferrin-PEI complexes is an important factor for gene expression in cultured cells. *Gene Ther* 5, 1425-1433.
- Osaki, M., Tatebe, S., Goto, A., Hayashi, H., Oshimura, M., and Ito, H. (1997). 5-Fluorouracil (5-FU) induced apoptosis in gastric cancer cell lines: role of the p53 gene. *Apoptosis* 2, 221-226.
- Oshima, R. G. (2002). Apoptosis and keratin intermediate filaments. *Cell Death Differ* 9, 486-492.
- Owens, D. W. and Lane, E. B. (2003). The quest for the function of simple epithelial keratins. *Bioessays* 25, 748-758.
- Parlato, S., Giammarioli, A. M., Logozzi, M., Lozupone, F., Matarrese, P., Luciani, F., Falchi, M., Malorni, W., and Fais, S. (2000). CD95 (APO-1/Fas) linkage to the actin cytoskeleton through ezrin in human T lymphocytes: a novel regulatory mechanism of the CD95 apoptotic pathway. *Embo J* 19, 5123-5134.
- Peifer, M. (1999). Signal transduction. Neither straight nor narrow. *Nature* 400, 213-215.
- Pelisek, J., Engelmann, M. G., Golda, A., Fuchs, A., Armeanu, S., Shimizu, M., Mekkaoui, C., Rolland, P. H., and Nikol, S. (2002). Optimization of nonviral transfection: variables influencing liposome-mediated gene transfer in proliferating vs. quiescent cells in culture and in vivo using a porcine restenosis model. *J Mol Med* 80, 724-736.
- Pelisek, J., Gaedtke, L., DeRouchey, J., Walker, G. F., Nikol, S., and Wagner, E. (2006). Optimized lipopolyplex formulations for gene transfer to human colon carcinoma cells under in vitro conditions. *J Gene Med* 8, 186-197.
- Perng, M. D., Cairns, L., van den, I. J., Prescott, A., Hutcheson, A. M., and Quinlan, R. A. (1999). Intermediate filament interactions can be altered by HSP27 and alphaB-crystallin. *J Cell Sci* 112 (Pt 13), 2099-2112.
- Petak, I. and Houghton, J. A. (2001). Shared pathways: death receptors and cytotoxic drugs in cancer therapy. *Pathol. Oncol. Res* 7, 95-106.

Petak, I., Tillman, D. M., and Houghton, J. A. (2000). p53 dependence of Fas induction and acute apoptosis in response to 5-fluorouracil-leucovorin in human colon carcinoma cell lines. *Clin. Cancer Res.* 6, 4432-4441.

Pizzato, M., Franchin, E., Calvi, P., Boschetto, R., Colombo, M., Ferrini, S., and Palu, G. (1998). Production and characterization of a bicistronic Moloney-based retroviral vector expressing human interleukin 2 and herpes simplex virus thymidine kinase for gene therapy of cancer. *Gene Ther* 5, 1003-1007.

Plank, C., Zatloukal, K., Cotten, M., Mechtler, K., and Wagner, E. (1992). Gene transfer into hepatocytes using asialoglycoprotein receptor mediated endocytosis of DNA complexed with an artificial tetra-antennary galactose ligand. *Bioconjug. Chem.* 3, 533-539.

Polakis, P. (1997). The adenomatous polyposis coli (APC) tumor suppressor. *Biochim. Biophys Acta* 1332, F127-F147.

Porfiri, E., Rubinfeld, B., Albert, I., Hovanes, K., Waterman, M., and Polakis, P. (1997). Induction of a beta-catenin-LEF-1 complex by wnt-1 and transforming mutants of beta-catenin. *Oncogene* 15, 2833-2839.

Preville, X., Schultz, H., Knauf, U., Gaestel, M., and Arrigo, A. P. (1998). Analysis of the role of Hsp25 phosphorylation reveals the importance of the oligomerization state of this small heat shock protein in its protective function against TNFalpha- and hydrogen peroxide-induced cell death. *J Cell Biochem* 69, 436-452.

Rao, K. S., Babu, K. K., and Gupta, P. D. (1996). Keratins and skin disorders. *Cell Biol. Int* 20, 261-274.

Ries, L. A. G., Eisner, M. P., Kosary, C. L., Hankey, B. F., Miller, B. A., Clegg, L., Mariotto, A., Feuer, E. J., and Edwards, B. K. (2002). http://seer.cancer.gov/csr/1975_2002/. SEER Cancer Statistics Review 1975-2002 National Cancer Institute. Bethesda, MD.

Rodriguez-Gabriel, M. A., Remacha, M., and Ballesta, J. P. (1998). Phosphorylation of ribosomal protein P0 is not essential for ribosome function but can affect translation. *Biochemistry* 37, 16620-16626.

Rogalla, T., Ehrnsperger, M., Preville, X., Kotlyarov, A., Lutsch, G., Ducasse, C., Paul, C., Wieske, M., Arrigo, A. P., Buchner, J., and Gaestel, M. (1999). Regulation of Hsp27 oligomerization, chaperone function, and protective activity against oxidative stress/tumor necrosis factor alpha by phosphorylation. *J Biol. Chem.* 274, 18947-18956.

- Rosenberg, S. A., Mule, J. J., Spiess, P. J., Reichert, C. M., and Schwarz, S. L. (1985). Regression of established pulmonary metastases and subcutaneous tumor mediated by the systemic administration of high-dose recombinant interleukin 2. *J Exp. Med* *161*, 1169-1188.
- Rosin-Arbesfeld, R., Townsley, F., and Bienz, M. (2000). The APC tumour suppressor has a nuclear export function. *Nature* *406*, 1009-1012.
- Rutman, R. J., Cantarow, A., and Paschkis, K. E. (1954). Studies in 2-acetylaminofluorene carcinogenesis. III. The utilization of uracil-2-C14 by preneoplastic rat liver and rat hepatoma. *Cancer Res.* *14*, 119-123.
- Samali, A. and Cotter, T. G. (1996). Heat shock proteins increase resistance to apoptosis. *Exp. Cell Res.* *223*, 163-170.
- Santini, M. T. and Rainaldi, G. (1999). Three-dimensional spheroid model in tumor biology. *Pathobiology* *67*, 148-157.
- Schmidt, W. M., Kalipciyan, M., Dornstauder, E., Rizovski, B., Steger, G. G., Sedivy, R., Mueller, M. W., and Mader, R. M. (2004). Dissecting progressive stages of 5-fluorouracil resistance in vitro using RNA expression profiling. *Int. J Cancer* *112*, 200-212.
- Schmoll, H. J., Buchele, T., Grothey, A., and Dempke, W. (1999). Where do we stand with 5-fluorouracil? *Semin. Oncol.* *26*, 589-605.
- Schreiber, S., Kampgen, E., Wagner, E., Pirkhammer, D., Trcka, J., Korschan, H., Lindemann, A., Dorffner, R., Kittler, H., Kasteliz, F., Kupcu, Z., Sinski, A., Zatloukal, K., Buschle, M., Schmidt, W., Birnstiel, M., Kempe, R. E., Voigt, T., Weber, H. A., Pehamberger, H., Mertelsmann, R., Brocker, E. B., Wolff, K., and Stingl, G. (1999). Immunotherapy of metastatic malignant melanoma by a vaccine consisting of autologous interleukin 2-transfected cancer cells: outcome of a phase I study. *Hum. Gene Ther* *10*, 983-993.
- Schwartzberg, L. S., Petak, I., Stewart, C., Turner, P. K., Ashley, J., Tillman, D. M., Douglas, L., Tan, M., Billups, C., Mihalik, R., Weir, A., Tauer, K., Shope, S., and Houghton, J. A. (2002). Modulation of the Fas signaling pathway by IFN-gamma in therapy of colon cancer: phase I trial and correlative studies of IFN-gamma, 5-fluorouracil, and leucovorin. *Clin. Cancer Res.* *8*, 2488-2498.
- Seipelt, J., Guarne, A., Bergmann, E., James, M., Sommergruber, W., Fita, I., and Skern, T. (1999). The structures of picornaviral proteinases. *Virus Res.* *62*, 159-168.
- Selivanova, G. (2004). p53: fighting cancer. *Curr. Cancer Drug Targets.* *4*, 385-402.

Shtutman, M., Zhurinsky, J., Simcha, I., Albanese, C., D'Amico, M., Pestell, R., and Ben Ze'ev, A. (1999). The cyclin D1 gene is a target of the beta-catenin/LEF-1 pathway. *Proc. Natl. Acad. Sci. U. S. A* *96*, 5522-5527.

Shumaker, D. K., Kuczmarski, E. R., and Goldman, R. D. (2003). The nucleoskeleton: lamins and actin are major players in essential nuclear functions. *Curr. Opin. Cell Biol.* *15*, 358-366.

Sladek, N. E. (1999). Aldehyde dehydrogenase-mediated cellular relative insensitivity to the oxazaphosphorines. *Curr. Pharm. Des* *5*, 607-625.

Sladek, N. E. (2003). Human aldehyde dehydrogenases: potential pathological, pharmacological, and toxicological impact. *J Biochem Mol Toxicol.* *17*, 7-23.

Smalley, M. J. and Dale, T. C. (2001). Wnt signaling and mammary tumorigenesis. *J Mammary. Gland. Biol. Neoplasia.* *6*, 37-52.

Sodeman, T., Bronk, S. F., Roberts, P. J., Miyoshi, H., and Gores, G. J. (2000). Bile salts mediate hepatocyte apoptosis by increasing cell surface trafficking of Fas. *Am. J Physiol Gastrointest. Liver Physiol* *278*, G992-G999.

Stewart, M. J., Malek, K., Xiao, Q., Dipple, K. M., and Crabb, D. W. (1995). The novel aldehyde dehydrogenase gene, ALDH5, encodes an active aldehyde dehydrogenase enzyme. *Biochem Biophys Res. Commun.* *211*, 144-151.

Strelkov, S. V., Herrmann, H., and Aebi, U. (2003). Molecular architecture of intermediate filaments. *Bioessays* *25*, 243-251.

Tai, H. H., Ensor, C. M., Tong, M., Zhou, H., and Yan, F. (2002). Prostaglandin catabolizing enzymes. *Prostaglandins Other Lipid Mediat.* *68-69*, 483-493.

Tchorzewski, M., Boldyreff, B., Issinger, O., and Grankowski, N. (2000). Analysis of the protein-protein interactions between the human acidic ribosomal P-proteins: evaluation by the two hybrid system. *Int. J Biochem Cell Biol.* *32*, 737-746.

Templeton, N. S. (2002). Cationic liposome-mediated gene delivery in vivo. *Biosci. Rep.* *22*, 283-295.

Tetsu, O. and McCormick, F. (1999). Beta-catenin regulates expression of cyclin D1 in colon carcinoma cells. *Nature* *398*, 422-426.

Tong, M. and Tai, H. H. (2004). Synergistic induction of the nicotinamide adenine dinucleotide-linked 15-hydroxyprostaglandin dehydrogenase by an androgen and interleukin-6 or forskolin in human prostate cancer cells. *Endocrinology* *145*, 2141-2147.

- Uchiumi, T., Wahba, A. J., and Traut, R. R. (1987). Topography and stoichiometry of acidic proteins in large ribosomal subunits from *Artemia salina* as determined by crosslinking. *Proc. Natl. Acad. Sci. U. S. A* *84*, 5580-5584.
- van Engeland, M., Nieland, L. J., Ramaekers, F. C., Schutte, B., and Reutelingsperger, C. P. (1998). Annexin V-affinity assay: a review on an apoptosis detection system based on phosphatidylserine exposure. *Cytometry* *31*, 1-9.
- van Tellingen, O. (2001). The importance of drug-transporting P-glycoproteins in toxicology. *Toxicol. Lett.* *120*, 31-41.
- Vasiliou, V. and Nebert, D. W. (2005). Analysis and update of the human aldehyde dehydrogenase (ALDH) gene family. *Hum. Genomics* *2*, 138-143.
- Vasiliou, V. and Pappa, A. (2000). Polymorphisms of human aldehyde dehydrogenases. Consequences for drug metabolism and disease. *Pharmacology* *61*, 192-198.
- Vasiliou, V., Pappa, A., and Estey, T. (2004). Role of human aldehyde dehydrogenases in endobiotic and xenobiotic metabolism. *Drug Metab Rev.* *36*, 279-299.
- Vasiliou, V., Pappa, A., and Petersen, D. R. (2000). Role of aldehyde dehydrogenases in endogenous and xenobiotic metabolism. *Chem. Biol. Interact.* *129*, 1-19.
- Vecsey-Semjen, B., Becker, K. F., Sinski, A., Blennow, E., Vietor, I., Zatloukal, K., Beug, H., Wagner, E., and Huber, L. A. (2002). Novel colon cancer cell lines leading to better understanding of the diversity of respective primary cancers. *Oncogene* *21*, 4646-4662.
- Weitz, J., Koch, M., Debus, J., Hohler, T., Galle, P. R., and Buchler, M. W. (2005). Colorectal cancer. *Lancet* *365*, 153-165.
- Wightman, L., Kircheis, R., Rossler, V., Carotta, S., Ruzicka, R., Kursa, M., and Wagner, E. (2001). Different behavior of branched and linear polyethylenimine for gene delivery in vitro and in vivo
1026. *J. Gene Med.* *3*, 362-372.
- Winder, S. J. and Walsh, M. P. (1990). Smooth muscle calponin. Inhibition of actomyosin MgATPase and regulation by phosphorylation. *J Biol. Chem.* *265*, 10148-10155.
- Wohlhueter, R. M., Mclvor, R. S., and Plagemann, P. G. (1980). Facilitated transport of uracil and 5-fluorouracil, and permeation of orotic acid into cultured mammalian cells. *J Cell Physiol* *104*, 309-319.

- Wu, S. and Storey, K. B. (2005). Up-regulation of acidic ribosomal phosphoprotein P0 in response to freezing or anoxia in the freeze tolerant wood frog, *Rana sylvatica*. *Cryobiology* 50, 71-82.
- Xu, Y. and Szoka, F. C., Jr. (1996). Mechanism of DNA release from cationic liposome/DNA complexes used in cell transfection. *Biochemistry* 35, 5616-5623.
- Yan, M., Rerko, R. M., Platzer, P., Dawson, D., Willis, J., Tong, M., Lawrence, E., Lutterbaugh, J., Lu, S., Willson, J. K., Luo, G., Hensold, J., Tai, H. H., Wilson, K., and Markowitz, S. D. (2004). 15-Hydroxyprostaglandin dehydrogenase, a COX-2 oncogene antagonist, is a TGF-beta-induced suppressor of human gastrointestinal cancers. *Proc. Natl. Acad. Sci. U. S. A* 101, 17468-17473.
- Yin, S., Li, X., Meng, Y., Finley, R. L., Jr., Sakr, W., Yang, H., Reddy, N., and Sheng, S. (2005). Tumor-suppressive Maspin Regulates Cell Response to Oxidative Stress by Direct Interaction with Glutathione S-Transferase. *J Biol. Chem.* 280, 34985-34996.
- Yoshimoto, R., Hori, M., Ozaki, H., and Karaki, H. (2000). Proteolysis of acidic calponin by mu-calpain. *J Biochem (Tokyo)* 128, 1045-1049.
- Zatloukal, K., Schneeberger, A., Berger, M., Schmidt, W., Koszik, F., Kutil, R., Cotten, M., Wagner, E., Buschle, M., Maass, G., and . (1995). Elicitation of a systemic and protective anti-melanoma immune response by an IL-2-based vaccine. Assessment of critical cellular and molecular parameters. *J Immunol.* 154, 3406-3419.
- Zhang, W., Shi, H. Y., and Zhang, M. (2005). Maspin overexpression modulates tumor cell apoptosis through the regulation of Bcl-2 family proteins. *BMC. Cancer* 5, 50.

8. ACKNOWLEDGEMENTS

First of all, I am very thankful to all my colleagues for affording an outstanding working atmosphere that along with their strong support decisively contributed to the accomplishment of this thesis.

Foremost, I want to thank Prof. Dr. Ernst Wagner for his scientific support and professional guidance as my supervisor and for being also a very pleasant colleague. Thanks a lot to him and his family for being the best local tourist guides of Vienna.

Special thanks go to Dr. Jaroslav Pelisek for the very enjoyable and fruitful collaboration and his aid with the lipopolyplexes experiments, for his encouraging suggestions and for carefully reviewing the manuscript.

Many thanks go to Dr. Carsten Culmsee for his introduction into confocal laser scanning microscopy, his competent contributions to this thesis and for carefully reviewing the manuscript. I also thank Dr. Manfred “Fredl” Ogris for his support in the optimization of flow cytometry analysis, his manifold advices, his accommodation with “Apfelstrudel” and “Hirter Märzen”, and for the invitation to his house in Carinthia.

I am very grateful to Jens Rauch, from the Department of Otorhinolaryngology, Head and Neck Surgery, Klinikum Großhadern, LMU Munich, for teaching me the practical basics in 2D electrophoresis and to his supervisor Dr. Olivier Gires for giving me the chance to become acquainted with this fascinating technology in his lab. Further, I want to thank Dr. Werner Spahl for introducing me to mass spectrometry and Dr. Barbara Mayer from the Department of Surgery, Klinikum Großhadern, LMU Munich for teaching me the basics in the cultivation of multicellular spheroids.

A big thank you to Ursula Biebel for the performance of plasmid purifications and further support in the everyday life in the lab, and also for the supply with sweets and cakes. Thanks a lot to Wolfgang Rödl for fixing my PC many times and to Dr. Martina Ruffer and Melinda Kiss for the pleasant collaboration in the supervision of the students’ course. I also thank Olga Brück for typing the numerous references into the Reference Manager Database, and Dr. Greg “The Kiwi” Walker and the *dict.leo.org* website for support in the English language.

I am also very appreciative to Dr. Chris Wrighton and Dr. Kai Lipinski from ML Research PLC, UK for the provision of the pCTP4-Luc plasmid and to Boehringer Ingelheim Austria for the provision of the human low passage colon cancer cell lines. Moreover, I thank Dr. Joachim Seipelt and Agnes Kisser from the Department of Medical Biochemistry, Medical University Vienna, for the allocation of the p2A-IRES-IL2 plasmid.

A great thank you to all PhD and master students for the enduring encouragement during my entire PhD time, for the many “after-work seminars” in the beer garden, pub or other facilities, for the “funny conventions” at the skiing lodge, the beer hall at the “Oktoberfest” or further occasions, and, foremost, for being the best colleagues that one can imagine. Thanks to Julia Kloeckner for not wearing the “weird skirt” too often, to Nicole Tietze for going with me “Backstage”, to Silke van der Piepen for the ski lessons, to Rahul Haware for the hottest curry ever, to Arun “John Travolta” Kotha for the hottest dancing show ever, to Alenka Schwerdt for the “kind quarreling”, to Michael Günther for his “Liebesmobil” transport company, to Lilja Thoenes for her delicious “Schweinebraten”, to Katharina von Gersdorff for stick out bravely next to me during the “sick voyage” back from Carinthia and for introducing me to flow cytometry, to Verena Ruß for the “taxi service” to my home, to Julia Fahrmeir for the accommodation with “Mangostane”, to Carolin Fella for the “friendly takeover” of the supervision of the students, to Stefan Landshamer for sharing a bed with me at the skiing lodge, to Sabine Boeckle for being there for me at the beginning of my PhD thesis, to Martin Meyer for sharing the “real men’s” lab with me and to Veronika Knorr who unfortunately not shared the lab with me.

Finally, I want to say a big thank you to the people that mean the most to me, foremost, to my father for his support and everything he has done for me, to all my friends for their encouragement and their appreciation that I could only rarely find time for them during the last years, and especially to Daniela Huschka: Thank you very much for your continuous help, your backing and your appreciation that I could not spend as much time with you as I wanted to do.

9. CURRICULUM VITAE

Personal data

Date of birth: 29.04.1976

Place of birth: Leonberg

Marital status: unmarried

Education

- | | |
|--------------------|---|
| 05/2002 to present | PhD thesis at the Department of Pharmaceutical Biology-Biotechnology, Ludwig Maximilian University, Munich, Germany; supervisor: Prof. Dr. Ernst Wagner |
| 10/2001 | Graduation with diploma |
| 02/2001–10/2001 | Diploma thesis at the Department of Molecular Virology, Max Planck Institute of Biochemistry, Martinsried, Germany. Establishment and characterization of Sendai virus mutants with mutations in the L gene |
| 03/1999–04/1999 | Internship at the Human Retrovirus Section, National Cancer Institute, Frederick, Maryland, USA.
Investigations of the Vpr protein of HIV |
| 11/1996–10/2001 | Studies of biology, Technical University Munich, Germany |
| 10/1995–10/1996 | Civilian service at Haus Roehling, Deutscher Orden, Mittenwald, Germany |
| 06/1995 | Graduation with Abitur |
| 09/1986–06/1995 | Upper-track Secondary School, Welfen Gymnasium, Schongau, Germany |